UNIVERSITY OF CALIFORNIA

SANTA CRUZ

THE ROLE OF TEMPERATURE IN THE ENVIRONMENTAL SURVIVAL AND TRANSMISSION OF *VIBRIO CHOLERAE*

A dissertation submitted in partial satisfaction of the requirements for the degree of

DOCTOR OF PHILOSOPHY

in

MICROBIOLOGY AND ENVIRONMENTAL TOXICOLOGY

by

Loni Townsley

September 2015

The Dissertation of Loni Townsley is approved:

_____
Professor Fitnat H. Yildiz, Chair

_____
Professor Karen M. Ottemann

_____
Professor Grant A. Hartzog

_____
Distinguished Professor Jon Zehr

_____
Tyrus Miller
Vice Provost and Dean of Graduate Studies

TABLE OF CONTENTS

LIST OF FIGURES

THE ROLE OF TEMPERATURE IN THE ENVIRONMENTAL SURVIVAL AND TRANSMISSION OF *VIBRIO CHOLERAE*

Loni Townsley

Abstract

V. cholerae the causative agent of the diarrheal disease cholera is able to thrive within the small intestines of human hosts, however, between epidemics is found as an autochthonous member of aquatic microbial communities throughout the world (Kaper, 1979; Gil, 2004; Huq, 2005). This pathogen must endure changes in environmental parameters such as temperature, salinity, pH, and iron availability between their human hosts and aquatic reservoirs as well as within the environment. Temperature is an important parameter that governs the prevalence and distribution of *V. cholerae* in the environment, impacts association between *V. cholerae* and zooplankton, and is a strong predictor of cholera outbreaks. Despite the influence that temperature has on the ecology of *V. cholerae,* the molecular details of how *V. cholerae* adapts to temperature change and the cellular processes that are influenced by temperature in order to facilitate temperature adaptation in *V. cholerae* remain unknown.

To gain a better understanding of how temperature impacts *V. cholerae,* we examined biofilm formation at various temperatures. In *V. cholerae,* biofilm formation is important for persistence in the environment and survival within

the human host. We found that low-temperature growth enhances biofilm formation in *V. cholerae* through an increase in levels of the intracellular signaling molecule cyclic diguanylate (c-di-GMP). Furthermore, we identified six diguanylate cyclases, *cdgA, cdgH, cdgK cdgL, cdgM,* and *vpvC*, which are responsible for increasing c-di-GMP levels at low temperatures that impact biofilm formation and motility in *V. cholerae.*

Next we analyzed the genome-wide transcriptional profile of *V. cholerae* grown at different temperatures and determined that genes involved in virulence, biofilm formation, type VI secretion (T6SS), and cold shock were modulated by temperature. Mutational analysis and phenotypic characterization of the most highly induced gene at low temperatures, *cspV* (coding for cold shock protein V) revealed that this cold shock gene is important for biofilm formation and T6SS-mediated interspecies killing. In order to examine the effect of CspV in a more biologically relevant system, we tested the ability of CspV to colonize live zooplankton and perform T6SS-killing of bacteria on the these plankton. The strain lacking *cspV* had a severe attachment defect on the plankton surface, as well as a T6SS-killing defect of *E. coli* and *Aeromonas sp.*, which suggests that this cold shock gene is important for environmental survival and transmission of *V. cholerae* to the human host.

Finally we begin to characterize a putative c-di-GMP effector/ protease system in *V. cholerae* that is predicted to be functionally homologous to the inside-out signal transduction system LapD/G in *Pseudomonas fluorescens.* We determined that temperature is a key signal in regulating this system likely through low-temperature modulation of cellular c-di-GMP levels and via temperature modulation of genes that encode two putative large adhesins, VCA0849 and VC1620. Based on our results we predict that at low temperatures c-di-GMP levels are increased, causing the putative receptor VCA1082-3 to bind c-di-GMP and inhibit degradation of VCA0849 by a predicted periplasmic protease VCA1081, thereby increasing biofilm compactness and thickness at low temperatures.

This dissertation describes mechanisms that promote the survival of *V. cholerae* in the environment and facilitate the transmission of this pathogen to human hosts. This research provides important insight into how environmental pathogens adapt to changes in temperature and persist in the environment and by this means perpetuate their infectious cycle.

This work is dedicated to my father Louis T. Montoya, my grandmother Yolanda Bevan, and my partner Phil A. Wadell for always believing in me.

Acknowledgements

I would like to thank my advisor Dr. Fitnat Yildiz for her invaluable advice, guidance, and hard work on this project and express my gratitude for the opportunity to work on cutting edge science with an incredibly talented group in her lab. I would like to thank each of my committee members Dr. Karen Ottemann, Dr. Grant Hartzog, and Dr Jon Zehr for their wonderful ideas and guidance on the project.

I would also like to sincerely thank Dr. Chad Saltikov for his support and encouragement, and a very special thank you to Dr. Zia Isola to whom I am inspired by her wisdom, generosity, and passion and humbled by the tremendous support she gave me. I would also like to thank the members of the Yildiz Lab, past and present, and the METX graduate students for setting an example with their hard work and dedication while still providing an incredibly supportive atmosphere.

Thank you Dr. Nick Fong for being for being an incredibly hard-working and talented Scientist who is also an amazing friend. I would like to genuinely thank all of my friends especially Sylvia Zamudio, Emma Hiolski, Alison Conrad, Dr. Andrew Cheng and Samar Abedrabbo for always being there for support, encouragement, and inspiration during these past few years.

Words cannot express my gratitude to my family for the efforts and sacrifices they made to give me the opportunities they never had. Many thanks to my

grandmother who demanded the very best from me and taught me how to be independent and believe in myself- I miss you every day, to my Mom who taught me discipline and diligence and always encouraged learning, and to my Father who taught me the value of hard work and determination but also to be passionate and curious about the world around me. Thank you to my brothers, George Ishii and Alan Ishii for being amazingly smart and talented and always supporting me. And finally, to my partner Phil Wadell- thank you so much for all that you have done, I am my best self at your side.

The text of this dissertation includes reprints of the following previously published material:

Townsley L., Yildiz F. H. (2015). Temperature affects c-di-GMP signalling and biofilm formation in *Vibrio cholerae*. *Environ. Microbiol.* [Epub ahead of print].

Chapter 1: Introduction

CHOLERA

The facultative human pathogen *Vibrio cholerae* is responsible for the diarrheal disease cholera, a major health burden in many developing countries within Africa, Asia, South and Central America where the disease is endemic. In addition, cholera is known to significantly impact non-endemic regions after natural disasters like the recent devastation in Haiti where, following a major earthquake, an ongoing cholera outbreak has infected a startling 6% of the population (Barzilay et al., 2013). The World Health Organization reports that an estimated 3-5 million cholera infections and 120,000 deaths occur around the globe annually, however it is predicted that only 5-10% of cholera cases the occur actually get reported (World Health Organization, 2014). Once ingested, through contaminated food or water, *V. cholerae* can infect the intestines causing profuse watery diarrhea and vomiting, which is often fatal if exigent treatment is not administered. *V. cholerae* remains a major public health concern and better prevention and treatment measures are urgently needed to alleviate the impact of this disease.

TEMPERATURE FLUCTUATION DURING THE LIFE CYCLE OF *V. CHOLERAE*

Between epidemics *V. cholerae* is found as an autochthonous member of aquatic microbial communities within brackish water, coastal waters, and fresh water lakes and rivers where they are exposed to seasonal and inter-annual fluctuations in environmental variables like temperature, salinity, and iron availability that play an important role in the ecology of *V. cholerae* (Colwell, 1996; Lipp et al., 2002). Environmental temperature is an important factor that affects the prevalence of this pathogen in the environment and also impacts *V. cholerae*/plankton interactions, which are important for the survival and transmission of this pathogen. In addition, *V. cholerae* must endure temperature fluctuation between the human host and the environment. Aquatic habitats where cholera is endemic exhibit a temperature range of about 12 °C -30°C, whereas the human host environment is a constant 37 °C (Gil et al., 2004). Thus, temperature adaptation is imperative to the survival of *V. cholerae* in the environment and upon entering and exiting the human host, and thereby facilitates the continuation of its infectious cycle.

Temperature variation in the environment

Temperature has a large influence on outbreaks of the disease cholera (Cowell et al., 1996). Studies aimed at monitoring the occurrence of *V. cholerae* in the environment have detected the pathogen more frequently during warmer months (Gil et al., 2004; A. Huq et al., 2005; Louis et al., 2003). Furthermore, case studies compared compared with environmental

monitoring data have concluded that surface water temperature is directly correlated with cholera epidemics (Huq et al., 2005; Lipp, et al., 2003). In fact, monitoring of sea surface temperature by remote satellite sensing along with environmental measurements has been useful in developing a prediction model for cholera (Constantin de Magny et al., 2008). Results from these studies confirm that temperature is important in governing the distribution and occurrence of *V. cholerae* in the aquatic environment and has a direct impact on outbreaks of the disease cholera.

Temperature is also an important parameter that governs the growth and distribution of plankton, which greatly impacts *V. cholerae* ecology. Cholera outbreaks rise when high water temperatures occur concomitantly with plankton blooms (Huq et al.,1983; Turner et al., 2014). Temperature influences plankton abundance, which in turn affects the survival, growth, and distribution of *V. cholerae* in the environment, but also impacts the association of *V. cholerae* with plankton. The presence of live zooplankton has been shown to greatly increase the survival of *V. cholerae* at 25°C and 30°C, but has no effect at or below 15°C (Huq et al., 1984). In addition, attachment of *V. cholerae* to chitinous zooplankton occurs more frequently at higher environmental temperatures (Huq et al., 1983), which is advantageous to the bacteria in a multitude of ways. First, attached *V. cholerae* are able to utilize chitin as sources of carbon and nitrogen (R R Colwell, 1970; Meibom et al., 2004). Second, contact with chitin induces type IV pili required for

competence (Meibom et al., 2005; Seitz et al., 2014) allowing *V. cholerae* to potentially increase its fitness by taking up and incorporating foreign DNA when closely associated with other bacteria on the plankton surface. Finally, attachment to plankton allows *V. cholerae* to disseminate, increasing the chance of exposure to human hosts and has been shown to be important in the transmission of *V. cholerae* (Broza et al., 2008; Rita R Colwell et al., 2003; Huq et al., 2010; Nahar et al., 2012)

Temperature shifts between host and environment

Upon ingestion, *V. cholerae* experiences an abrupt increase in temperature. A shift to body temperature (37°C) from lower temperatures causes an increase in heat shock proteins in *V. cholerae* (Sahu et al.,1994; Slamti et al., 2007). The heat shock response in gram negative bacteria is transcriptionally controlled by the heat shock sigma factor sigma 32, or RpoH. The sequence of *rpoH* in *V. cholerae* is 70% identical to that in *E. coli,* and over-expression of RpoH from *E. coli* is able to activate transcription of heat shock response genes in *V. cholerae* (Slamti et al., 2007). Most of the genes induced upon high-temperature shift in *V. cholerae* include those that encode proteins that influence protein fate such as proteases and chaperones (Slamti et al, 2007) to restore proper protein folding during heat stress. The heat shock response is important for establishing infection within the gastrointestinal tract of the host, as an *rpoH* deletion mutant is attenuated for virulence within the

suckling mouse intestine (Slamti et al., 2007). In addition to genes that facilitate high-temperature shift survival, virulence factor expression is directly controlled by temperature, through translational control of the major virulence regulator ToxT, which is responsible for activating genes that encode the cholera toxin (CT) and toxin-coregulated pilus (TCP) required for virulence (Weber et al., 2014). ToxT contains a fourU anti-Shine-Dalgarno element located within its 5' UTR region that is inhibited from base pairing with the protein's Shine Dalgarno sequence at high temperatures, promoting translation under these conditions (G. G. Weber et al., 2014). The ability to adapt to temperature upshift is essential for virulence in *V. cholerae* and high temperatures provide an important signal to the pathogen to control the timing of the virulence gene network.

When *V. cholerae* is expelled from the human host, into the environment, it experiences a sudden decrease in temperature. Despite its significant influence on the life cycle of *V. cholerae*, very little is known about the effects that low temperatures have on the physiology of this pathogen. There are four predicted cold shock protein (CSP) homologues in *V. cholerae*, and one study determined that two that are cold inducible, CspA and CspV (Datta et al., 2003). CSPs are putative chaperones that prevent mRNA secondary structure formation by melting stem loops and modulating mRNA folding (Rodrigues & Tiedje, 2008). Each of these proteins contains a Y-box domain characteristic of an ancient family with conserved nucleic acid binding

domains (Phadtare, 2004). Datta et al found that the mRNA sequences of both the *V. cholerae* CSPs exhibit some significant differences when compared to their *E*. *coli* homologues. While there is an AT rich UP element, the long 5' UTR and cold box sequences normally found in CSPs are absent in *V. cholerae's* CSPs (Datta et al., 2003), *V. cholerae* CSPs are highly basic as opposed to the acidic Csps found in *E*. *coli,* and chloramphenicol inhibition of translation does not induce CSPs in *V. cholerae* as it does in *E. coli* (Datta et al., 2003). Currently it is unknown what affect these differences have on protein function or regulation in *V. cholerae*. CspV is highly expressed when *V*. *cholerae* is released from the human intestines back into the environment (Merrell et al., 2002), suggesting that it has an important role in environmental adaptation and survival.

THE COLD SHOCK RESPONSE

Low temperature environments impose numerous challenges to bacterial cell physiology; thus, the fundamental processes carried out by the cell must be significantly modified in order to survive temperature downshifts. Therefore there is a general trend in most species studied that the majority of cold shock induced proteins function in membrane alterations, DNA packaging, transcription and translation aiding, RNA degradation, and ribosome assembly (Gualerzi, 2003).

Membrane fluidity

As temperatures decrease outside the cell, the lipid composition of the cell membrane transitions to a ridged gel state (Hébraud & Potier, 1999; Phadtare & Inouye, 2004). This decrease in fluidity affects active transport and protein secretion by the cell, and compromises the ability of the membrane to provide protection from the external environment (Phadtare & Inouye, 2004). The cell membrane is the first barrier to the outside environment; therefore, it must be quickly modified to maintain its physical and functional integrity in cold conditions. Bacteria employ numerous methods for modifying membrane fluidity, also called homoviscous adaptation. The three most well studied membrane alterations, in respect to cold shock adaptation, are (a) the introduction of cis configured carbon double bonds, (b) the alteration of fatty acid branching, and (c) the shortening of fatty acid chain length (Weber et al., 2001). Most bacteria utilize multiple alteration mechanisms to increase membrane fluidity at low temperatures. In *Bacillus*, desaturation mechanisms quickly respond to and restore membrane fluidity, then, if cold conditions persist, branching and chain length is altered to maintain membrane fluidity. It has been established that cold temperatures alters lipid A synthesis (Hébraud & Potieret, 1999). *Shewanella oneidensis* cold shock experiments have shown that expression of genes required for lipopolysaccharide (LPS) biosynthesis is induced at low temperatures (Gao et al., 2006). Additionally, *Pseudomonas fluorescence* has been shown to increase its cell wall

thickness two-fold in response to low temperatures, however the underlying mechanism of this response has yet to be elucidated (Shivaji & Prakash, 2010).

DNA supercoiling

Cold stress causes a transient increase in negative supercoiling (Peter et al., 2004) and these changes to DNA structure can influence RNA polymerase binding and alter expression of target genes. This is primarily due to the numerous DNA associated proteins that are induced by cold shock, including the Histone U39 protein (HU-β), Histone-like nucleoid-structuring protein (H-NS), and Gyrase A (Rodrigues & Tiedje, 2008). Alternative topology proteins are induced in some other species in response to cold shock, however they too increase negative supercoiling. For instance, in *Shewanella oneidensis* microarray experiments have shown that DNA topoisomerase III is cold induced to increase negative supercoiling as opposed to *gyrA* in *E.coli* (Gao et al., 2006). Cold induced changes in DNA topology can alter gene expression in many ways. Expression can be increased through promoter melting which facilitates transcription initiation by increasing RNA polymerase recognition (Drolet, 2006). In *E. coli*, the recA promoter is induced upon cold shock by an increase of negative supercoiling at the -10 and -35 region, which enhances the recognition of the sigma 70 promoter site (Phadtare, 2004). On the contrary, the transcription of some genes is disrupted by the

increase of R-loop formations between nascent RNA and their DNA template strands which occurs during excess supercoiling (Baaklini et al., 2004). The expression of nearly 7% of the entire genome is significantly affected by alterations in chromosomal supercoiling in *E. coli* (Peter et al., 2004).

RNA secondary structure

Major obstacles to translation are imposed by poor ribosome assembly and the stabilization of RNA secondary structures at low temperatures (Chen & Shakhnovich, 2010; Tinoco et al., 1999; Phadtare, 2004). Cold shock proteins (CSPs) are thought to prevent mRNA secondary structure formation by melting stem loops and modulating mRNA folding (Rodrigues & Tiedje, 2008). CspA is among the first and most abundant proteins induced upon cold shock in many bacteria. In *E. coli*, CspA is induced to an astounding 13% of total protein content in cells shocked from 37 °C to 15 °C (Jiang et al., 1993). While CSP transcription is increased upon cold shock the dramatic induction of these proteins seems to be primarily post-transcriptional. The regulatory elements of *cspA* include; an A-T rich upstream sequence that is speculated to be a transcriptional pausing site by forming temperature-sensitive secondary structures, a cold box domain at the 5'end that stabilizes mRNA at low temperatures, and a downstream box that facilitates preferential ribosome binding in cold conditions (Shivaji & Prakash, 2010). The cold box domain often lies within an unusually long 5' UTR sequence (Chen &

Shakhnovich, 2010) which appears to be important for CSP regulation (Jiang et al., 1996).

In addition to CSPs, RNA exoribonucleases and helicases are induced upon cold shock to modulate mRNA processing (D'Amico et al., 2006). Polynucleotide phosphorylase (PNPase) is an important exoribonuclease that is essential to the cold shock response; however, its exact function during cold shock is unknown (Gualerzi, 2003). PNPase concentration increases over 10-fold after cold shock (Gualerzi, 2003). Like the CSPs, this is largely due to an increase in mRNA stability and translation efficiently at low temperatures (Phadtare & Severinov, 2010). Strains lacking *pnp* have severe growth defects at low temperatures (4-10 ° C) yet show no growth imparity at high temperatures (37° C or 42° C) in both *E. coli* and *Yersinia enterica* (Haddad et al., 2009). CsdA, a DEAD-Box helicase important for translation initiation and degradation of mRNA, is also highly induced upon cold shock (Phadtare & Severinov, 2010). Like PNPase, CsdA is essential at low temperatures, however overproduction of RNase R, an exoribonulease, can complement *csdA* mutations (Phadtare & Severinov, 2010). Interestingly, RNase R cannot complement PNPase, despite their functional similarities (Phadtare & Severinov, 2010). Furthermore, CsdA and PNPase cannot complement each other, indicating distinct targets for mRNA modulation for each of these proteins (Phadtare & Severinov, 2010). SrmB is another cold inducible DEAD-Box helicase that chaperones mRNA and aids in ribosome

assembly (Charollais et al., 2003; Nishi et al., 1988). The strains lacking *srmB* exhibit slow growth at low temperatures (Phadtare & Severinov, 2010). Both CsdA and SrmB aid in unwinding nucleic acid duplexes, 50s assembly, and RNA chaperoning; however, these proteins are not functionally redundant as they cannot complement each other in deletion mutants (Nishi et al., 1988). RNA degradation is important for controlling the levels of CSPs as well. PNPase and CsdA continue to accumulate later in the cold shock response to prevent excessively high levels of cold shock proteins. While CSPs are essential for growth in cold conditions, their mRNA outcompetes bulk mRNA and therefore represses growth (Gualerzi, 2003). Furthermore, CSPs are lethal at high concentrations (Ermolenko & Makhatadze, 2002). Thus, once cold resistance has been established in the cell, it is important to degrade CSPs so that growth can resume (Ermolenko & Makhatadze, 2002).

Ribosome stalling

In addition to the translation initiation challenges imposed by mRNA secondary structures, cold conditions also cause poor ribosome assembly. Upon cold shock, there is a transient decrease in polysomes and increase in inactive 70, 50, and 30S ribosomes (Chen & Shakhnovich, 2010). Hence ribosome associated proteins are induced upon cold shock. In *E. coli*, three ribosome associated proteins IF2, RbfA, and CsdA are highly induced at cold temperatures (Thieringer et al., 1998). As mentioned above, CsdA is a

DEAD-Box helicase important for RNA unwinding, but also participates in ribosome assembly (Chen & Shakhnovich, 2010). IF2 aides in the binding of tRNA to the 30S subunit, and RbfA is a 30S ribosome binding factor (Thieringer et al., 1998). Like CsdA, RbfA is required for optimal growth at cold temperatures (Chen & Shakhnovich, 2010). RbfA, IF2, and CsdA associate with 70s subunits to attain a cold resistant translatable state thereby allowing cell growth at cold temperatures (Phadtare & Severinov, 2010).

Sensing low temperatures

Ribosome staling is proposed to be a major sensor for the cold response networks. It has been shown that artificially stalling ribosomes, through use of antibiotics, triggers the cold shock response at normal physiological temperatures. Exposure of cells to chloramphenicol, erythromycin, and tetracycline induce expression of cold shock proteins (Jiang et al., 1993). Furthermore, at low temperatures there is a decrease in the concentration of guanosine 5'-triphosphate- 3'diphosphate and guanosine 5'-diphosphate-3'-diphosphaste, collectively abbreviated as (p)ppGpp (VanBogelen & Neidhardt, 1990). This provides a means of relaying the signal to induce the cold shock response. (p)ppGpp, is produced by stalled ribosomes during deficiencies in charged tRNA and poor nutrient conditions (VanBogelen & Neidhardt, 1990). Both *relA* and *spoT* mutants, unable to synthesize

(p)ppGpp, show a greater induction of cold shock proteins as well as faster cold adaptation when exposed to low temperature (Jones et al., 1992) indicating that (p)ppGpp may provide a means to relay cold sensing signals from stalled ribosomes to a elicit a genetic response, and control the magnitude of the cold shock response through regulation of cold shock gene expression.

Membrane sensing by two component regulatory systems is another means of relaying temperature signals to the cold shock response network. In *Bacillus subtilis* the decreased membrane fluidity caused by low temperatures is sensed by the transmembrane domain of the sensor kinase DesK that phosphorylates the response regulator DesR, which subsequently binds the *des* promoter activating the D5-desaturase responsible for introducing double bonds into preexisting fatty acids of phospholipids inside the cell membrane (Russell, 2008).

CELLULAR PROCESSES IMPORTANT FOR *V cholerae* ECOLOGY

Biofilm Formation

Biofilm formation is crucial to the environmental persistence as well as transmission of *V. cholerae.* Biofilms are surface-attached bacterial communities enclosed in an extra-polymeric matrix that are known to exhibit

enhanced tolerance to protozoan grazing (Matz & Kjelleberg, 2005) and toxic compounds (Bilecen et al., 2015; Yildiz & Schoolnik, 1999). In the environment *V. cholerae* are known to form biofilms on the surfaces of marine plankton (Huq et al., 1983). Additionally, biofilm-like aggregates of *V. cholerae* have been found in the surface waters of Bangladesh in a partially dormant 'conditionally viable state (Faruque et al., 2006). These conditionally viable environmental cells (CVECs) are revived as fully virulent cells when inoculated into rabbit intestines (Faruque et al., 2006). In addition, *V. cholerae* biofilms have been shown to be more infectious than their planktonic counterparts (Tamayo et al., 2010).

In *V. cholerae* there are three kinds of type IV pili that mediate surface attachment, the mannose-sensitive hemagglutinin pilus (MSHA) (Watnick et al., 1999), the toxin co-regulated pilus (TCP) (Taylor et al., 1987), and the chitin regulated pilus (ChiRP) (Meibom et al. 2004). Upon attachment, cells produce an extracellular matrix composed of *Vibrio* polysaccharides (VPS), matrix proteins, and extracellular DNA (Fong & Yildiz, 2007; Seper et al., 2011; Yildiz & Schoolnik, 1999). The VPS biosynthesis genes are encoded by *vps*U (VC0916), *vpsA-K*, VC0917-27 (*vps*-I cluster); *vpsL-Q*, VC0934-9 (*vps*-II cluster) (Fong et al., 2010) and are required for mature biofilm formation. Matrix proteins RbmA, RbmC, and Bap1 are required for maintaining the structural integrity of the biofilm (Fong et al., 2006; Fong & Yildiz, 2007).

Biofilm formation is highly regulated. Cyclic diguanylate (c-di-GMP) is an important second messenger that controls the expression of *vps* genes. c-di-GMP is an intracellular signaling molecule that is synthesized or degraded in response to external stimuli, which relays the signal to downstream receptors to control the life style switch between a free living and biofilm lifestyle (Fong & Yildiz, 2007). c-di-GMP is produced by Diguanylate cyclases (DGC), which contain GGDEF domains, and degraded by phosphodiesterases (PDE), which contain an EAL or HD-GYP domain (Römling et al., 2013). *V. cholerae* genome contains 62 genes predicted to encode proteins containing GGDEF or EAL domains capable of degrading or producing c-di-GMP (Beyhan et al., 2008). In *V. cholerae*, c-di-GMP receptors identified thus far include two riboswitches, five PilZ domain proteins, biofilm regulators VpsR and VpsT, degenerate GGDEF domain containing protein CdgG, and flagellar biosynthesis regulator FlrA (Beyhan et al., 2008; Krasteva et al., 2010; Pratt et al., 2007; Srivastava et al., 2011; Srivastava et al., 2013; Sudarsan et al., 2008). At present, little is known regarding the integration of environmental signals into the c-di-GMP network and biofilm formation.

In Chapter 1 we demonstrate that biofilm formation is enhanced at low temperatures through an increase in c-di-GMP levels and identify the DGCs responsible for modulating c-di-GMP levels in a temperature-dependent manner. Additionally, in Chapter 2 we further elucidate the molecular mechanism of temperature-modulated biofilm formation by establishing that

low-temperature biofilm formation is additionally controlled though modulation of expression of the cold shock protein *cspV.* In Chapter 3 we reveal the role of a c-di-GMP receptor and putative large adhesion protein in formation and c-di-GMP signaling at low temperatures.

Type VI secretion

Resent studies have demonstrated that the type VI secretion system (T6SS) is important for interspecies competition (Basler & Mekalanos, 2013), virulence (Pukatzki et al., 2006); , and natural transformation (Borgeaud et al., 2015) in *V. cholerae*. The T6SS apparatus spans the cell envelope with an inner tube composed of hemolysin coregulated protein (Hcp) polymers and an outer tube, also called the contractile sheath, formed by VipA and VipB polymers capped with a spike complex of trimeric VgrG proteins (Basler et al., 2012; Pukatzki et al., 2007). Effectors are delivered by contraction of the contractile sheath, which ejects the inner tube along with VgrG and the effectors towards the target cell. Four T6SS effectors have been identified in *V. cholerae.* VrgG1 (valine-glycine repeat protein G), has actin cross-linking activity; VrgG3 has peptidoglycan-degrading activity; TseL (T6SS effector lipase), has lipase activity and VasX (virulence-associated secretion protein X), causes cytoplasmic membrane perturbation (Brooks et al., 2013; Dong et al., 2013; Miyata et al., 2013; Pukatzki et al., 2007). Effector activity is antagonized in strains harboring their corresponding immunity proteins:

TsiV3, TsiV1, and TsiV2 (Brooks et al., 2013; Dong et al., 2013; Miyata et al., 2013; Unterweger et al., 2014).

T6SS genes are organized into one large cluster (VCA0105-VCA0124) and two auxiliary clusters (VCA0017-VCA0022 and VC1415-VC1421) (Pukatzki et al., 2006; Zheng et al., 2011). VasH is a transcriptional regulator that activates the T6SS auxiliary clusters and *vgrG3*, but does not affect expression of the structural genes encoded on the large cluster (Kitaoka et al., 2011). Hcp production is positively regulated by HapR, the global regulator cyclic AMP (cAMP) receptor protein, CRP, and negatively regulated by the QS regulator, LuxO, and the global regulator, TsrA (Ishikawa et al., 2009; Zheng et al., 2010).

In Chapter 2 we determine that T6SS gene expression and function are impacted by temperature and *cspV.* Additionally, we demonstrate that *cspV* is required for T6SS-mediated killing of *Aeromonas* on the surface of live *D. magna.*

CONCLUSION

V. cholerae is a facultative human pathogen that spends a significant portion of its life cycle in aquatic reservoirs where it is subjected to temperature fluctuation. Furthermore, *V. cholerae* must endure drastic shifts in temperature between the human host and the environment. Temperature has

been identified as an important factor that not only governs the occurrence and distribution of *V. cholerae* within the environment, but also affects *Vibrio*-plankton interactions that are crucial to the survival of this pathogen. Nonetheless, very little is known regarding the affect of temperature stress on the physiology and cellular processes of *V. cholerae*. This work aims to elucidate the molecular mechanisms utilized by *V. cholerae* cope with life at low temperatures and reveal the impact of temperature on cellular processes imperative to the survival, persistence, and transmission of this pathogen.

Baaklini, I., Hraiky, C., Rallu, F., Tse-Dinh, Y.-C., & Drolet, M. (2004). RNase HI overproduction is required for efficient full-length RNA synthesis in the absence of topoisomerase I in *Escherichia coli*. *Molecular Microbiology*, *54*(1), 198–211.

Barzilay, E. J., Schaad, N., Magloire, R., Mung, K. S., Boncy, J., Dahourou, G. a, Tappero, J. W. (2013). Cholera surveillance during the Haiti epidemic--the first 2 years. *The New England Journal of Medicine*, *368*, 599–609.

Basler, M., Ho, B. T., & Mekalanos, J. J. (2013). Tit-for-tat: Type VI secretion system counterattack during bacterial cell-cell interactions. *Cell*, *152*(4), 884–894.

Basler, M., Pilhofer, M., Henderson, G. P., Jensen, G. J., & Mekalanos, J. J. (2012). Type VI secretion requires a dynamic contractile phage tail-like structure. *Nature*, *483*(7388), 182–186.

Beyhan, S., Odell, L. S., & Yildiz, F. H. (2008). Identification and characterization of cyclic diguanylate signaling systems controlling rugosity in *Vibrio cholerae*. *Journal of Bacteriology*, *190*(22), 7392–405.

Bilecen, K., Fong, J. C. N., Cheng, A., Jones, C. J., Zamorano-Sánchez, D., & Yildiz, F. H. (2015). Polymyxin B Resistance and Biofilm Formation in *Vibrio cholerae* Are Controlled by the Response Regulator CarR. *Infection and Immunity*, *83*(3), 1199–1209.

Borgeaud, S., Metzger, L. C., Scrignari, T., & Blokesch, M. (2015). The type VI secretion system of *Vibrio cholerae* fosters horizontal gene transfer. *Scienc*, *347*(6217), 63–67.

Brooks, T. M., Unterweger, D., Bachmann, V., Kostiuk, B., & Pukatzki, S. (2013). Lytic activity of the Vibrio cholerae type VI secretion toxin VgrG-3 is inhibited by the antitoxin TsaB. *Journal of Biological Chemistry*, *288*(11), 7618–7625.

Broza, M., Gancz, H., & Kashi, Y. (2008). The association between non-biting midges and *Vibrio cholerae*. *Environmental Microbiology*, *10*(12), 3193–3200.

Charollais, J., Pflieger, D., Vinh, J., Dreyfus, M., & Iost, I. (2003). The DEAD-box RNA helicase SrmB is involved in the assembly of 50S ribosomal subunits in *Escherichia coli*. *Molecular Microbiology*, *48*(5), 1253–1265.

Chen, P., & Shakhnovich, E. I. (2010). Thermal adaptation of viruses and bacteria. *Biophysical Journal*, *98*(7), 1109–18.

Colwell, R. R. (1970). Polyphasic taxonomy of the genus vibrio: numerical taxonomy of *Vibrio cholerae*, *Vibrio parahaemolyticus*, and related *Vibrio* species. *J Bacteriol*, *104*(I), 410–433.

Colwell, R. R. (1996, December 20). Global climate and infectious disease: the cholera paradigm. *Science (New York, N.Y.)*.

Colwell, R. R., Huq, A., Islam, M. S., Aziz, K. M. a, Yunus, M., Khan, N. H., Russek-Cohen, E. (2003). Reduction of cholera in Bangladeshi villages by simple filtration. *Proceedings of the National Academy of Sciences of the United States of America*, *100*(3), 1051–1055.

Constantin de Magny, G., Murtugudde, R., Sapiano, M. R. P., Nizam, A., Brown, C. W., Busalacchi, A. J., Colwell, R. R. (2008). Environmental signatures associated with cholera epidemics. *Proceedings of the National Academy of Sciences of the United States of America*, *105*(46), 17676–17681.

D'Amico, S., Collins, T., Marx, J.-C., Feller, G., & Gerday, C. (2006). Psychrophilic microorganisms: challenges for life. *EMBO Reports*, *7*(4), 385–9.

Datta, P. P., & Bhadra, R. K. (2003). Cold Shock Response and Major Cold Shock Proteins of *Vibrio cholerae*. *Society*, *69*(11), 6361–6369.

Dong, T. G., Ho, B. T., Yoder-Himes, D. R., & Mekalanos, J. J. (2013). Identification of T6SS-dependent effector and immunity proteins by Tn-seq in *Vibrio cholerae*. *Proceedings of the National Academy of Sciences of the United States of America*, *110*(7), 2623–8.

Drolet, M. (2006). Growth inhibition mediated by excess negative supercoiling: the interplay between transcription elongation, R-loop formation and DNA topology. *Molecular Microbiology*, *59*(3), 723–30.

Ermolenko, D. N., & Makhatadze, G. I. (2002). Bacterial cold-shock proteins. *Cellular and Molecular Life Sciences : CMLS*, *59*, 1902– 1913.

Faruque, S. M., Biswas, K., Udden, S. M. N., Ahmad, Q. S., Sack, D. a, Nair, G. B., & Mekalanos, J. J. (2006). Transmissibility of cholera: in vivo-formed biofilms and their relationship to infectivity and persistence in the environment. *Proceedings of the National Academy of Sciences of the United States of America*, *103*(16), 6350–5.

Fong, J. C. N., Karplus, K., Schoolnik, G. K., & Yildiz, F. H. (2006). Identification and Characterization of RbmA, a Novel Protein Required for the Development of Rugose Colony Morphology and Biofilm Structure in *Vibrio cholerae*. *Journal of Bac*, *188*(3), 1049–1059.

Fong, J. C. N., Syed, K. a., Klose, K. E., & Yildiz, F. H. (2010). Role of *Vibrio* polysaccharide (vps) genes in VPS production, biofilm formation and *Vibrio cholerae* pathogenesis. *Microbiology*, *156*(9), 2757–2769.

Fong, J. C. N., & Yildiz, F. H. (2007). The rbmBCDEF gene cluster modulates development of rugose colony morphology and biofilm formation in Vibrio cholerae. *Journal of Bacteriology*, *189*(6), 2319–30.

Gao, H., Yang, Z. K., Wu, L., Thompson, D. K., & Zhou, J. (2006). Global transcriptome analysis of the cold shock response of *Shewanella* oneidensis MR-1 and mutational analysis of its classical cold shock proteins. *Journal of Bacteriology*, *188*(12), 4560–9.

Gil, A. I., Louis, V. R., Rivera, I. N. G., Lipp, E., Huq, A., Lanata, C. F., Colwell, R. R. (2004). Occurrence and distribution of *Vibrio cholerae* in the coastal environment of Peru. *Environmental Microbiology*, *6*(7), 699–706.

Gualerzi, C. (2003). Transcriptional and Post-transcriptional Control of Cold-shock Genes. *Journal of Molecular Biology*, *331*(3), 527–539.

Haddad, N., Burns, C. M., Bolla, J. M., Prévost, H., Fédérighi, M., Drider, D., & Cappelier, J. M. (2009). Long-Term Survival of *Campylobacter jejuni* at Low Temperatures Is Dependent on Polynucleotide Phosphorylase Activity. *Applied and Environmental Microbiology*, *75*(23),

Hébraud, M., & Potier, P. (1999). Cold shock response and low temperature adaptation in psychrotrophic bacteria. *Journal of Molecular Microbiology and Biotechnology*, *1*(2), 211–9. Retrieved from http://www.ncbi.nlm.nih.gov/pubmed/10943552

Huq, a, Small, E. B., West, P. a, Huq, M. I., & Colwell, R. R. (1983). Ecological relationships between *Vibrio cholerae* and planktonic crustacean Ecological Relationships Between *Vibrio cholerae* and Planktonic Crustacean Copepods, *45*(1), 275–283.

Huq, a., West, P. a., Small, E. B., Huq, M. I., & Colwell, R. R. (1984). Influence of water temperature, salinity, and pH on survival and growth of toxigenic *Vibrio cholerae* serovar O1 associated with live copepods in

laboratory microcosms. *Applied and Environmental Microbiology*, *48*(2), 420–424.

Huq, A., Sack, R. B., Nizam, A., Longini, I. M., Nair, G. B., Ali, A., Colwell, R. R. (2005). Critical Factors Influencing the Occurrence of *Vibrio cholerae* in the Environment of Bangladesh. *Society*, *71*(8), 4645–4654.

Huq, A., Yunus, M., Sohel, S., Bhuiya, A., Emch, M., Luby, S. P., & Russek-cohen, E. (2010). Simple Sari Cloth Filtration of Water Is Sustainable and Continues To Protect Villagers from Cholera in Matlab, Bangladesh, *1*(1), 1–5.

Ishikawa, T., Rompikuntal, P. K., Lindmark, B., Milton, D. L., & Wai, S. N. (2009). Quorum sensing regulation of the two hcp alleles in *Vibrio cholerae* O1 strains. *PLoS ONE*, *4*(8).

Jiang, W., Jones, P., & Inouye, M. (1993). Chloramphenicol induces the transcription of the major cold shock gene of *Escherichia coli*, cspA. *Journal of Bacteriology*, *175*(18), 5824–8.

Jones, P. G., Cashel, M., Glaser, G., & Neidhardt, F. C. (1992). Function of a relaxed-like state following temperature downshifts in *Escherichia coli*. *Journal of Bacteriology*, *174*(12), 3903–14.

Kitaoka, M., Miyata, S. T., Brooks, T. M., Unterweger, D., & Pukatzki, S. (2011). *VasH* is a transcriptional regulator of the type VI secretion system functional in endemic and pandemic *Vibrio cholerae*. *Journal of Bacteriology*, *193*(23), 6471–6482.

Krasteva, P. V, Fong, J. C. N., Shikuma, N. J., Beyhan, S., Navarro, M. V. a S., Yildiz, F. H., & Sondermann, H. (2010). *Vibrio cholerae* VpsT regulates matrix production and motility by directly sensing cyclic di-GMP. *Science (New York, N.Y.)*, *327*(5967), 866–868.

Lipp, E. K., Huq, A., & Colwell, R. R. (2002). Effects of Global Climate on Infectious Disease : the Cholera Model Effects of Global Climate on Infectious Disease : the Cholera Model, *15*(4).

Louis, V. R., Russek-cohen, E., Choopun, N., Rivera, I. N. G., Gangle, B., Jiang, S. C., Colwell, R. R. (2003). Predictability of *Vibrio cholerae* in Chesapeake Bay. *Applied and Environmental Microbiology*, *69*(5), 2773–2785.

Matz, C., & Kjelleberg, S. (2005). Off the hook - How bacteria survive protozoan grazing. *Trends in Microbiology*, *13*(7), 302–307.

Meibom, K. L., Blokesch, M., Dolganov, N. a, Wu, C.-Y., & Schoolnik, G. K. (2005). Chitin induces natural competence in *Vibrio cholerae*. *Science (New York, N.Y.)*, *310*(5755), 1824–1827.

Meibom, K. L., Li, X. B., Nielsen, A. T., Wu, C.-Y., Roseman, S., & Schoolnik, G. K. (2004). The *Vibrio cholerae* chitin utilization program. *Proceedings of the National Academy of Sciences of the United States of America*, *101*(8), 2524–2529.

Merrell, D. S., Butler, S. M., Qadri, F., Dolganov, N. a, Alam, A., Cohen, M. B., Camilli, A. (2002). Host-induced epidemic spread of the cholera bacterium. *Nature*, *417*(6889), 642–5.

Miyata, S. T., Unterweger, D., Rudko, S. P., & Pukatzki, S. (2013). Dual Expression Profile of Type VI Secretion System Immunity Genes Protects Pandemic *Vibrio cholerae*. *PLoS Pathogens*, *9*(12), 1–18.

Nahar, S., Sultana, M., Naser, M. N., Nair, G. B., Watanabe, H., Ohnishi, M., Alam, M. (2012). Role of shrimp chitin in the ecology of toxigenic *Vibrio cholerae* and cholera transmission. *Frontiers in Microbiology*, *2*(JAN), 1–8.

Nishi, K. et al. (1988). An eIF-4A-like protein is a suppressor of an Escherichia coli mutant defective in 50S ribosomal subunit assembly. *Nature*, *336*, 496–498.

Peter, B. J., Arsuaga, J., Breier, A. M., Khodursky, A. B., Brown, P. O., & Cozzarelli, N. R. (2004). Genomic transcriptional response to loss of chromosomal supercoiling in *Escherichia coli*. *Genome Biology*, *5*(11), R87.

Phadtare, S. (2004). Recent developments in bacterial cold-shock response. *Current Issues in Molecular Biology*, *6*(2), 125–36.

Phadtare, S., & Inouye, M. (2004). Genome-Wide Transcriptional Analysis of the Cold Shock Response in Wild-Type and Strains of *Escherichia coli* Genome-Wide Transcriptional Analysis of the Cold Shock Response in.

Phadtare, S., & Severinov, K. (2010). RNA remodeling and gene regulation by cold shock proteins. *RNA Biology*, *7*(6), 788–95. Retrieved from

Pratt, J. T., Tamayo, R., Tischler, A. D., & Camilli, A. (2007). PilZ domain proteins bind cyclic diguanylate and regulate diverse processes in *Vibrio cholerae*. *Journal of Biological Chemistry*, *282*(17), 12860–12870.

Pukatzki, S., Ma, A. T., Revel, A. T., Sturtevant, D., & Mekalanos, J. J. (2007). Type VI secretion system translocates a phage tail spike-like protein into target cells where it cross-links actin. *Proceedings of the National Academy of Sciences of the United States of America*, *104*, 15508–15513.

Pukatzki, S., Ma, A. T., Sturtevant, D., Krastins, B., Sarracino, D., Nelson, W. C., Mekalanos, J. J. (2006). Identification of a conserved bacterial protein secretion system in Vibrio cholerae using the Dictyostelium host model system. *Proceedings of the National Academy of Sciences of the United States of America*, *103*(5), 1528–1533.

Rodrigues, D. F., & Tiedje, J. M. (2008). Coping with our cold planet. *Applied and Environmental Microbiology*, *74*(6), 1677–86.

Römling, U., Galperin, M. Y., & Gomelsky, M. (2013). Cyclic di-GMP: the first 25 years of a universal bacterial second messenger. *Microbiology and Molecular Biology Reviews : MMBR*, *77*(1), 1–52.

Russell, N. J. (2008). Membrane components and cold sensing. In *Psychrophiles: from biodiversity to biotechnology*. Springer Berlin Heidelberg. 177-190

Sahu, G. K., Chowdhury, R., & Das, J. (1994). Heat shock response and heat shock protein antigens of *Vibrio cholerae*. *Infection and Immunity*, *62*(12), 5624–31. Retrieved from

Seitz, P., Pezeshgi Modarres, H., Borgeaud, S., Bulushev, R. D., Steinbock, L. J., Radenovic, A., Blokesch, M. (2014). ComEA Is Essential for the Transfer of External DNA into the Periplasm in Naturally Transformable *Vibrio cholerae* Cells. *PLoS Genetics*, *10*(1).

Seper, A., Fengler, V. H. I., Roier, S., Wolinski, H., Kohlwein, S. D., Bishop, A. L., Schild, S. (2011). Extracellular nucleases and extracellular DNA play important roles in *Vibrio cholerae* biofilm formation. *Molecular Microbiology*, *82*(4), 1015–1037.

Shivaji, S., & Prakash, J. S. S. (2010). How do bacteria sense and respond to low temperature? *Archives of Microbiology*, *192*(2), 85–95.

Slamti, L., Livny, J., & Waldor, M. (2007). Global gene expression and phenotypic analysis of a Vibrio cholerae rpoH deletion mutant. *Journal of Bacteriology*. Retrieved from

Srivastava, D., Harris, R. C., & Waters, C. M. (2011). Integration of cyclic di-GMP and quorum sensing in the control of *vpsT* and *aphA* in *Vibrio cholerae*. *Journal of Bacteriology*, *193*(22), 6331–41.

Srivastava, D., Hsieh, M.-L., Khataokar, A., Neiditch, M. B., & Waters, C. M. (2013). Cyclic di-GMP inhibits *Vibrio cholerae* motility by repressing induction of transcription and inducing extracellular polysaccharide production. *Molecular Microbiology*, *90*(6), 1262–76.

Sudarsan, N., Lee, E. R., Weinberg, Z., Moy, R. H., Kim, J. N., Link, K. H., & Breaker, R. R. (2008). Riboswitches in eubacteria sense the second messenger cyclic di-GMP. *Science (New York, N.Y.)*, *321*(5887), 411–413.

Tamayo, R., Patimalla, B., & Camilli, A. (2010). Growth in a biofilm induces a hyperinfectious phenotype in Vibrio cholerae. *Infection and Immunity*, *78*(8), 3560–9.

Taylor, R. K., Miller, V. L., Furlong, D. B., & Mekalanos, J. J. (1987). Use of *phoA* gene fusions to identify a pilus colonization factor coordinately regulated with cholera toxin. *Proceedings of the National Academy of Sciences of the United States of America*, *84*(9), 2833–2837.

Thieringer, H. a, Jones, P. G., & Inouye, M. (1998). Cold shock and adaptation. *BioEssays : News and Reviews in Molecular, Cellular and Developmental Biology*, *20*(1), 49–57.

Tinoco, I., & Bustamante, C. (1999). How RNA folds. *Journal of molecular biology*, *293*(2), 271-281.

Turner, J. W., Malayil, L., Guadagnoli, D., Cole, D., & Lipp, E. K. (2014). Detection of *Vibrio parahaemolyticus, Vibrio vulnificus* and *Vibrio cholerae* with respect to seasonal fluctuations in temperature and plankton abundance. *Environmental Microbiology*, *16*(4), 1019–1028.

Unterweger, D., Miyata, S. T., Bachmann, V., Brooks, T. M., Mullins, T., Kostiuk, B., Pukatzki, S. (2014). The *Vibrio cholerae* type VI secretion system employs diverse effector modules for intraspecific competition. *Nature Communications*, *5*, 3549.

VanBogelen, R. a, & Neidhardt, F. C. (1990). Ribosomes as sensors of heat and cold shock in *Escherichia coli*. *Proceedings of the National Academy of Sciences of the United States of America*, *87*(15), 5589–93.

Watnick, P. I., Fullner, K. J., & Kolter, R. (1999). A role for the mannose-sensitive hemagglutinin in biofilm formation by *Vibrio cholerae* El Tor. *Journal of Bacteriology*, *181*(11), 3606–9.

Weber, G. G., Kortmann, J., Narberhaus, F., & Klose, K. E. (2014). RNA thermometer controls temperature-dependent virulence factor expression in *Vibrio cholerae*. *Proceedings of the National Academy of Sciences*, *111*(39), 14241–14246.

Weber, M. H., Klein, W., Müller, L., Niess, U. M., & Marahiel, M. a. (2001). Role of the *Bacillus subtilis* fatty acid desaturase in membrane adaptation during cold shock. *Molecular Microbiology*, *39*(5), 1321–9.

World Health Organization. (2014). Cholera, 2013. *Weekly Epidemiological Record*, (31), 345–356.

Yildiz, F. H., & Schoolnik, G. K. (1999). *Vibrio cholerae* O1 El Tor: identification of a gene cluster required for the rugose colony type, exopolysaccharide production, chlorine resistance, and biofilm formation. *Proceedings of the National Academy of Sciences of the United States of America*, *96*(7), 4028–4033.

Zheng, J., Ho, B., & Mekalanos, J. J. (2011). Genetic analysis of anti-amoebae and anti-bacterial activities of the type vi secretion system in *Vibrio cholerae*. *PLoS ONE*, *6*(8).

Zheng, J., Shin, O. S., Cameron, D. E., & Mekalanos, J. J. (2010). Quorum sensing and a global regulator TsrA control expression of type VI secretion and virulence in *Vibrio cholerae*. *Pnas*, *107*(49), 21128–21133.

Chapter 2: Temperature affects c-di-GMP signaling and biofilm formation in *Vibrio cholerae*

Loni Townsley and Fitnat H. Yildiz

Abstract

Biofilm formation is crucial to the environmental survival and transmission of *Vibrio cholerae*, the facultative human pathogen responsible for the disease cholera. During its infectious cycle *V. cholerae* experiences fluctuations in temperature within the aquatic environment and during the transition between human host and aquatic reservoirs. In this study, we report that biofilm formation is induced at low temperatures through increased levels of the signaling molecule, cyclic diguanylate (c-di-GMP). Strains harboring in-frame deletions of all *V*. *cholerae* genes that are predicted to encode diguanylate cyclases (DGCs) or phosphodiesterases (PDEs) were screened for their involvement in low-temperature-induced biofilm formation and *Vibrio* polysaccharide (VPS) gene expression. Of the 52 mutants tested, deletions of six DGCs and three PDEs were found to affect these phenotypes at low temperatures. Unlike wild type, a strain lacking all six DGCs did not exhibit a low-temperature-dependent increase in c-di-GMP, indicating that these DGCs are required for temperature modulation of c-di-GMP levels. This study uncovers the role of temperature in environmental regulation of biofilm formation and c-di-GMP signaling.

INTRODUCTION

Vibrio cholerae, the causative agent of the diarrheal disease cholera, is a natural inhabitant of aquatic environments (Faruque, 1998; Alam, 2006). The

ability of this pathogen to form biofilms, matrix-enclosed surface-associated communities, is important for enhancing environmental survival and increasing infectivity and transmission (Alam, 2006; Charles, 2011; Faruque, 1998; 2006; Cowell, 2003; Harris, 2012; Huq; 1996; Nelson, 2009; Tamayo, 2010). In *V. cholerae*, biofilm formation is controlled by a complex regulatory network and is dependent on the production of *Vibrio* exopolysaccharides (VPS) and biofilm matrix proteins that facilitate cell-cell and cell-surface interactions (Berk, 2012; Fong, 2006; 2007; 2010; Yildiz, 1999; 2009). Although, key regulators of biofilm formation and their genetic interactions have been studied, little is known regarding the mechanisms by which environmental signals are integrated into the biofilm regulatory network.

c-di-GMP is an intracellular signaling molecule that controls diverse cellular processes including biofilm formation, motility, and virulence (Römling, 2013). c-di-GMP is synthesized by diguanylate cyclases (DGCs), which contain GGDEF domains, and degraded by phosphodiesterases (PDEs), which contain EAL or HD-GYP domains (Ryan, 2006; Ryjenkov, 2005; Schmidt, 2005). Many proteins with GGDEF, EAL or HD-GYP domains also harbor additional domains including REC, PAS and GAF domains which strongly suggests that the activity of c-di-GMP metabolizing enzymes can be modulated by sensing domains. Examples of such proteins are as follows. The *Ax*PDEA1 protein in *Acetobacter xylinum* contains a heme-binding PAS domain, which increases its PDE activity when bound to oxygen (Chang,

2001). The globin-coupled DGCs BpeGReg, DosD, and YddV in *Bordetella pertussis*, *Shewanella putrefaciens,* and *Escherichia coli* (respectively) promote c-di-GMP synthesis upon oxygen binding (Wan, 2009; Wu, 2013; Kitanishi, 2010). And finally, in *E. coli,* the YcgF protein contains a BLUF domain at the N-terminus and an EAL domain at the C-terminus that relieves repression of biofilm-associated genes at low temperatures (Tschowri, 2009). Levels of c-di-GMP can also be affected by sensor proteins that interact with DGCs or PDEs. For instance, in *Rhodopseudomonas palustris*, the BLUF protein PapB enhances PDE activity of PapA in response to blue light conditions (Kanazawa, 2010). Moreover, proteins with H-NOX (heme-nitric oxide/oxygen-binding) domains have been shown to modulate DGC activity and biofilm formation in response to nitric oxide (NO) (Plate, 2012). Once produced, c-di-GMP is sensed by different types of receptors that interact with a multitude of target proteins and regulate diverse cellular processes (Sondermann, 2012).

The genome of *V. cholerae* A1552 encodes 30 proteins with predicted GGDEF domains, 11 with EAL domains, 11 with both GGDEF and EAL domains, and 9 with HD-GYP domains (Galperin, 2001). *V. cholerae* GGDEF/EAL domain proteins often include sensory input domains (Galperin, 2001) that are likely responsible for modulating enzymatic activities of DGCs and PDEs. At present, few studies have identified environmental signals that affect c-di-GMP signaling in *V. cholerae*. The activity of the *V. cholerae* DGC

Vc Bhr-DGC is controlled by the redox state of the non-heme di-iron within the Bhr (bacterial hemerythrin) domain. Specifically, the DGC activity has been shown to be 10-times higher when the iron is in its diferrous state, which occurs under anaerobic conditions (Schaller, 2012). Polyamine norspermidine levels affect biofilm formation through the regulatory pathway involving the phosphodiesterase MbaA (Karatan, 2005; Cockerell, 2014). Furthermore, it was recently demonstrated that growth medium and growth conditions significantly impact c-di-GMP levels in *V. cholerae*, through modulation of DGC and PDE cellular activity (Koestler, 2013), however the specific signal(s) responsible for this phenotype was not determined. Additionally bile and bicarbonate, signals encountered by *V. cholerae* during infection, were also shown to impact c-di-GMP levels (Koestler, 2014). Taken together, these findings support the notion that diverse environmental conditions modulate c-di-GMP signaling in *V. cholerae*. Receptors of c-di-GMP identified in *V. cholerae* thus far include 2 riboswitches, 5 PilZ domain proteins, biofilm regulators VpsR and VpsT, degenerate GGDEF domain containing protein CdgG, and flagellar biosynthesis regulator, FlrA (Pratt, 2007; Krasteva, 2010; Srivastava 2011; Sudarsan, 2008; Beyhan, 2008; Srivastava 2013). While components of c-di-GMP signaling networks are being identified, molecular mechanisms by which c-di-GMP signaling operates remain unclear.

V. cholerae is a facultative pathogen that is able to grow in both the human host and aquatic reservoirs during its life cycle. Thus, *V. cholerae* must endure significant temperature shifts during the transition between human hosts and the aquatic environment. Furthermore, *V. cholerae* experiences seasonal and inter-annual changes in temperature within aquatic reservoirs; and it has been demonstrated that cholera outbreaks are highly correlated with sea surface temperature and seasonal temperature fluctuation (Gil, 2004; Huq, 2005; Turner, 2013). However, despite its critical influence on the life cycle of *V. cholerae*, little is known about the effects that temperature has on the physiology of *V. cholerae*.

In this study we show that a decrease in growth temperature enhances biofilm formation in *V. cholerae* through increased c-di-GMP levels. We determined that six DGCs, *cdgA* (VCA0074), *cdgH* (VC1067), *cdgK* (VC1104), *cdgL* (VC2285), *cdgM* (VC1376), and *vpvC* (VC2454) are required for a low-temperature increase in c-di-GMP levels and biofilm formation. These results collectively show that c-di-GMP signaling is critical for integration of environmental signals with biofilm formation.

RESULTS

Growth at low temperatures increases biofilm formation

V. cholerae experiences temperature changes during its lifecycle and biofilms are crucial to the environmental persistence and transmission of this organism. We therefore asked whether biofilm formation would be affected by temperature. We analyzed the ability of *V. cholerae* to form biofilms at 15°C, 25°C, and 37°C as the pathogen experiences this temperature range during its life cycle (Gil, 2004; Huq, 2005) and *V. cholerae* have been isolated from aquatic environments at these temperatures (Gil, 2004; Turner, 2013). To determine if temperature affects biofilm formation, biofilms were formed under static conditions using wild-type *V. cholerae*. We found that biofilms formed at low temperatures (15°C and 25°C) exhibited increased biomass, thickness, and were more structured compared to those formed at 37°C (Fig. 1). COMSTAT analysis (Table 1) revealed that biofilm biomass is 19.8-fold and 6.8-fold higher at 15°C and 25°C, respectively, when compared to those formed at 37°C. We note that it was previously demonstrated using crystal violet staining assay that biofilm formation in a *V. cholerae* O1 strain and several non-O1 strains was slightly increased at 30°C when compared to 37°C (Hoštacká, 2010), corroborating our results that biofilm forming ability of *V. cholerae* is enhanced at lower temperatures.

Figure 1. *V. cholerae* biofilm formation at various temperatures Three-dimensional biofilm structures of wild-type *V. cholerae* formed at 15°C, 25°C, and 37°C after 24 hours incubation in static biofilm chambers. Images of horizontal (*xy*) and vertical (*xz*) projections of biofilms are shown. The results shown are from one representative experiment of three independent experiments. Scale bars = 40 μm.

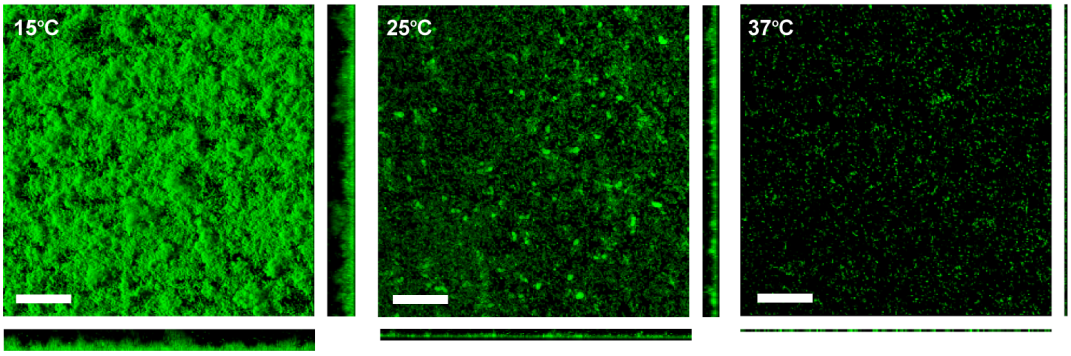

Table 1: COMSTAT analysis of biofilms formed by wild-type *V. cholerae* grown at 15°C, 25°C , and 37°C in static chambers in LB for 24 hours.

Temperature (˚C)	Biomass ($\mu m^3/\mu m^2$)	Thickness (μm)		Roughness coefficient
		Average	Maximum	
15	6.15 (0.46)	6.40 (0.28)	17.01 (5.47)	0.37 (0.03)
25	2.12 (0.76)	2.05 (0.66)	9.53 (0.87)	0.85 (0.35)
37	0.31 (0.32)	0.73 (0.92)	6.60 (1.21)	1.67 (0.34)

Growth at low temperatures increases cellular c-di-GMP levels

Since biofilm formation was impacted by temperature and enhanced c-di-GMP levels induce biofilm formation, we reasoned that cellular c-di-GMP levels may change with growth temperature. Cellular c-di-GMP quantification in wild-type *V. cholerae* grown for 24 hours at different temperatures revealed that c-di-GMP levels were approximately 1.5-fold higher at 25°C when compared to 37°C ($P < 0.05$), and approximately 5-fold higher at 15°C when compared to 37°C ($P < 0.005$) (Fig. 2A). Because *V. cholerae* must endure shifts in temperature during its transition between human host and the environment, we analyzed if c-di-GMP synthesis could be induced by a shift from high to low temperature. To this end, *V. cholerae* was grown at 37°C until mid-exponential phase then subjected to a low-temperature shift (25°C and 15°C) for 1 hour. Cellular c-di-GMP levels in these cultures were quantified and compared to control cultures that were kept at 37°C. We observed that c-di-GMP levels were over 2-fold higher after the shift from 37°C to 15°C ($P < 0.0005$), however there was no significant change after the shift to 25°C at this time point (Fig. 2B). Cultures maintained at 37°C showed an almost 2-fold decrease in c-di-GMP after 1 hour ($P < 0.005$) (Fig. 2B). In *V. cholerae* cellular c-di-GMP levels decrease as cell density increases; thus, a decrease in cellular c-di-GMP levels is expected (Koestler, 2013). These results show that c-di-GMP levels are increased at lower temperatures.

Having determined that biofilm formation and cellular c-di-GMP levels are increased in cells grown at low temperatures, we next evaluated the impact of the overexpression of a DGC (CdgA) and a PDE (CdgC) on biofilm formation at 15°C. We determined that overexpression of CdgA or CdgC from an arabinose inducible promoter resulted in an increase and a decrease in biofilm formation, respectively (Fig. 2C, Table 2).

Figure 2. c-di-GMP levels in *V. cholerae* grown at various temperatures c-di-GMP was extracted from whole cells and quantified using HPLC-MS/MS. (A) c-di-GMP levels in *V. cholerae* cells grown at 37°C, 25°C, or 15°C for 24 hours. (B) c-di-GMP levels in cells grown at 37°C then subjected to a low-temperatures. *V. cholerae* cells grown at 37°C to OD_{600} of 0.4 then shifted to 25°C,15°C or kept at 37°C, for one hour; and c-di-GMP levels were quantified. Error bars indicate standard deviations of four biological replicates. *$P < 0.05$, ** $P < 0.005$, n.s., $P > 0.05$. Biofilms formed after incubation at 15°C for 24 hours by wild-type *V. cholerae* harboring either *cdgA* or *cdgC* on an overexpression plasmid in LB with 0%, 0.05%, or 0.2% arabinose. The results shown are from one representative experiment of three independent experiments. Scale bars represent 40 μm.

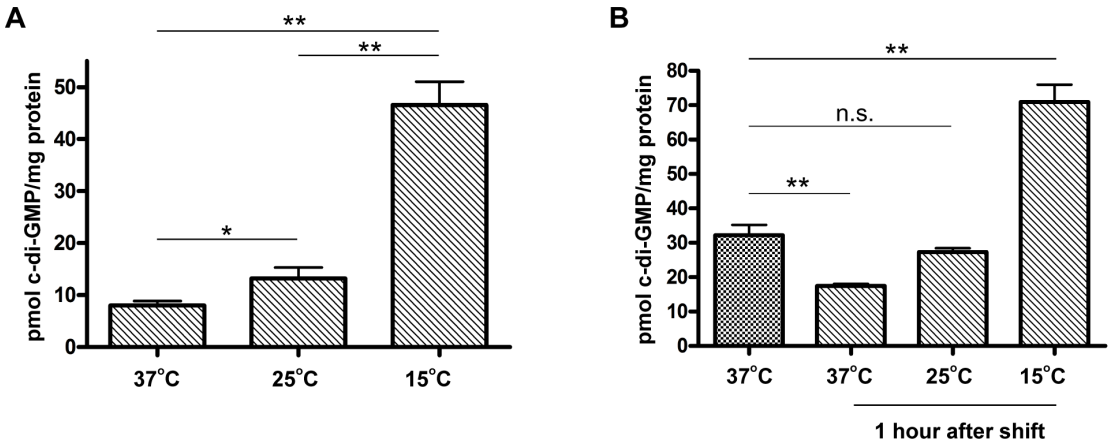
A
**
**
*
pmol c-di-GMP/mg protein
0
10
20
30
40
50
37°C
25°C
15°C
B
**
n.s.
**
pmol c-di-GMP/mg protein
0
10
20
30
40
50
60
70
80
37°C
37°C
25°C
15°C
1 hour after shift

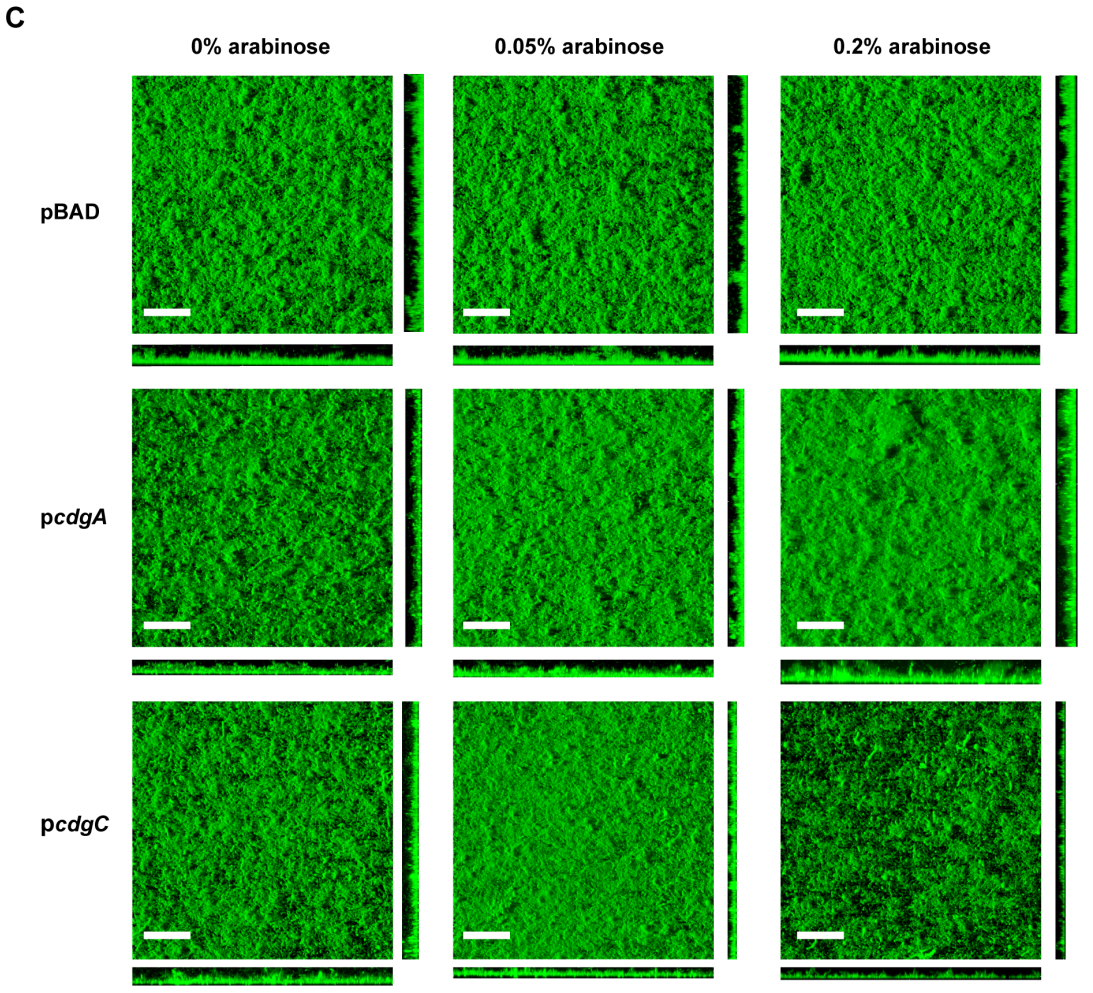
C
0% arabinose
0.05% arabinose
0.2% arabinose
pBAD
pcdgA
pcdgC

Table 2: COMSTAT analysis of biofilms formed by wild-type *V. cholerae* overexpressing either a DGC or PDE at 15°C, in static chambers in LB + 0%, 0.05%, or 0.2% arabinose for 24 hours.

		Thickness (μm)		
Plasmid	**Biomass ($\mu m^3/\mu m^2$)**	**Average**	**Maximum**	**Roughness coefficient**
pBAD-0%	6.15 (1.11)	6.88 (0.98)	15.54 (2.57)	0.26 (0.03)
pBAD-0.05%	5.65 (0.92	5.20 (0.42)	17.89 (2.33)	0.38 (0.08)
pBAD-0.2%	6.37 (0.90)	5.92 (1.06)	16.13 (1.09)	0.35 (0.06)
p*cdgA*-0%	8.20 (1.37)	8.75 (0.46)	20.53 (0.62)	0.28 (0.02)
p*cdgA*-0.05%	9.47 (1.12)	9.70 (1.16)	28.18 (0.45)	0.30 (0.09)
p*cdgA*-0.2%	10.52 (0.88)	10.88 (2.11)	28.77 (0.66)	0.24 (0.07)
p*cdgC*-0%	5.10 (0.35)	4.84 (0.45)	10.73 (0.40)	0.31 (0.05)
p*cdgC*-0.05%	4.91 (0.18)	4.055 (0.33)	10.44 (0.62)	0.20 (0.08)
p*cdgC*-0.2%	4.22 (0.12)	3.59 (0.28)	9.72 (0.80)	0.26 (0.11)

Identification of DGCs that control vpsL expression at low temperatures

We next wanted to determine if there are specific DGCs and/or PDEs responsible for modulating c-di-GMP metabolism in response to low temperatures**.** We previously generated 52 isogenic mutants with in-frame deletions of almost all of the predicted c-diGMP-related proteins of *V. cholerae* (Beyhan, 2008; Liu, 2010; Shikuma, 2012). To identify specific DGCs that contribute to low-temperature-induced c-di-GMP production, we measured promoter activity of the *vps genes* using a luciferase transcriptional reporter *vpsLp-lux* in wild-type *V. cholerae* and 31 strains containing in-frame deletions of each gene encoding a protein with a predicted GGDEF domain. In *V. cholerae, vpsL* is the first gene in the *vps*-II cluster, which together with the *vps*-I cluster genes, encode proteins that are required for VPS production and biofilm formation. Because *vpsL* transcription is positively regulated by c-di-GMP, we used the expression of *vpsL* as an indicator of cellular c-di-GMP levels. To measure *vpsL* expression, each strain was grown at 37°C until it reached an OD_{600} of 0.4, at which time they were shifted to 15°C for one hour and luminescence was measured (Supplementary Fig.1). A total of six mutants, Δ*cdgA*, Δ*cdgH*, Δ*cdgK*, Δ*cdgL*, Δ*cdgM*, and Δ*vpvC,* were found to exhibit an over 2-fold decrease in *vpsL* expression compared to wild type ($P < 0.05$) (Fig. 3A). We also measured *vpsL* expression in these strains after 24 hours of growth at 15°C (Fig. 3B). Δ*cdgH*, Δ*cdgL*, and Δ*cdgM* still exhibited an over 2-fold decrease in *vpsL* expression whereas Δ*cdgA*, Δ*cdgK*, and

Δ*vpvC* exhibited an approximately 1.5-fold decrease when compared to wild type ($P < 0.05$) (Fig. 3B). These results show that multiple DGCs are involved in *vpsL* regulation and likely in c-di-GMP homeostasis at low temperatures.

Figure 3. Analysis of *vpsL* expression in DGC mutants *vpsL* expression in wild-type *V. cholerae* and strains that harbor in-frame deletions of genes encoding proteins with GGDEF domains. *V. cholerae* cells were grown at (A) 37°C to OD_{600} of 0.4 then shifted to 15°C for one hour or (B) at 15°C for 24 hours with no shift. Expression is reported in luminescence counts min^{-1} ml^{-1}/OD_{600}. Error bars indicate standard deviations of three biological replicates. All strains exhibited a statistically significant difference when compared with wild type ($P < 0.05$). (C) Schematic showing predicted domains for each DGC, black boxes represent predicted transmembrane domains within each protein.

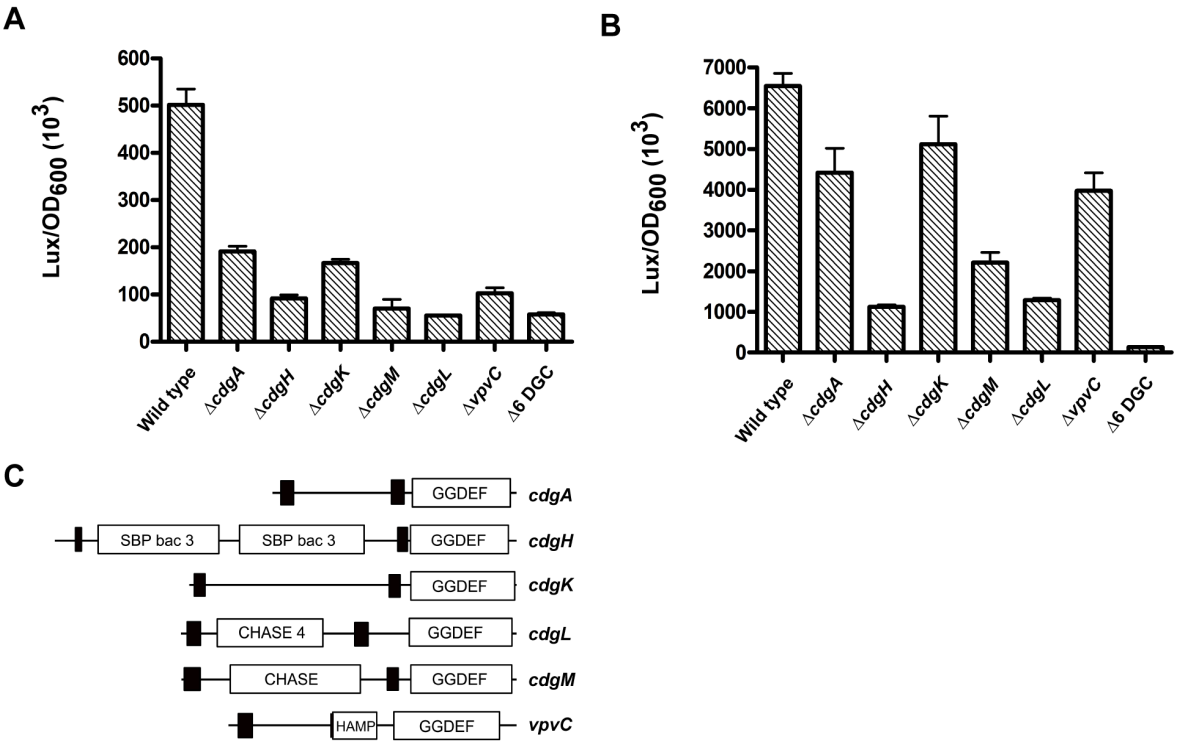

We hypothesized that each of these DGCs could contribute additively to low temperature-mediated increase in *vpsL* expression. Therefore, we created a strain lacking all six DGCs, designated as ∆6 DGC. We then analyzed *vpsL* gene expression in ∆6 DGC strain following a temperature shift from 37 °C to 15 °C, and also in cells grown at 15°C for 24 hours (Fig. 3A and B). The ∆6 DGC mutant exhibited an approximately 10-fold and 25-fold lower *vpsL* expression when compared to wild type following a low-temperature shift and constant incubation at 15°C ($P < 0.005$) (Fig. 3A and B), supporting the hypothesis that multiple DGC are contributing to cellular c-di-GMP levels at low temperatures.

To further understand how these DGCs could contribute to low temperature sensing, we checked if these proteins are predicted to harbor sensory input domains (Fig. 3C). CdgH contains a tandem bacterial extracellular solute-binding domain 3 (SBP bac 3). Periplasmic solute-binding proteins of Gram-negative bacteria can be classified into eight families (Tam, 1993). Family 3 proteins bind to polar amino acids and opines. CdgM has a Cyclases/Histidine kinases Associated Sensory Extracellular domain (CHASE). This domain is predicted to bind diverse low molecular weight ligands, such as the cytokinin-like adenine derivatives or peptides. CdgH and CdgM activity was recently shown to be enhanced by bile acids, an environmental signal critical for sensing host environment (Koestler, 2014). CdgL harbors a CHASE 4 domain. While ligand-binding specifies of CHASE

4 domain is yet to be determined, it is reported that in bacteria this domain is found exclusively with diguanylate cyclases (Mougel, 2001). VpvC has a Histidine kinases, Adenyl cyclases, Methyl-accepting proteins and Phosphatases domain (HAMP). HAMP domains are involved in transmembrane signaling by relaying stimulus-induced conformational changes to cytoplasmic signaling domains (Parkinson, 2010). It is yet to be determined how these domains could be involved in sensing or responding low-temperature mediated changes to cell physiology. In contrast to the four DGCs discussed above, CdgA and CdgK periplasmic sensing domains have not been formally described.

Identification of DGCs that regulate biofilm formation at low temperatures

Since our objective was to identify c-di-GMP signaling proteins contributing to both c-di-GMP levels and biofilm formation at low temperatures, we further characterized mutants discussed above for their ability to form biofilms at 15°C. We observed that Δ*cdgH,* Δ*cdgK,* Δ*cdgL,* and Δ*cdgM* exhibited less biofilm formation than wild type (Fig. 4 and Table 3), consistent with the *vpsL* expression data (Fig. 3A). Δ*vpvC* and Δ*cdgA* exhibited a small but reproducible decrease in biofilm formation when compared to wild type (Fig 4 and Table 3). These data show that each DGC affects biofilm formation at low temperatures to a different degree.

Figure 4. Biofilm formation in strains lacking DGCs Biofilms formed by wild-type *V. cholerae* and strains containing in-frame deletions of genes encoding DGCs (*cdgA*, *cdgH*, *cdgK*, *cdgL*, *cdgM*, *vpvC* and a Δ6 mutant) after incubation at 15°C for 24 hours. The results shown are from one representative experiment of three independent experiments. Scale bars represent 40 μm.

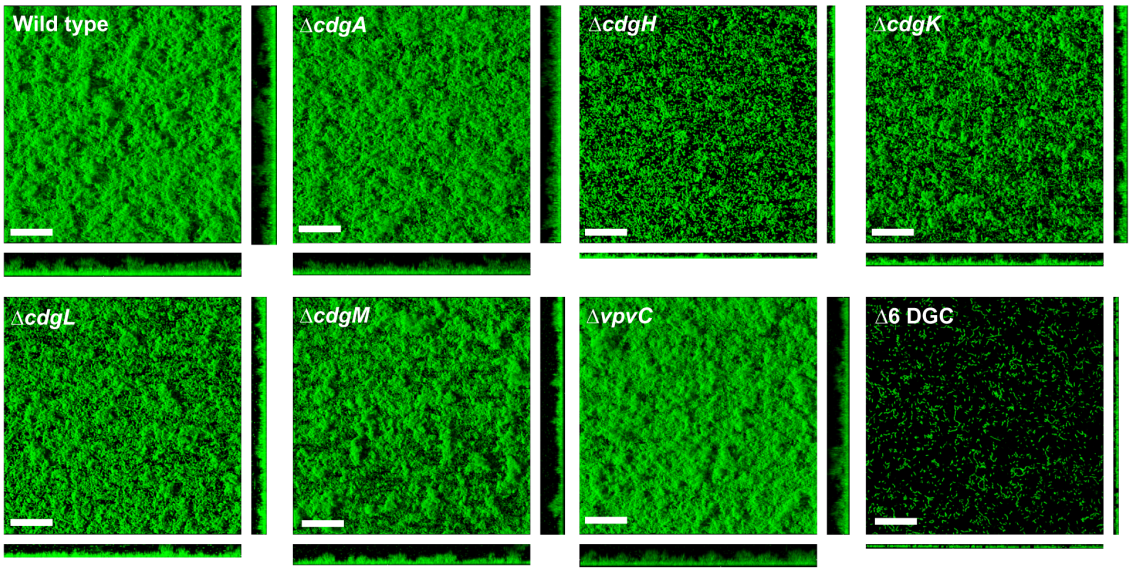

Table 3: COMSTAT analysis of biofilms formed by wild-type *V. cholerae* and DGC/PDE mutants grown at 15°C, in static chambers in LB for 24 hours.

Strain	Gene Name	Domain	Biomass ($\mu m^3/\mu m^2$)	Thickness (μm)		Roughness coefficient
				Average	Maximum	
Wild type	N/A	N/A	7.18 (2.3)	7.65 (2.2)	20.97 (3.5)	0.42 (0.08)
ΔVC0137	*cdgJ*	EAL	8.80 (0.9)	9.22 (0.4)	24.79 (1.4)	0.36 (0.02)
ΔVC0653	*rocS*	GGDEF-EAL	10.1 (1.2)	10.80 (1.0)	29.48 (2.7)	0.34 (0.06)
ΔVC1067	*cdgH*	GGDEF	1.81 (0.4)	1.58 (0.3)	6.75 (0.4)	0.96 (0.26)
ΔVC1104	*cdgK*	GGDEF	4.04 (0.1)	4.14 (0.2)	16.28 (0.2)	0.69 (0.04)
ΔVC1376	*cdgM*	GGDEF	3.91 (0.8)	3.68 (1.4)	14.52 (0.6)	0.51 (0.23)
ΔVC2285	*cdgL*	GGDEF	2.67 (0.3)	2.41 (0.4)	8.36 (0.2)	0.90 (0.15)
ΔVC2454	*vpvC*	GGDEF	7.67 (0.9)	7.96 (0.5)	22.88 (0.8)	0.35 (0.02)
ΔVCA0074	*cdgA*	GGDEF	6.00 (2.3)	6.41 (2.3)	23.32 (0.6)	1.32 (0.40)
ΔVCA0785	*cdgC*	GGDEF-EAL	8.82 (0.1)	9.48 (3.3)	24.95 (3.3)	0.35 (0.06)
Δ6 DGC		GGDEF	0.39 (0.1)	0.47 (0.0)	6.01 (0.6)	1.72 (0.05)
Δ3 PDE		EAL	1.33 (0.1)	1.86 (0.4)	27.28 (4.9)	1.11 (0.39)

To further confirm the contribution of these DGCs to biofilm formation at low temperatures, we generated complementation plasmids where expression of DGC genes were placed under the control of an arabinose-inducible promoter of the pBAD plasmid. Each plasmid was then introduced to their respective deletion strain and biofilm formation was analyzed and quantified. We determined that each DGC gene was able to complement the biofilm defect of its corresponding deletion strain (Table 4).

Table 4: COMSTAT analysis of biofilms formed by wild type *V. cholerae* and DGC mutants harboring complementation plasmids. Biofilms were grown at 15°C, in static chambers in LB for 24 hours.

Strain	Gene Name	Biomass ($\mu m^3/\mu m^2$)	Thickness (μm)		Roughness coefficient
			Average	Maximum	
Wild type	vector	7.23 (0.75)	7.61 (1.12)	20.77 (1.33)	0.34 (0.05)
Δ*cdgA*	vector	4.60 (0.40)	4.84 (0.69)	15.55 (2.59)	0.37 (0.05)
	p*cdgA*	6.69 (1.55)	7.47 (2.35)	22.35 (6.54)	0.37 (0.04)
Δ*cdgH*	vector	3.83 (0.37)	3.96 (0.11)	9.97 (1.02)	0.30 (0.02)
	p*cdgH*	6.10 (0.61)	6.90 (1.32)	14.67 (0.51)	0.33 (0.05)
Δ*cdgK*	vector	5.07 (1.23)	4.93 (1.52)	14.08 (3.77)	0.40 (0.15)
	p*cdgK*	7.50 (3.25)	7.74 (3.84)	17.6 (4.62)	0.34 (0.08)
Δ*cdgL*	vector	1.94 (0.43)	2.42 (0.61)	12.03 (1.64)	0.85 (0.14)
	p*cdgL*	5.61 (0.92)	5.59 (1.34)	12.04 (1.81)	0.32 (0.01)
Δ*cdgM*	vector	4.69 (0.92)	5.17 (1.90)	14.08 (4.16)	0.35 (0.05)
	p*cdgM*	6.13 (1.79)	7.39 (3.08)	19.21 (6.50)	0.40 (0.03)
Δ*vpvC*	vector	4.47 (0.62)	4.51 (0.91)	12.47 (2.69)	0.36 (0.04)
	p*vpvC*	5.74 (1.09)	5.98 (1.51)	15.25 (4.61)	0.32 (0.02)
Δ6 DGC	vector	1.14 (0.05)	1.14 (0.05)	4.69 (0.51)	1.27 (0.03)
	p*cdgA*	6.57 (0.42)	6.46 (0.23)	21.71 (1.02)	0.36 (0.02)
	p*cdgH*	1.98 (0.18)	2.35 (0.23)	13.79 (1.02)	0.86 (0.01)
	p*cdgK*	1.24 (0.13)	1.16 (0.34)	5.28 (0.88)	1.11 (0.03)
	p*cdgL*	1.89 (0.26)	2.33 (0.27)	10.85 (1.06)	0.86 (0.01)
	p*cdgM*	1.29 (0.12)	1.92 (0.30)	4.40 (0.88)	1.34 (0.03)
	p*vpvC*	2.33 (0.40)	2.22 (0.34)	7.04 (0.88)	0.69 (0.18)

Next, biofilm formation of the Δ6 DGC mutant was analyzed after incubation at 15°C for 24 hours. The Δ6 DGC mutant exhibited a severe defect in biofilm formation at 15°C with an 18-fold decrease in biomass and a 16-fold and 3-fold decrease in average and maximum thickness, respectively, when compared to biofilms formed by the wild-type strain (Fig. 4A and Table 2). We then evaluated the ability of each complementation plasmid to restore biofilm formation at 15°C in the Δ6 DGC mutant (Table 4). Thus, we introduced p*cdgA*, p*cdgH*, p*cdgK*, p*cdgL*, p*cdgM*, or p*vpvC* into the Δ6 DGC strain. We then analyzed and quantified biofilm formation by measuring total biomass, average and maximum thickness, and the roughness coefficient. The Δ6 DGC strain harboring p*cdgA* was able to complement the Δ6 DGC strain to wild-type levels. Partial complementation was observed with p*cdgH* and p*cdgL*, and p*vpvC* (Table 3). On the other hand, the Δ6 DGC strain harboring p*cdgM* and p*cdgK* exhibited a low but reproducible increase in biofilm properties compared to the Δ6 DGC harboring the vector alone. These results suggest that these DGCs may differ in their ability to produce c-di-GMP thus contribute differently to low temperature biofilm formation.

To better evaluate the ability of each DGC to produce c-di-GMP at 15°C, we analyzed cellular c-di-GMP levels in the Δ6 DGC strain harboring individual complementation plasmids. The expression of each gene resulted in an increase in cellular c-di-GMP levels of the Δ6 DGC strain (Fig. 5A). However, each DGC differed in its ability to produce c-di-GMP. Overall, biofilm

formation and cellular c-di-GMP levels resulting from complementation were corroboratory.

Figure 5. c-di-GMP levels in complementation strains A) c-di-GMP levels in wild type *V. cholerae* cells harboring pBAD and the Δ6 DGC strain harboring pBAD only or pBAD expressing *cdgA*, *cdgH*, *cdgK*, *cdgL*, *cdgM*, or *vpvC* genes grown in LB with 0.1% arabinose at 15°C for 24 hours. Error bars indicate standard deviations of four biological replicates comparing the Δ6 DGC strain harboring each complementation plasmid to pBAD only. *P < 0.05, ** P < 0.005.

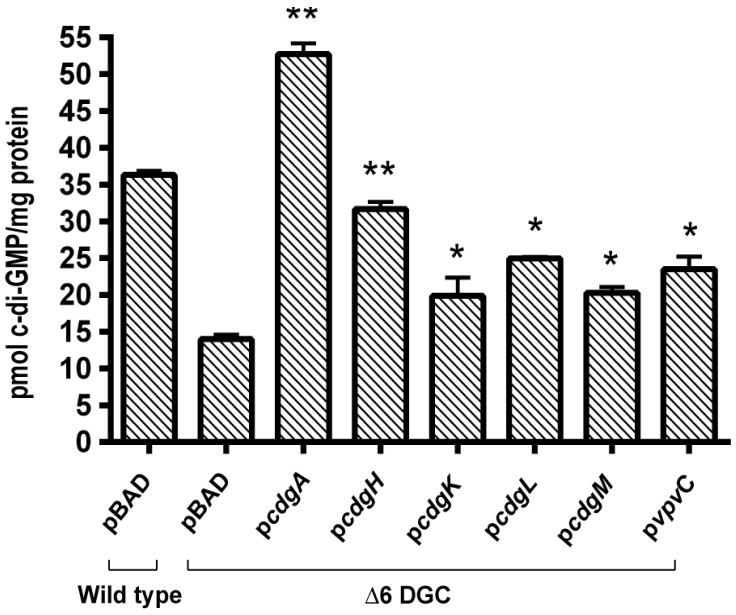

Analysis of motility phenotypes of DGC mutants

c-di-GMP inversely regulates motility and biofilm formation in *V. cholerae*. To understand the effect of the six DGCs on cell motility at low temperatures, we analyzed the motility phenotype of each mutant at 15°C on LB motility plates. While Δ*cdgH*, Δ*cdgK*, Δ*cdgL* and Δ*vpvC* mutants exhibited an increase in migration (Fig. 6A), Δ*cdgA* and Δ*cdgM*, and did not show a major difference in migration compared to wild type. In previous studies performed at 30°C, Δ*cdgH*, Δ*cdgK* and Δ*cdgL* exhibited increased motility however a Δ*vpvC* mutant did not (Liu, 2010), indicating the increase in motility in Δ*vpvC* is low-temperature specific. All strains harboring their respective complementation plasmids exhibited decreased motility compared to the same strains carrying vector only ($P < 0.05$) (Fig. 6A). This outcome further supports that all the above-mentioned DGCs were active at 15ºC and able to produce c-di-GMP. We also analyzed the motility phenotype of wild type harboring a plasmid where expression of *cdgA*, *cdgH*, *cdgK*, *cdgL*, *cdgM*, or *vpvC* was controlled from an arabinose-inducible promoter at 37°C and 15°C. At 37°C, wild type harboring p*cdgA*, p*cdgH*, p*cdgK*, and *cdgL* exhibited a decrease in motility compared to vector only ($P < 0.005$), while *pcdgM* and p*vpvC* did not (Fig. 6B). At 15°C, expression of each gene decreased motility when compared to vector only control ($P < 0.05$) (Fig. 6B and C). These results suggest that *cdgM* and *vpvC* affect motility specifically at low temperatures.

Figure 6. Motility in strains lacking DGCs (A) Diameters of migration zones of DGC deletion strains harboring pBAD or their respective complementation plasmid. Migration of Δ*cdgH,* Δ*cdgK,* Δ*cdgL,* and Δ*vpvC* were increased relative to wild type ($P < 0.05$) while *cdgA* and *cdgM* did not differ significantly. (B and C) Diameters of migration zones of wild-type *V. cholerae* harboring a pBAD plasmid where expression of *cdgA*, *cdgH*, *cdgK*, *cdgL*, *cdgM*, or *vpvC* is controlled from an arabinose-inducible promoter. Strains were grown on motility plates with 0.1% arabinose. The diameter of migration zones were measured after (B) 8 hours incubation at 37°C and (C) three days incubation at 15°C. The results represent an average of three biological replicates; error bars indicate standard deviations. *$P < 0.05$, ** $P < 0.005$, n.s., $P > 0.05$.

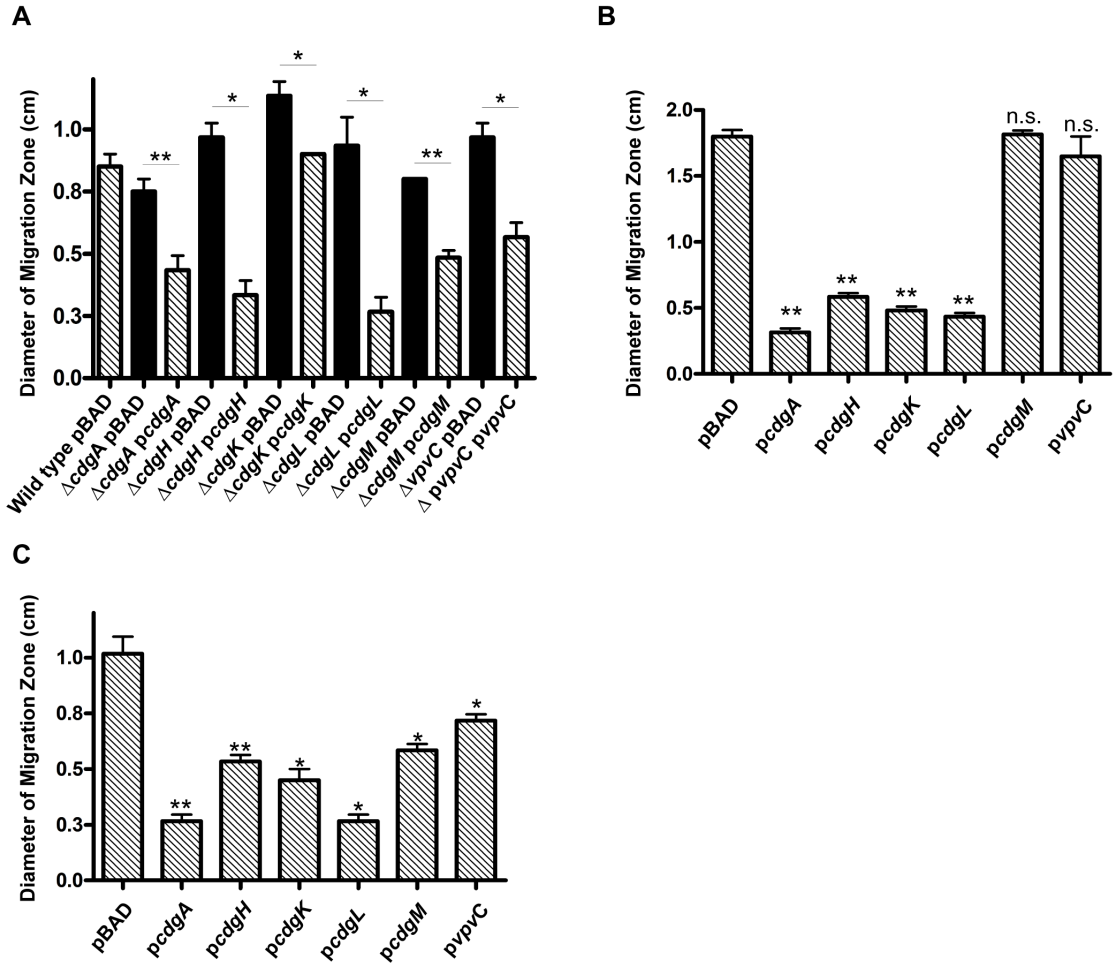
A
Diameter of Migration Zone (cm)
0.0
0.3
0.5
0.8
1.0
Wild type pBAD
ΔcdgA pBAD
ΔcdgA pcdgA
ΔcdgH pBAD
ΔcdgH pcdgH
ΔcdgK pBAD
ΔcdgK pcdgK
ΔcdgL pBAD
ΔcdgL pcdgL
ΔcdgM pBAD
ΔcdgM pcdgM
ΔvpvC pBAD
Δ pvpvC pvpvC
B
Diameter of Migration Zone (cm)
0.0
0.5
1.0
1.5
2.0
n.s.
n.s.
pBAD
pcdgA
pcdgH
pcdgK
pcdgL
pcdgM
pvpvC
C
Diameter of Migration Zone (cm)
0.0
0.3
0.5
0.8
1.0
pBAD
pcdgA
pcdgH
pcdgK
pcdgL
pcdgM
pvpvC

Identification of PDEs that control vps expression and biofilm formation at low temperatures

Having identified DGCs that contribute to *vps* gene expression and biofilm formation, we also entertained the possibility that at low temperatures a decrease in PDE activity or abundance could also modulate cellular c-di-GMP levels, and in turn *vps* expression and biofilm formation. To identify specific PDEs that regulate low-temperature-induced biofilm formation, we measured *vpsL* expression in the 22 strains containing in-frame deletions of each gene encoding a protein with a predicted EAL, or GGDEF and EAL domain (Supplementary Fig.1). A total of three mutants, Δ*cdgC* (VCA0785), Δ*cdgJ* (VC0137), and Δ*rocS* (VC0653) were found to exhibit an over 2-fold increase in *vpsL* expression compared to wild type ($P < 0.05$) (Fig. 7A). We also observed that a set of mutants ΔVC0398, ΔVC0658, ΔVC1934, ΔVC2750, and ΔVCA0080 exhibited over 2-fold decrease in *vpsL* expression. However, for this study, we focused only on the strains that exhibited an increase in *vpsL* expression. We also generated a Δ3 PDE mutant with deletions in Δ*cdgC*, Δ*cdgJ*, and Δ*rocS*. The Δ3 PDE mutant exhibited 13-fold higher *vpsL* expression when compared to wild type ($P < 0.05$) (Fig. 7A).

Figure 7. Phenotypic analysis of PDEs mutants (A) *vpsL* expression (B) pellicle and colony morphology and (C) biofilm formation of wild-type *V. cholerae* and strains containing single in-frame deletions of genes encoding PDEs (*cdgC*, *cdgJ*, *rocS*) and a Δ3 PDE strain. Expression of *vpsL* and biofilm formation was analyzed in cells that were grown at 15°C for 24 hours. Colony morphology was evaluated after 48 h of growth on LB agar at room temperature. Scale bars in colony morphology and confocal images represent 1 mm and 40 μm respectively. (D) Schematic showing predicted domains for each PDE, black boxes represent predicted transmembrane domains within each protein.

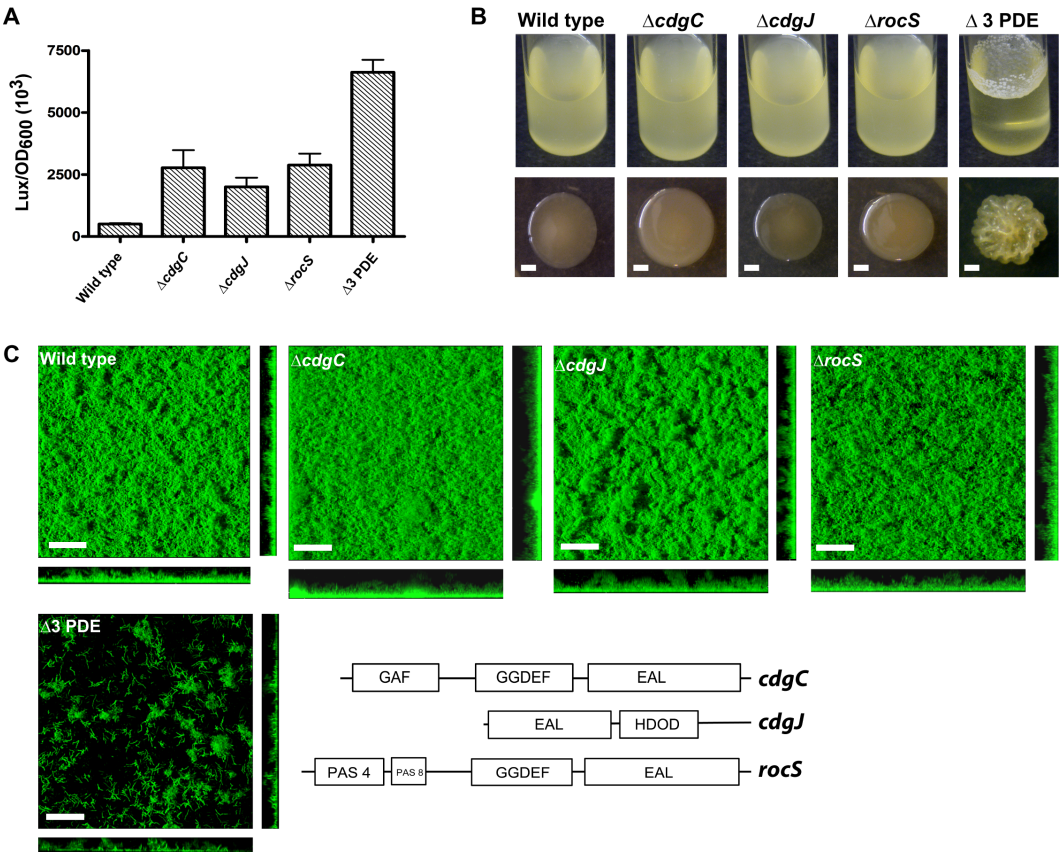

Typically, strains with enhanced biofilm matrix production are able to form pellicle biofilms at the air-liquid interface and corrugated colonies on agar plates. We analyzed pellicle formation and colony corrugation in Δ*cdgC*, Δ*cdgJ*, Δ*rocS*, and the Δ3 PDE mutant. We determined that single deletion mutants did not form pellicle biofilms or corrugated colonies, whereas the Δ3 PDE mutant did form both pellicle biofilms and corrugated colonies (Fig.7B) which is indicative of increased production of VPS and biofilm matrix proteins (Yildiz, 1999; Fong, 2007).

When we analyzed biofilm formation under static conditions using CSLM, Δ*cdgC,* Δ*cdgJ*, and Δ*rocS* mutants exhibited an increase in biofilm formation relative to wild type at 15°C (Fig. 7C and Table 3). The Δ3 PDE mutant exhibited a defect in biofilm formation at 15°C with a 5-fold decrease in biomass, a 4-fold decrease in average thickness, and a 1.3-fold increase in maximum thickness when compared to biofilms formed by the wild-type (Fig. 8C and Table 3). As discussed above the Δ3 PDE mutant has enhanced ability to form pellicles. When biofilms are formed under static conditions cells that are distributed between the air-liquid and solid-liquid interfaces; therefore biofilms imaged by CSLM at the solid-liquid interface may not be a true representation of the biofilm forming ability of the Δ3 PDE mutant. These results collectively show that these 6 DGCs and 3 PDEs are additively affecting *vps* gene expression and biofilm formation at low temperatures.

Analysis of the contribution of DGCs and PDEs for enhancement of c-di-GMP levels at low temperatures

To examine the contribution of the DGCs to the low-temperature induction of c-di-GMP, we first analyzed c-di-GMP levels in each of the DGC mutants grown at 15°C for 24 hours (Fig.8A). We determined that c-di-GMP levels in Δ*cdgA*, Δ*cdgH*, Δ*cdgK*, Δ*cdgL*, and Δ*cdgM* single deletion strains were approximately 1.5-fold lower that wild type ($P < 0.05$) when grown at 15°C for 24 hours; however, there was no decrease in c-di-GMP in the Δ*vpvC* mutant. In a Δ2 DGC strain lacking *cdgL* and *cdgM*, the strains with lowest *vpsL* expression at 15°C, we observed a 1.7-fold decrease ($P < 0.05$) and in a Δ6 DGC strain lacking all 6 DGCs a 2.1-fold decrease ($P < 0.005$) in c-di-GMP relative to that of wild type. c-di-GMP levels were not completely abolished in the Δ6 DGC strain, suggesting that under the conditions utilized in this study other DGCs could also contribute to c-di-GMP levels.

Figure 8. Analysis of c-di-GMP levels in DGC and PDE mutants of *V. cholerae* (A) c-di-GMP quantification of wild-type and strains containing in-frame deletions of DGCs grown at 15°C for 24 hours. (B) c-di-GMP quantification of *V. cholerae* wild-type and ∆3 PDE and ∆6 DGC strains grown at 37°C to an OD_{600} of 0.4 then shifted to 15°C for one hour. Error bars indicate standard deviations of four biological replicates. *P < 0.05, ** P < 0.005, n.s., P > 0.05.

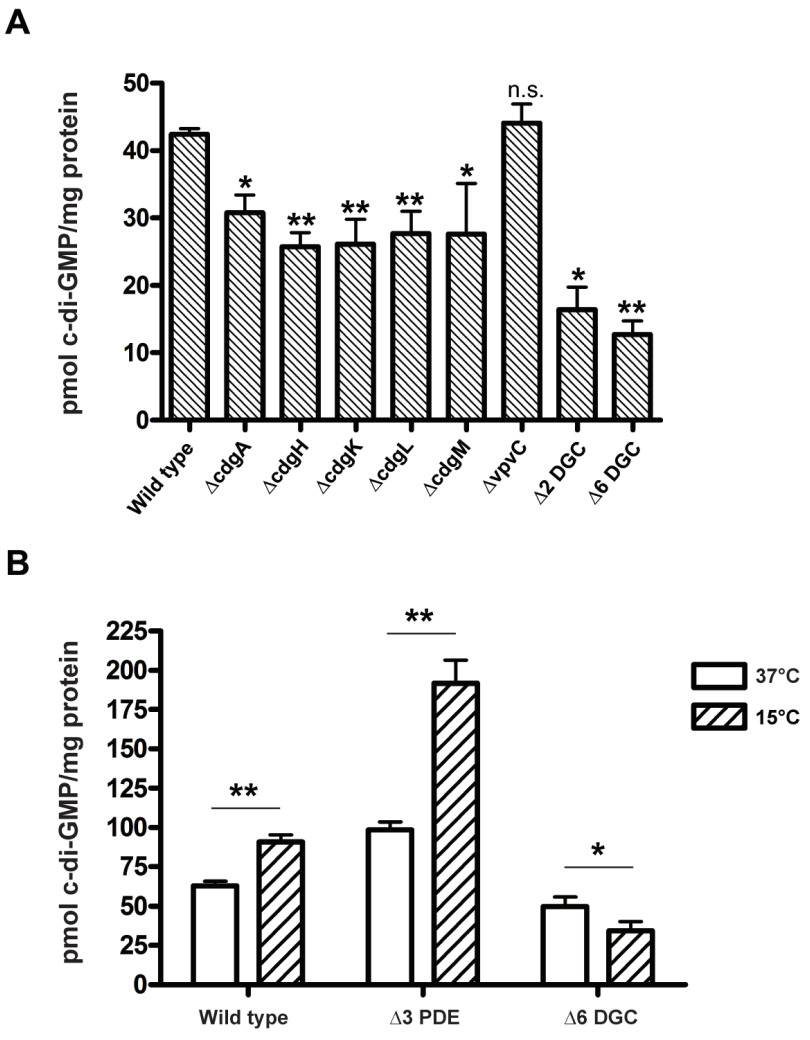

To determine if the DGCs discussed above are involved in the induction of c-di-GMP levels observed after shifting cells from 37°C to 15°C, we determined the amount of c-di-GMP produced by the ∆6 DGC strains under these conditions and compared them to wild type. Results showed that c-di-GMP levels in ∆6 DGC grown at 37°C were not significantly different than that of wild type ($P > 0.05$) (Fig. 8B). This suggests that these DGCs are not required to maintain the basal level of the c-di-GMP pool at 37°C. However, when the ∆6 DGC strain was shifted to 15°C c-di-GMP levels were not induced as observed in wild type, but instead reduced 1.5-fold ($P < 0.05$) (Fig. 8B). These results strongly suggest that these DGCs are required for increasing c-di-GMP in response to low temperatures. It is also possible that reduced phosphodiesterase activity might also contribute to the observed increase in c-di-GMP levels at low temperature. To explore this possibility we determined the c-di-GMP levels in the ∆3 PDE strain and found that they were 1.5-fold higher than wild type even before the shift (37°C) ($P < 0.05$), and 2-fold higher than wild type after the shift to 15°C ($P < 0.05$) (Fig. 7A). This indicates that these PDEs are not responsible for low temperature-mediated increase in c-di-GMP levels.

Analysis of DGCs expression

The increase in c-di-GMP levels observed at 15°C could be caused by an increase in the abundance or activity of these six DGCs. To determine if

expression of these genes is altered by growth at low temperatures or by temperature shift, we determined the transcript abundance for each gene using Real-Time PCR. First, we found that mRNA transcript levels of *cdgA, cdgH, cdgK, cdgL* and *cdgM* are increased 15.3, 6.1, 3.8, 3.4, and 7.2-fold ($P < 0.05$), respectively, after 24 hours of growth at 15°C compared to 37°C (Fig. 9A). However, levels of *vpvC* were not significantly different between these conditions (Fig. 9A). Next, we found that one hour after a shift from 37°C to 15°C expression of *cdgA* and *cdgM* was slightly increased 1.7 and 1.2 respectively ($P < 0.05$); however, transcript levels of *cdgH*, *cdgK*, *cdgL*, and *vpvC* were not increased (Fig. 9B) despite the increase of c-di-GMP levels at this time point. This suggests that post-transcriptional regulation is required for modulating c-di-GMP levels in response to temperature shift.

Figure 9. Comparison of DGC gene expression in *V. cholerae* grown at 37°C and 15°C Message levels of DGCs were determined by Real-Time PCR using total RNA isolated from wild-type *V. cholerae* grown in LB incubated at (A) 37°C and 15°C for 24 hours. Impact of low temperature shift on expression was analyzed using total RNA isolated from wild-type *V. cholerae* grown at (B) 37°C to 0.4 OD_{600} then shifted to 15 °C or maintained at 37 °C for one hour. The Pfaffl method was used to compare expression levels of each gene-of-interest to that of 16s rRNA, and relative expression was calculated by normalizing expression at 15°C by that at 37°C. **P* < 0.05, ** *P* < 0.005, n.s., *P* > 0.05.

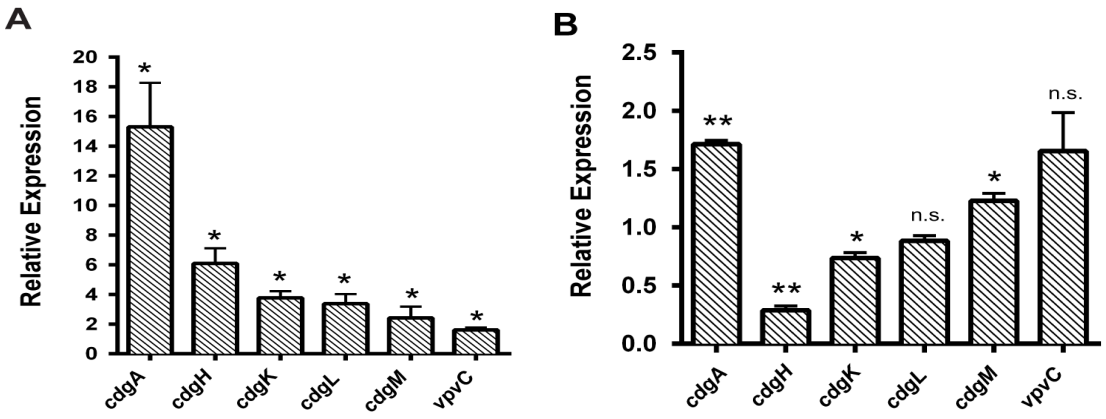

Effects of temperature on c-di-GMP signaling in other facultative pathogens

Because c-di-GMP is a ubiquitous signaling molecule in bacteria, and temperature changes are encountered by a wide variety of bacteria, we hypothesized that temperature might also affect c-di-GMP signaling in other facultative pathogens. We selected *P. aeruginosa* PAO1, a Gram-negative opportunistic pathogen that is ubiquitous in the environment and *L. monocytogenes,* a Gram-positive pathogen that is capable of growing at low temperatures. To test if c-di-GMP levels were affected by temperature in these two pathogens, cells were grown at 15°C, 25°C, and 37°C for 24 hours and c-di-GMP levels were quantified. Our results revealed that there was a significant increase in c-di-GMP levels at low temperatures in *P. aeruginosa* with 11.50 pmol/mg protein at 15°C, 2.07 pmol/mg protein at 25°C, and 3.15 pmol/mg protein at 37°C (Fig. 10A). Yet growth temperature did not have the same drastic effect on c-di-GMP levels in *L. monocytogenes* with 14.05 pmol/mg protein at 15°C, 16.63 pmol/mg protein at 25°C, and 13.78 pmol/mg protein at 37°C (Fig. 10B). These results indicate that c-di-GMP levels can be affected by temperature in other environmental pathogens but may vary between species.

Figure 10. Analysis of c-di-GMP levels in *P. aeruginosa* and *L. monocytogenes* grown at different temperatures (A) *P. aeruginosa* and (B) *L. monocytogenes* grown at 15°C, 25°C, and 37°C for 24 hours, c-di-GMP was extracted from whole cells and quantified using HPLC-MS/MS. Error bars indicate standard deviations of four biological replicates. *$P < 0.05$, ** $P < 0.005$, n.s., $P > 0.05$.

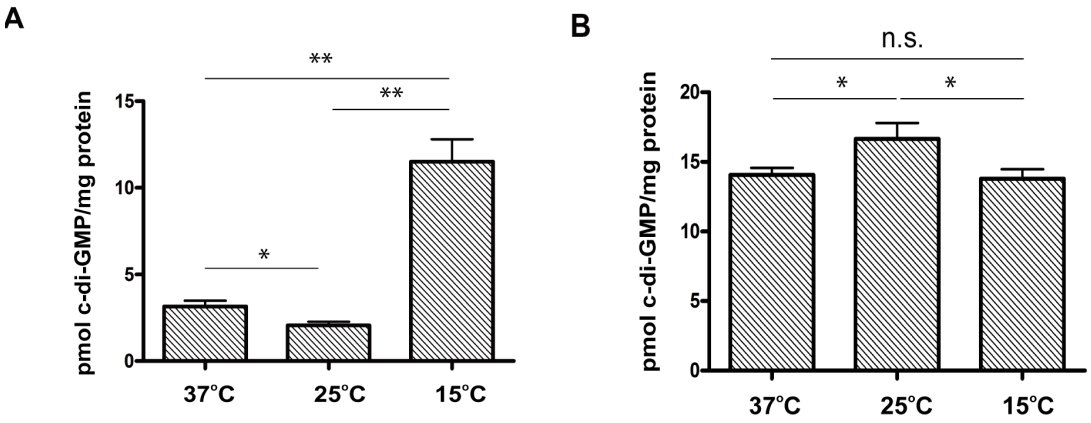

DISCUSSION

The objective of this study was to determine how temperature affects biofilm formation in *V. cholerae.* We determined that low temperature increases biofilm formation in part through increased cellular c-di-GMP levels. We found that six DGCs (*cdgA, cdgH, cdgK, cdgL, cdgM,* and *vpvC*) are required for a low-temperature increase in c-di-GMP levels and biofilm formation. Previous studies by our group have identified these DGCs to be important for c-di-GMP signaling and biofilm formation at 30°C in LB (Lim, 2006; Beyhan, 2006; Beyhan, 2007; Beyhan, 2008; Fong, 2008; Liu, 2010; Shikuma, 2012). Shikuma *et al* demonstrated that 5 of these 6 DGCs (*cdgA, cdgH, cdgK, cdgL, cdgM*) affect c-di-GMP levels when cultures are grown at 30°C (Shikuma, 2012) and contribute to *vps* gene expression by providing c-di-GMP pool necessary for activation of c-di-GMP sensor VpsT. In this study we showed that these 6 DGCs are critical for environmental regulation of c-di-GMP signaling and biofilm formation.

Cellular c-di-GMP levels could be controlled by changes in abundance of c-di-GMP metabolizing enzymes. Studies have shown that either transcription or translation of genes encoding c-di-GMP signaling enzymes could be modulated in response to environmental signals. In *E. coli*, transcription of genes encoding GGDEF/EAL domain proteins is increased at 28°C when compared to 37°C (Sommerfeldt, 2009). It has been previously documented

that translation of the DGC VCA0939 is activated through quorum sensing Qrr sRNA (Hammer, 2007; Zhao, 2013) demonstrating that DGC levels could be controlled post-transcriptionally under some conditions. Here we show that expression of 5 DGCs (*cdgA, cdgH*, *cdgK*, *cdgL* and *cdgM*) is increased in cells grown at 15°C for 24 hours. In contrast, short cold-shifts did not lead to a significant increase in transcription of four of these DGC genes. Surprisingly, mRNA message abundance of *cdgH* and *cdgK* was lower one hour after cold-shift. It is yet to be determined if translation of any of these genes or protein stability are impacted by growth temperature.

Cellular c-di-GMP levels could also be controlled by changes in the activities of DGCs upon environmental signal sensing. We observed that these DCCs differ in their ability to complement the biofilm phenotype of a Δ6 DGC strain at 15°C. This suggests that these DGCs may not be equally active at low temperatures, which was corroborated by our c-di-GMP measurements in the Δ6 DGC strain harboring over-expression plasmids of with each DGC. Alternatively, DGCs might contribute to an increase in the c-di-GMP pools locally or may not on their own surpass the threshold level of c-di-GMP necessary to rescue the biofilm defect in Δ6 DGC strain. The mechanisms responsible for the differences in activities of these DGCs is yet to be determined.

As mentioned above, four of these DGCs harbor a sensory input domains. These domains could potentially allow these DGCs to sense environmental signals like low temperature and modulate their activity accordingly, but another possibility is that these proteins sense temperature via their transmembrane domains. All 6 of the DGCs in this study contain transmembrane domains and are predicted to localize in the membrane. Studies of other bacteria have shown that membrane fluidity is affected by temperature (Cronan, 1975; Garwin, 1980; Aguilar, 2001; Zhu, 2005), which could be a means of integrating temperature sensing into the c-di-GMP network. Specialized sensing domains or changes to protein structure due to membrane fluidity could be important for relaying temperature signals to these DGCs. We are currently investigating how the activity of these DGCs is impacted by environmental signals.

At present we do not know if there are specific downstream effectors responsible for converting c-di-GMP levels to phenotypic outputs at low temperatures. It is likely that VpsT is required for integrating an increase in c-di-GMP levels to an increase in biofilm formation at low temperatures. Likewise, the effect on motility could be mediated at the transcriptional level by FlrA. It is also likely that a yet-to-be determined effector could work at the transcrional and/or potstranscriptonal level to relay the increase in c-di-GMP levels to the biofilm regulatory network at low temperatures.

Temperature affects biofilm formation in other bacteria such as *Staphylococcus epidermidis*, *E. coli*, *Legionella pneumophila*, and *Burkholderia pseudomallei* (Fitzpatrick, 2005; White-Ziegler, 2008; Piao, 2006; Ramli, 2012). The mechanism for temperature-mediated biofilm formation and the involvement of c-di-GMP in these microbes, however, has yet to be elucidated. In this study we revealed that c-di-GMP levels are also regulated by temperature in an opportunistic human pathogen, *P. aeruginosa*, indicating that integration of environmental signal perception to c-di-GMP signaling is a common phenomenon of bacteria. c-di-GMP levels were not as dramatically affected by growth temperature in the Gram-positive pathogen, *L. monocytogenes. L. monocytogenes* is able to grow at a wider temperature range than *V. cholerae*, therefore it is possible that the temperatures used in this study may not be broad enough to see an effect in this organism.

Our study demonstrates that temperature is a crucial environmental signal that modulates biofilm formation and c-di-GMP signaling in *V. cholerae*. Multiple DGCs modulate cellular c-di-GMP levels in response to low-temperature, which in turn increases biofilm formation and represses motility.

EXPERIMENTAL PROCEDURES

Bacterial strains and growth conditions

V. cholerae O1 El Tor A1552 was used as our wild-type strain. *E. coli* CC118λ*pir* and S17-1λ*pir* were used for cloning and conjugation, respectively. *P. aeruginosa* PAO1 and *L. monocytogenes* 10403S were used for experiments designed to determine temperature effect on c-di-GMP levels. Luria Bertani (LB) medium (1% tryptone, 0.5% yeast extract, 0.2M NaCl; pH 7.5) was used to grow all strains. Temperature-shift experiments were performed by inoculating overnight-grown cultures of *V. cholerae* in a 1:200 dilution in LB and incubating at 37°C until exponential phase (OD_{600}=0.4); cultures were then shifted to 15°C and 25°C for the time indicated. Constant temperature experiments were performed by inoculating overnight-grown cultures in a 1:200 dilution in LB followed by incubation at 15°C, 25°C, or 37°C for 24 hours. When needed, chloramphenicol was used at 5 μg/ml, and ampicillin and rifampicin were used at 100 μg/ml, except for biofilm complementation analysis where ampicillin was used at 25 μg/ml. L-arabinose was added to growth medium at a final concentration of 0.1% (wt/vol) for complementation and DGC activity experiments.

Plasmid Construction

Overexpression plasmids were constructed by cloning the open reading frame of each gene of interest into pBAD/Myc-His B (Invitrogen) using ligation-independent cloning (LIC) and sequenced by QB3 Macrolab (Berkeley, CA).

Generation of in-frame deletion mutants

Deletion mutants were generated using previously published protocols (Fong, 2006). Briefly, approximately 500 bp up and downstream of the gene of interest was amplified by PCR using two sets of deletion primers. These two PCR products were then joined via splicing by overlap extension PCR (Fong, 2006) and cloned into a pGP704-*sacB*28 suicide plasmid. The deletion plasmids were maintained in *E. coli* CC118 (λ *pir*). Biparental matings were carried out with *V. cholerae* A1552 and the conjugative strain *E. coli* S17-1 (*λ pir*) harboring the deletion plasmid. Ampicillin- and rifampin-resistant transconjugants, resulting from single homologous recombinations, were selected and subjected to sucrose-based selection. Ampicillin-sensitive and sucrose-resistant *V. cholerae* deletion strains, which had undergone double homologous recombinations, were selected and verified by PCR.

Generation of GFP-tagged strains.

V. cholerae strains were tagged with green fluorescent protein (GFP) according to the procedure previously described (Fong, 2006). Briefly,

triparental matings were carried out with donor *E. coli* S17-1 (λ *pir*) carrying pMCM11, helper *E. coli* S17-1 (λ *pir*) harboring pUX-BF13, and various *V. cholerae* strains. Transconjugants were selected on thiosulfate-citrate-bile salts-sucrose (Difco) agar medium containing gentamicin at 30°C. GFP-tagged *V. cholerae* strains were verified by PCR.

Biofilm Imaging

V. cholerae from overnight-grown cultures were diluted into LB broth to an OD_{600} of about 0.02, then 3 ml were inoculated into glass chambers (Lab-Tek) and incubated statically at 15°C, 25°C, or 37°C. After 24 hours, planktonic bacteria were removed by gently inverting the chambers and washed gently twice with LB. Biofilm formation was visualized using confocal laser-scanning microscopy (CLSM) with an LSM 5 Pascal laser-scanning microscope (Zeiss). Three-dimensional images were reconstructed using Imaris 7.6 and analyzed using COMSTAT (Heydorn, 2000). Each experiment included three independent biological replicates and three images were taken for each replicate.

Determination of intracellular c-di-GMP levels

c-di-GMP extraction was performed as described previously (Liu, 2010). Briefly, 40 ml of culture was centrifuged at 3220 *g* for 30 min. Cell pellets were allowed to dry briefly then re-suspended in 1 ml extraction solution (40%

acetonitrile, 40% methanol, 0.1% formic acid, 19.9% water), and incubated on ice for 5 min . Samples were then centrifuged at 16,100 *g* for 5 min and 800 µl of supernatant was dried under vacuum and then lyophilized. Samples were re-suspended in 50 µl of 184 mM NaCl and analyzed by liquid chromatography-tandem mass spectrometry (LC-MS/MS) on a Thermo-Electron Finnigan LTQ mass spectrometer coupled to a surveyor HPLC. The Synergin Hydro 4u Fusion-RP 80A column (150 mm x 2.00 mm diameter; 4-µm particle size) (Phenomenex, Torrance, CA) was used for reverse-phase liquid chromatography. Solvent A was 0.1% acetic acid in 10 mM ammonium acetate, solvent B was 0.1% formic acid in methanol. The gradient used was as follows: time (t) = 0-4 min, 98% solvent A, 2% solvent B; t = 10-15 minutes, 5% solvent A, 95% solvent B. The injection volume was 20 µl and the flow rate for chromatography was 200 µl/minutes.

The amount of c-di-GMP in samples was calculated with a standard curve generated from pure c-di-GMP suspended in 184 mM NaCl (Biolog Life Science Institute, Bremen, Germany). Concentrations used for standard curve generation were 50 nM, 100 nM, 500 nM, 2 µM, 3.5 µM, 5 µM, 7.5 µM, and 10 µM. The assay is linear from 50 nM to 10 µM with an R2 of 0.999. c-di-GMP levels were normalized to total protein per ml of culture.

To determine protein concentration, 4 ml from each culture was pelleted, the supernatant was removed, and cells were lysed in 1 ml of 2% sodium dodecyl

sulfate. Total protein in the samples was estimated with BCA assay (Thermo Fisher) using bovine serum albumin (BSA) as standards. Each c-di-GMP quantification experiment was performed with four biological replicates. Levels of c-di-GMP were compared between temperatures in *V. cholerae* and *P. aeruginosa* using a two-tailed student's *t* test. Levels of c-di-GMP in *L. monocytogenes* were compared between temperatures using the Mann Whitney U test.

Luminescence Assays

V. cholerae wild type, and DGD/PDE mutants harboring the *vpsL*-lux plasmid where grown overnight (15-17 hours) aerobically in LB supplemented with chloramphenicol. Cells were diluted 1:200 in LB + chloramphenicol and grown at 37°C until OD_{600}= 0.4, at which time cultures were shifted to 15°C. One hour after shift, luminescence was measured using a Victor3 Multi-label Counter (PerkinElmer) and is reported as counts min^{-1} ml^{-1}/ OD_{600}. Assays were repeated with at least two biological replicates for all 52 strains tested, and three biological replicates for the six DGC, three PDE, Δ6DGC, and Δ3PDE strains. Four technical replicates were measured for all assays. Statistical analysis was performed using two-tailed student's *t* test. All six DGC and three PDE strains exhibited a *P* value of < 0.05 when compared to wild type.

Motility Assays

LB soft-agar (0.3% agar) motility plates were used to determine motility phenotypes of each strain. Single colonies were stabbed into LB motility plates with and without 0.1% arabinose. Plates were incubated at 37°C for 8 hours or 15°C for 3 days at which time the diameter of the migration zone was measured. Assays were repeated with at least three biological replicates. Statistical analysis was performed using two-tailed student's *t* test.

Expression analysis - Real Time PCR

Total RNA was isolated from *V. cholerae* cells that were grown in LB either at 15°C or 37°C for 24 hours or from *V. cholerae* cells that were exposed to cold-shift. For this experiment overnight-grown cultures of *V. cholerae* were diluted 1:200 in LB and incubated at 37°C until exponential phase (OD_{600}=0.4); cultures were then shifted to 15°C or maintained at 37°C for one hour. 2 ml aliquots were collected by centrifugation, immediately resuspended in 1 ml of Trizol reagent (Invitrogen) and 0.2 ml of chloroform was added into each tube. Tubes were shaken, incubated at room temperature for 5 minutes and then centrifuged for 20 minutes at 12,000 g, 4°C. Aqueous layer was collected into a new tube. Isopropanol (250 µl) and 250 µl high salt solution (0.8 M Na-citrate, 1.2 M NaCl) was added and the suspension was incubated for 10 minutes at room temperature to precipitate the RNA. Isopropanol was removed by centrifugation for 30 minutes at 12,000 g, 4°C. Pellets were washed with 1 ml of 75% ethanol, and ethanol was

removed by centrifugation for 5 minutes at 7,500 g, 4°C. Pellets were dried at room temperature for 10 minutes. Dried pellets were then resuspended in nuclease-free water. To remove contaminating DNA, total RNA was incubated with TURBO DNase (Ambion), and the RNeasy Mini kit (QIAGEN) was used to clean up the RNA after DNase digestion.

cDNA was synthesized using iScript cDNG Synthesis Kit (Bio-Rad) from 1 µg of total RNA. Real-time PCR was performed using a Bio-Rad CFX1000 thermal cycler and Bio-Rad CFX96 real-time imager with specific primer pairs (designed within the coding region of the target genes) and SsoAdvanced SYBR green supermix (Bio-Rad). Results are from two independent experiments performed in triplicate. All samples were normalized to the expression of the housekeeping gene 16S using the Pfaffl method (Pfaffl, 2004). Relative expression was calculated by normalizing expression at 15°C by that at 37°C. Statistical analysis was performed using two-tailed student's *t* test.

ACKNOWLEDGEMENTS

This work was supported by a NIH grant AI102584 to F.H.Y. L. T. was supported in part by the National Human Genome Research Institute (NHGRI) funded Research Mentoring Institute (RMI) at UC Santa Cruz and the Eugene Cota-Robles (ECR) Fellowship. c-di-GMP quantification was performed at the UCSC Mass Spectrometry Facility, which is funded by NIH grant S10-RR20939 (MS equipment grant). We kindly thank Q. Zhang for help with the HPLC/MS-MS experiments and analysis. B. Abrams at the UCSC Microscopy center for help with confocal microscopy. V. Auerbuch for the *Listeria monocytogenes* 10403S strain. We also thank M. Gomelsy, K. Ottemann, M. Camps, J.N.C. Fong, D. Zamorano-Sanchez, and other members of the Yildiz group for helpful discussions and reading of this manuscript.

REFERENCES

Aquilar, P.S., Hernandez-Arriaga, A.M., Cybulski, L.E., Erazo, A.C. & de Mendoza, D. (2001) Molecular basis of thermosensing: a two component signal transduction thermometer in *Bacillus subtilis*. EMBO J.20: 1681–1691.

Alam M, Sultana M, Nair GB, Sack RB, Sack DA, Siddique AK, Ali A, Huq A, Colwell RR. (2006) Toxigenic *Vibrio cholerae* in the aquatic environment of Mathbaria, Bangladesh. Appl. Environ. Microbiol. 72: 2849– 2855.

Berk, V., Fong, J. C. N., Dempsey, G. T., Develioglu, O. N., Zhuang, X., Liphardt, J., Chu, S. (2012) Molecular architecture and assembly principles of *Vibrio cholerae* biofilms. Science. 337(6091): 236–9.

Beyhan S, Tischler AD, Camilli A, Yildiz FH (2006) Transcriptome and phenotypic responses of *Vibrio cholerae* to increased cyclic di-GMP level. J Bacteriol 188: 3600–3613.

Beyhan, S., Bilecen, K., Salama, S. R., Casper-Lindley, C., & Yildiz, F. H. (2007) Regulation of rugosity and biofilm formation in *Vibrio cholerae*: comparison of VpsT and VpsR regulons and epistasis analysis of *vpsT*, *vpsR*, and *hapR*. J Bacteriol. 189(2): 388–402.

Beyhan, S., Odell, L. S., & Yildiz, F. H. (2008) Identification and characterization of cyclic diguanylate signaling systems controlling rugosity in *Vibrio cholerae*. J Bacteriol. 190(22): 7392–405.

Chang, A. L., Tuckerman, J. R., Gonzalez, G., Mayer, R., Weinhouse, H., Volman, G., February, V. (2001) Phosphodiesterase A1, a Regulator of Cellulose Synthesis in *Acetobacter xylinum* , Is a Heme-Based Sensor. Biochemistry 40(12): 3420–3426.

Charles, R. C., & Ryan, E. T. (2011) Cholera in the 21st century. Curr Opin Infect Dis, 24(5): 472–7.

Cockerell, S. R., Rutkovsky, A. C., Zayner, J. P., Cooper, R. E., Porter, L. R., Pendergraft, S. S., & Karatan, E. (2014). *Vibrio cholerae* NspS, a homologue of ABC-type periplasmic solute binding proteins, facilitates transduction of polyamine signals independent of their transport. Microbiology, 160(5), 832-843.

Colwell RR, Huq A, Islam MS, Aziz KM, Yunus M, Khan NH, Mahmud A, Sack RB, Nair GB, Chakraborty J, Sack DA, Russek-Cohen E. (2003)

Reduction of cholera in Bangladeshi villages by simple filtration. Proc. Natl. Acad. Sci. U. S. A. 100: 1051–1055.

Cronan, J.E. Jr & Gelmann, E.P. (1975) Physical properties of membrane lipids: biological relevance and regulation. Bacteriol. Rev.39: 232–256.

Datta PP, Bhadra RK. (2003) Cold Shock Response and Major Cold Shock Proteins of *Vibrio cholerae*. Society. 69(11): 6361-6369.

Faruque, S. M., Albert, M. J., Mekalanos, J. J., Faruque, S. M., & Albert, M. J. (1998) Epidemiology, Genetics, and Ecology of Toxigenic *Vibrio cholerae* Epidemiology, Genetics, and Ecology of Toxigenic *Vibrio cholerae*. Microbiol Mol Biol Rev, 62(4): 1301–1314.

Faruque SM, Biswas K, Udden SM, Ahmad QS, Sack DA, Nair GB, Mekalanos JJ. (2006) Transmissibility of cholera: *in vivo*-formed biofilms and their relationship to infectivity and persistence in the environment. Proc. Natl. Acad. Sci. U. S. A. 103: 6350–6355.

Fitzpatrick, F., Humphreys, H., & O'gara, J. P. (2005) Evidence for low temperature regulation of biofilm formation in *Staphylococcus epidermidis*. J Med Microbiol. 54(Pt 5): 509–10.

Fong, J. C. N., Karplus, K., Schoolnik, G. K., Yildiz, F. H., (2006) Identification and Characterization of RbmA, a Novel Protein Required for the Development of Rugose Colony Morphology and Biofilm Structure in *Vibrio cholerae*. J Bacteriol. 188(3), 1049–1059.

Fong J.C. and Yildiz F.H. (2007) The *rbmBCDEF* Gene Cluster Modulates Development of Rugose Colony Morphology and Biofilm Formation in *Vibrio cholerae*. J Bacteriol. 189(6): 2319–2330.

Fong J.C. and Yildiz F.H. (2008) Interplay between cyclic AMP-cyclic AMP receptor protein and cyclic di-GMP signaling in *Vibrio cholerae* biofilm formation. J. Bacteriol. 190(20): 6646-6659.

Fong JC, Syed KA, Klose KE, Yildiz FH. (2010) Role of *Vibrio* polysaccharide(*vps*) genes in VPS production, biofilm formation and *Vibrio cholerae* pathogenesis. Microbiology 156: 2757–2769.

Galperin, M. Y., A. N. Nikolskaya, and E. V. Koonin. (2001) Novel domains of the prokaryotic two-component signal transduction systems. FEMS Microbiol. Lett. 203: 11-21.

Garwin, J.L., Klages, A.L. & Cronan, J.E. Jr. (1980) β-ketoacyl-acyl carrier protein synthase II of *Escherichia coli*. Evidence for function in the thermal regulation of fatty acid synthesis. J.Biol. Chem 255: 3263–3265.

Gil, A. I., Louis, V. R., Rivera, I. N. G., Lipp, E., Huq, A., Lanata, C. F., Colwell, R. R. (2004) Occurrence and distribution of *Vibrio cholerae* in the coastal environment of Peru. Environ Microbiol 6(7), 699–706.

Hammer, B. K., & Bassler, B. L. (2007). Regulatory small RNAs circumvent the conventional quorum sensing pathway in pandemic *Vibrio cholerae*. Proc Natl Acad Sci, 104(27), 11145-11149.

Harris, J. B., Larocque, R. C., Qadri, F., Ryan, E. T., & Calderwood, S. B. (2012) Cholera. Lancet Infect Dis 379(9835): 2466–2476.

Hasegawa, K., Masuda, S., & Ono, T. (2006) Light induced structural changes of a full-length protein and its BLUF domain in YcgF(Blrp), a blue-light sensing protein that uses FAD (BLUF). Biochemistry, 45(11): 3785–93.

Hengge, R. (2009) Principles of c-di-GMP signalling in bacteria. Nature Rev Microbiol 7(4), 263–73.

Heydorn, a, Nielsen, a T., Hentzer, M., Sternberg, C., Givskov, M., Ersbøll, B. K., & Molin, S. (2000) Quantification of biofilm structures by the novel computer program COMSTAT. Microbiology 146(10): 2395–407.

Hostacká, a, Ciznár, I., & Stefkovicová, M. (2010) Temperature and pH affect the production of bacterial biofilm. Folia Microbiol 55(1): 75–8.

Huq A, West PA, Small EB, Huq MI, Colwell RR. (1984) Influence of water temperature, salinity, and pH on survival and growth of toxigenic *Vibrio cholerae* serovar O1 associated with live copepods in laboratory microcosms. Appl. Environ. Microbiol. 48: 420–424.

Huq A, Xu B, Chowdhury MA, Islam MS, Montilla R, Colwell RR. (1996) A simple filtration method to remove plankton-associated *Vibrio cholerae* in raw water supplies in developing countries. Appl. Environ. Microbiol. 62: 2508–2512.

Huq, A., Sack, R. B., Nizam, A., Longini, I. M., Nair, G. B., Ali, A., Colwell, R. R. (2005). Critical Factors Influencing the Occurrence of *Vibrio cholerae* in the Environment of Bangladesh. Appl Environ Microbiol. 71(8): 4645-54

Ishitsuka, Y., Araki, Y., Tanaka, A., Igarashi, J., Ito, O., & Shimizu, T. (2008). Arg97 at the heme-distal side of the isolated heme-bound PAS domain of a heme-based oxygen sensor from *Escherichia coli* (Ec DOS) plays critical roles in autoxidation and binding to gases, particularly O2. Biochemistry 47(34): 8874–84.

Kanazawa, T., Ren, S., Maekawa, M., Hasegawa, K., Arisaka, F., Hyodo, M., Masuda, S. (2010) Biochemical and physiological characterization of a BLUF protein-EAL protein complex involved in blue light-dependent degradation of cyclic diguanylate in the purple bacterium *Rhodopseudomonas palustris*. Biochemistry 49(50): 10647–55.

Karatan, E., Duncan, T. R., Watnick, P. I. (2005) NspS, a Predicted Polyamine Sensor, Mediates Activation of *Vibrio cholerae* Biofilm Formation by Norspermidine. J Bacteriol. 187(21): 7434-43.

Kitanishi, K., Kobayashi, K., Kawamura, Y., Ishigami, I., Ogura, T., Nakajima, K., Shimizu, T. (2010) Important roles of Tyr43 at the putative heme distal side in the oxygen recognition and stability of the Fe(II)-O2 complex of YddV, a globin-coupled heme-based oxygen sensor diguanylate cyclase. Biochemistry 49(49): 10381–93.

Koestler, B. J., & Waters, C. M. (2013) Exploring environmental control of cyclic di-GMP signaling in *Vibrio cholerae* by using the ex vivo lysate cyclic di-GMP assay (TELCA). Appl Environ Microbiol 79(17): 5233–41.

Koestler, B. J., & Waters, C. M. (2014) Bile Acids and Bicarbonate Inversely Regulate Intracellular Cyclic di-GMP in *Vibrio cholerae*. Infect and Immun 82(7): 3002–3014.

Krasteva, P. V., J. C. Fong, N. J. Shikuma, S. Beyhan, M. V. Navarro, F. H. Yildiz, and H. Sondermann. (2010) *Vibrio cholerae* VpsT regulates matrix production and motility by directly sensing cyclic di-GMP. Science 327:866-868.

Lim, B., Beyhan, S., Meir, J., & Yildiz, F. H. (2006). Cyclic-diGMP signal transduction systems in *Vibrio cholerae*: modulation of rugosity and biofilm formation. Mol Microbiol, 60(2), 331-348.

Liu, X., Beyhan, S., Lim, B., Linington, R. G., & Yildiz, F. H. (2010). Identification and characterization of a phosphodiesterase that inversely regulates motility and biofilm formation in *Vibrio cholerae.* J Bacteriol 192(18), 4541-4552.

Nelson, E. J., Harris, J. B., Morris, J. G., Calderwood, S. B., & Camilli, A. (2009) Cholera transmission: the host, pathogen and bacteriophage dynamic. Nature Rev Microbiol 7(10): 693–702.

Parkinson, J. S. (2010). Signaling mechanisms of HAMP domains in chemoreceptors and sensor kinases. Annu Rev Microbiol, 64, 101-122.

Pfaffl, M.W. (2001) A new mathematical model for relative quantification in real-time RT–PCR. Methods 50: 215–216.

Piao, Z., Sze, C. C., Barysheva, O., Piao, Z., Sze, C. C., Barysheva, O., Yoshida, S. (2006) Temperature-Regulated Formation of Mycelial Mat-Like Biofilms by *Legionella pneumophila*. Appl Environ Microbiol 72(2): 1613-22.

Plate, L., & Marletta, M. A. (2012). Nitric oxide modulates bacterial biofilm formation through a multicomponent cyclic-di-GMP signaling network. Mol Cell, 46(4), 449-460.

Pratt, J. T., R. Tamayo, A. D. Tischler, and A. Camilli. (2007) PilZ domain proteins bind cyclic diguanylate and regulate diverse processes in *Vibrio cholerae*. J. Biol. Chem. 282: 12860-12870.

Qi, Y., Rao, F., Luo, Z., & Liang, Z.-X. (2009) A flavin cofactor-binding PAS domain regulates c-di-GMP synthesis in AxDGC2 from *Acetobacter xylinum*. Biochemistry 48(43): 10275–85.

Ramli, N. S. K., Eng Guan, C., Nathan, S., & Vadivelu, J. (2012) The effect of environmental conditions on biofilm formation of *Burkholderia pseudomallei* clinical isolates. PloS one 7(9): e44104.

Romling, U., Sierralta, W.D., Eriksson, K., *and* Normark, S. *(*1998*)* Multicellular and aggregative behaviour of *Salmonella typhimurium* strains is controlled by mutations in the agfD promoter. *Mol Microbiol* **28***:* 249–264.

Römling, U., Galperin, M. Y., & Gomelsky, M. (2013) Cyclic di-GMP: the first 25 years of a universal bacterial second messenger. Microbiology and Molecular Biology Reviews: MMBR, 77(1): 1–52.

Ryan, R. P., Y. Fouhy, J. F. Lucey, L. C. Crossman, S. Spiro, Y. W. He, L. H. Zhang, S. Heeb, M. Camara, P. Williams, and J. M. Dow. 2006. Cell-cell signaling in *Xanthomonas campestris* involves an HD-GYP domain protein that functions in cyclic di-GMP turnover. Proc. Natl. Acad. Sci. U. S. A. 103: 6712-6717.

Ryjenkov, D. A., M. Tarutina, O. V. Moskvin, and Gomelsky M. (2005) Cyclic diguanylate is a ubiquitous signaling molecule in bacteria: insights into biochemistry of the GGDEF protein domain. J. Bacteriol. 187: 1792-1798.

Schaller, R. a, Ali, S. K., Klose, K. E., & Kurtz, D. M. (2012) A bacterial hemerythrin domain regulates the activity of a *Vibrio cholerae* diguanylate cyclase. Biochemistry, 51(43): 8563–70.

Schmidt, A. J., D. A. Ryjenkov, and Gomelsky M. (2005) The ubiquitous protein domain EAL is a cyclic diguanylate-specific phosphodiesterase: enzymatically active and inactive EAL domains. J. Bacteriol. 187: 4774-4781.

Shikuma, N. J., Fong, J. C. N., & Yildiz, F. H. (2012) Cellular levels and binding of c-di-GMP control subcellular localization and activity of the *Vibrio cholerae* transcriptional regulator VpsT. PLoS pathogens, 8(5): e1002719.

Sommerfeldt, N., Possling, A., Becker, G., Pesavento, C., Tschowri, N., & Hengge, R. (2009) Gene expression patterns and differential input into curli fimbriae regulation of all GGDEF/EAL domain proteins in *Escherichia coli*. Microbiology 155(4): 1318–31.

Sondermann, H., Shikuma, N. J., & Yildiz, F. H. (2012). You've come a long way: c-di-GMP signaling. Curr Opin Microbiol, 15(2), 140-146.

Srivastava, D., Harris R. C., Waters, C. M. (2011) Integration of cyclic di-GMP and quorum sensing in the control of *vpsT* and *aphA* in *Vibrio cholerae* J. Bacteriol. 193(22): 6331-6341.

Srivastava, D., & Waters, C. M. (2012) A tangled web: regulatory connections between quorum sensing and cyclic Di-GMP. J. Bacteriol. 194(17): 4485–93.Srivastava, D., Hsieh ML, Khataokar A., Neiditch M. B., Waters C. M. (2013) Cyclic di-GMP inhibits *Vibrio cholera* motility by repressing induction of transcription and inducing extracellular polysaccharides. Mol Microbiol. 90(6):1262-76.

Stauder, M., Vezzulli, L., Pezzati, E., Repetto, B., & Pruzzo, C. (2010) Temperature affects *Vibrio cholerae* O1 El Tor persistence in the aquatic environment via an enhanced expression of GbpA and MSHA adhesins. Environ Microbiol Rep 2(1): 140–4.

Sudarsan, N., E. R. Lee, Z. Weinberg, R. H. Moy, J. N. Kim, K. H. Link, and R. R. Breaker. (2008) Riboswitches in eubacteria sense the second messenger cyclic di-GMP. Science 321: 411-413.

Tam, R., & Saier, M. H. (1993). Structural, functional, and evolutionary relationships among extracellular solute-binding receptors of bacteria. Microbiol Rev 57(2), 320-346.

Tamayo R, Schild S, Pratt JT, Camilli A (2008) Role of cyclic di-GMP during el tor biotype *Vibrio cholerae* infection: characterization of the in vivo-induced cyclic di-GMP phosphodiesterase CdpA. Infect Immun 76: 1617–1627

Tamayo R, Patimalla B, Camilli A. (2010) Growth in a biofilm induces a hyperinfectious phenotype in *Vibrio cholerae*. Infect Immun 78: 3560–3569.

Tischler, A. D., & Camilli, A. (2004) Cyclic diguanylate (c-di-GMP) regulates *Vibrio cholerae* biofilm formation. Mol Microbiol 53(3): 857–69.

Tschowri, N., Busse, S., & Hengge, R. (2009) The BLUF-EAL protein YcgF acts as a direct anti-repressor in a blue-light response of *Escherichia coli*. Genes Dev 23(4): 522–34.

Turner, J. W., Malayil, L., Guadagnoli, D., Cole, D., & Lipp, E. K. (2013) Detection of *Vibrio parahaemolyticus*, *Vibrio vulnificus* and *Vibrio cholerae* with respect to seasonal fluctuations in temperature and plankton abundance. Environ Microbiol (4):1019-28.

Wan, X., Tuckerman, J. R., Saito, J. a, Freitas, T. A. K., Newhouse, J. S., Denery, J. R., Alam, M. (2009) Globins synthesize the second messenger bis-(3'-5')-cyclic diguanosine monophosphate in bacteria. J Mol Biol 388(2): 262–70.

Waters, C. M., W. Lu, J. D. Rabinowitz, and B. L. Bassler. (2008) Quorum sensing controls biofilm formation in *Vibrio cholerae* through modulation of cyclic di-GMP levels and repression of *vpsT*. J. Bacteriol. 190: 2527-2536.

White-Ziegler, C. a, Um, S., Pérez, N. M., Berns, A. L., Malhowski, A. J., & Young, S. (2008) Low temperature (23 degrees C) increases expression of biofilm-, cold-shock- and RpoS-dependent genes in *Escherichia coli* K-12. Microbiology 154(1): 148–66.

Wu, C., Cheng, Y.-Y., Yin, H., Song, X.-N., Li, W.-W., Zhou, X.-X., Yu, H.-Q. (2013) Oxygen promotes biofilm formation of *Shewanella putrefaciens* CN32 through a diguanylate cyclase and an adhesin. Sci Rep 3.

Yildiz, F.H., and Schoolnik, G.K. (1999) Vibrio cholerae O1 El Tor: Identification of a gene cluster required for the rugose colony type,

exopolysaccharide production, chlorine resistance, and biofilm formation. Proc Natl Acad Sci 96: 4028–4033.

Yildiz, F.H., Liu X.S., Heydorn A., Schoolnik G.K. (2004) Molecular analysis of rugosity in a *Vibrio cholerae* O1 El Tor phase variant. Mol. Microbiol. 53:497-515.

Yildiz, F. H., & Visick, K. L. (2009). Vibrio biofilms: so much the same yet so different. Trends Microbiol 17(3), 109-118.

Zhao, X., Koestler, B. J., Waters, C. M., & Hammer, B. K. (2013). Post-transcriptional activation of a diguanylate cyclase by quorum sensing small RNAs promotes biofilm formation in *Vibrio cholerae*. Mol Microbiol, 89(5), 989-1002.

Zhu J., Mekalanos J.J. (2003) Quorum sensing-dependent biofilms enhance colonization in *Vibrio cholerae.* Dev. Cell 5: 647-656.

Zhu, K., Bayles, D.O., Xiong, A., Jayaswal, R.K. & Wilkinson, B.J. (2005) Precursor and temperature modulation of fatty acid composition and growth of *Listeria monocytogenes* cold-sensitive mutants with transposon-interrupted branched-chain α-ketoacid dehydrogenase. Microbiology 151: 615–623.

Supplementary Fig. 1 Townsley and Yildiz

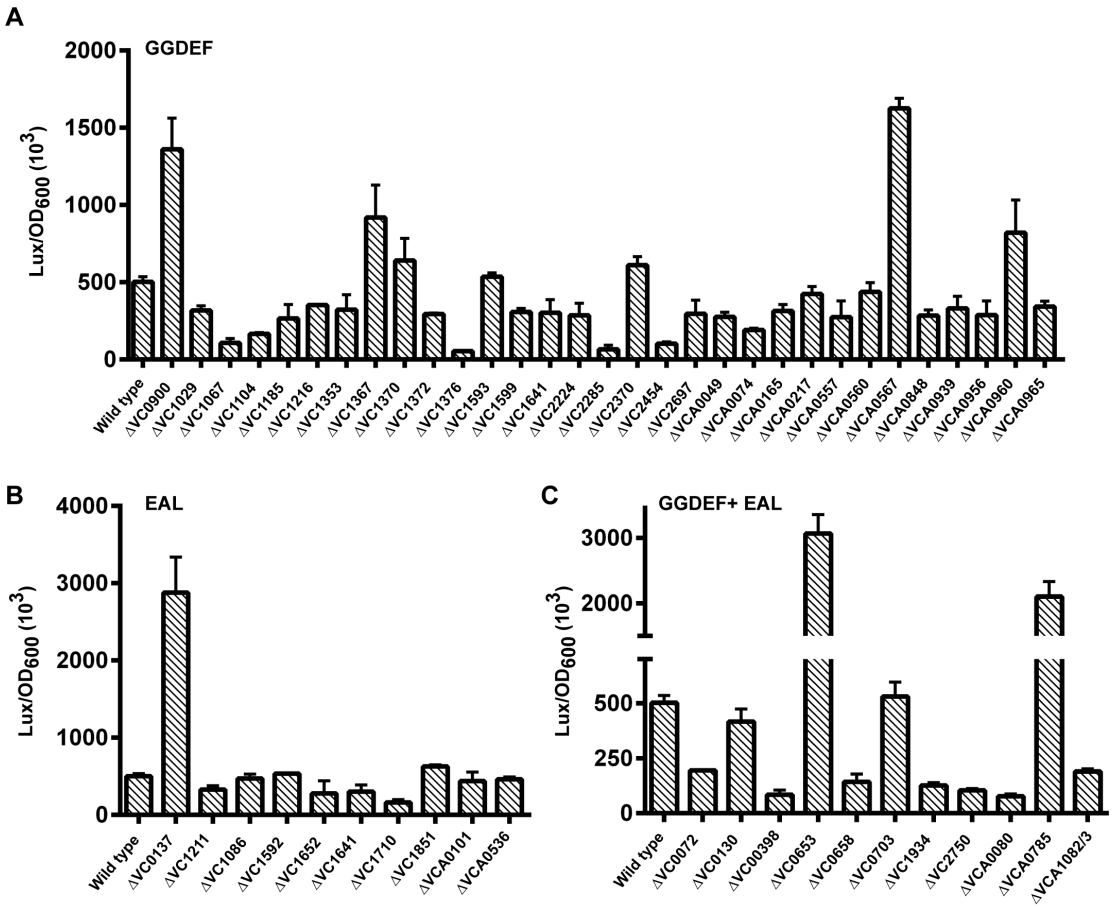

Chapter 3: Cold shock gene *cspV* regulates type VI secretion and biofilm formation in *Vibrio cholerae*

Loni Townsley, Sanjin Mehic, Marilou Sison Mangus, and Fitnat H Yildiz

ABSTRACT

The ability to sense and adapt to temperature fluctuation is critical to the aquatic survival, transmission, and infectivity of *Vibrio cholerae*, the causative agent of cholera. We determined the genome-wide transcriptional profile of *V. cholerae* upon shift from human body temperature (37°C) to lower temperatures, 15°C and 25°C, which mimic environmental temperatures. Genes involved in the cold shock response, biofilm formation, type VI secretion, and virulence were differentially regulated upon shifts from 37°C to 15°C or 25°C. Characterization of a mutant lacking the cold shock gene, *cspV*, whose expression was induced over 50-fold upon temperature down-shift to 15°C, revealed that *cspV* regulates the transcription of genes involved in biofilm matrix production and type VI secretion. We determined that *cspV* controls biofilm formation through modulation of the second messenger c-di-GMP, and also regulates type VI-mediated inter-species killing in a temperature dependent manner. A strain lacking *cspV* had a significant defect for the colonization of the aquatic crustacean *Daphnia magna* when compared with wild type. Type VI-mediated killing was significantly decreased in the *cspV* mutant on the surface of live *D. magna*. Attachment of *V. cholerae* to plankton is important for its survival, dissemination and transmission. Collectively these studies reveal that *cspV* is a major regulator of the temperature down-shift response and plays an important role in

controlling cellular processes crucial to the environmental survival and infectious cycle of *V. cholerae.*

INTRODUCTION

Vibrio cholerae is the facultative human pathogen responsible for the diarrheal disease cholera. Between epidemics, *V. cholerae* is found in aquatic reservoirs such as estuaries, coastal waters, and fresh water lakes and rivers where it is exposed to seasonal and inter-annual fluctuations in temperature (Alam et al., 2006; Faruque et al., 1998; Lipp et al., 2002). Multiple studies have demonstrated a significant positive correlation between the occurrence of *V. cholerae* and surface water temperature in a variety of aquatic environments (Baffone et al., 2006; Gil et al., 2004; Huq et al., 2005a; Lipp et al., 2003; Louis et al., 2003; Turner et al., 2014). Furthermore, surveillance of cholera outbreaks in rural, geographically separated areas in Bangladesh and along the coast of Peru, where cholera is endemic, have revealed a significant correlation between cases of the disease cholera and elevated sea surface temperatures (Gil et al., 2004; Huq et al., 2005; Turner et al., 2009). In addition to temperature fluctuation in the environment, *V. cholerae* must also endure a drastic shift in temperature during the transition between the human host and the environment. Aquatic habitats where cholera is endemic exhibit a temperature range of about 12 °C to 30°C, whereas the human host environment is a constant 37 °C (Gil et al., 2004).

Temperature is hypothesized as a key signal to differentiate between host and environment, facilitating virulence factor expression in the human host and genes associated with environmental survival upon expulsion. While studies aimed at understanding the importance of temperature up-shift in *V. cholerae* have shed light on mechanisms crucial to the survival of this pathogen inside the human host (Parsot & Mekalanos, 1990; Weber et al., 2014), less information is available regarding how *V. cholerae* survive and adapt to the down-shift in temperature the pathogen experiences upon exiting the human host and entry into the environment.

Low-temperature environments impose numerous challenges to bacterial cell physiology. As temperatures decrease, the lipid composition of the cell membrane transitions from its usual liquid crystalline state to a more rigid gel state (Hébraud & Potier, 1999; Phadtare & Inouye, 2004). Translation is impeded as low temperature causes poor ribosome assembly and the formation of extensive RNA secondary structures (Chen & Shakhnovich, 2010; Tinoco et al., 1999; Phadtare et al., 2004). In response to a shift to low-temperatures in *E. coli,* the bacterium up-regulates sgenes that encode for proteins involved in ribosome function, helicase activity, exoribonuclease activity, and cold shock proteins (Phadtare et al., 2004). Cold shock proteins (often) act as RNA chaperones, and are predicted to counteract the wide-spread effects of RNA secondary structure stabilization (Phadtare & Severinov, 2010; Rodrigues & Tiedje, 2008). In *E. coli*, the cold shock

domain of the CspA protein binds co-operatively to single-stranded DNA and RNA without sequence specificity (Schindelin et al., 1994; Wang et al., 1999). A previous study identified two cold shock proteins, CspA and CspV, which are highly induced when exponentially growing *V. cholerae* were shifted from 37°C to lower temperatures (Datta & Bhadra, 2003). Yet, despite its significant influence on the life cycle of *V. cholerae* little is known about how these proteins and low-temperature shifts affect the physiology and cellular processes of this pathogen.

Biofilm formation, a cellular process critical for the infection cycle of *V. cholerae* is regulated by temperature (Townsley & Yildiz, 2015). Biofilms are cell aggregates or surface-attached bacterial communities enclosed in an extracellular matrix. In the non-host environment, *V. cholerae* forms biofilms on the surfaces of plankton that greatly increases the survival of this pathogen and facilitates dissemination by increasing the chance of exposure to human hosts (Broza et al., 2008; Colwell et al., 2003; Huq et al., 1983; Nahar et al., 2012). Additionally, biofilm-like aggregates of *V. cholerae* have been found in the surface waters of Bangladesh in a partially dormant 'conditionally viable' state (Faruque et al., 2006). *V. cholerae* biofilms have been shown to be more infectious than their planktonic counterparts, on a per cell basis (Tamayo et al., 2010). These studies thus show that *V. cholerae* is often found in biofilms in the environment, and the biofilm form both survives better and is highly infections.

Biofilm cells are surrounded by extracellular matrix. The extracellular matrix of *V. cholerae* is composed of VPS (*Vibrio* polysaccharides) (Fong et al., 2010; Yildiz & Schoolnik, 1999) and matrix proteins, *rbmA*, *rbmC*, and Bap1 (Fong et al., 2006; Fong & Yildiz, 2007). The *vps*-I (*vpsU-K*) and *vps*-II (*vpsL-Q*) operons are responsible for biosynthesis of VPS and required for mature biofilm formation (Yildiz, & Schoolnik, 1999; Fong et al., 2010). Transcriptional regulation of biofilm genes is controlled by activators AphA, VpsR, and VpsT, and the repressor HapR. Response regulators VpsR and VpsT bind the *vps* promoter directly (Zamorano-Sánchez et al., 2015) while AphA, which is a transcriptional activator of virulence, affects biofilm formation through *vpsT* (Yang et al., 2010). Transcription of the genes that encode VPS and the matrix proteins is increased when levels of the intracellular messenger, cyclic diguanylate (c-di-GMP) are high (Beyhan et al., 2006; Tischler & Camilli, 2004) as DNA binding ability and activity of VpsT is dependent on c-di-GMP. HapR is the master quorum sensing regulator that represses biofilm formation at high cell density through direct binding of the *vps* regulatory region and *vpsT* (Waters et al., 2008).

The type VI secretion system (T6SS) is important for interspecies competition (Basler et al., 2013), virulence (Pukatzki et al., 2006), and natural transformation (Borgeaud et al., 2015) in *V. cholerae*. The T6SS can deliver effector proteins into neighboring cells in a contact-dependent manner (Ho et al., 2014; Silverman & Brunet, 2012). Effectors in *V. cholerae* include; VrgG1

and VrgG3 (valine-glycine repeat protein G), which have actin cross-linking activity and peptidoglycan-degrading activity, respectively (Brooks et al., 2013; Dong et al., 2013; Ma et al., 2009; Pukatzki et al., 2007); TseL, which exhibits lipase activity (Dong et al., 2013; Russell et al., 2013); and VasX, which perturbs the cytoplasmic membrane of target cells (Dong et al., 2013; Miyata et al., 2013). Corresponding immunity proteins, TsiV3, TsiV1, and TsiV2, provide protection by antagonizing effector activity (Dong et al., 2013; Unterweger et al., 2014). The T6SS apparatus includes a base that spans the cell envelope, an inner tube composed of polymers of the hemolysin coregulated protein (Hcp), and an outer contractile sheath that is formed by polymers of VipA and VipB (Basler et al., 2012; Pukatzki et al., 2007). The genes encoding the T6SS components are organized into one large cluster (VCA0105-VCA0124) and two auxiliary clusters (VCA0017-VCA0022 and VC1415-VC1421) (Pukatzki et al., 2006; Zheng et al, 2011). The T6SS genes are positively regulated by HapR and the global regulator cyclic AMP (cAMP) receptor protein CRP, and transcriptional regulator VasH and negatively regulated by the quorum sensing regulator LuxO and global regulator TsrA, which is homologous to the heat-stable nucleoid-structuring protein (H-NS) (Ishikawa et al., 2009; Kitaoka et al., 2011; Zheng et al., 2010). Additionally, a recent study reported that T6SS genes are induced on chitinous surfaces through competence regulators, Tfox and QstR (Borgeaud et al., 2015), suggesting that T6SS might be important during the environmental phase of

V. cholerae's life cycle. Previous studies have also indicated that T6SS may be affected by temperature in *V. cholerae* (Ishikawa et al., 2012); however, it remains unclear if temperature impacts inter-species killing.

In this study, we identified V. cholerae genes that are temperature regulated by examination of the genome-wide transcriptional profile of *V. cholerae* upon a shift from high temperature (37°C) to low temperatures (15°C and 25°C). We found that the expression of genes encoding cold-shock proteins, pathogenesis, biofilm formation and type VI secretion system (T6SS) were differentially regulated upon cold-shift. Follow up experiments confirmed that each of these cellular processes are affected by temperature. Mutational analysis and phenotypic characterization of the most highly induced gene, *cspV*, revealed that this cold shock gene affects biofilm formation and type VI secretion in *V. cholerae.* Furthermore, a *cspV* mutant had a significant defect in colonizing the chitinous zooplankton *Daphnia magna* and T6SS-mediated killing of *Aeromonas sp.* attached to *D. magna.*

RESULTS

Transcriptional profile upon cold-shift

Temperature is an important signal that can be used by *V. cholerae* to distinguish between the human host and the environment. To better understand how *V. cholerae* responds to temperature downshift, *V. cholerae* was grown in LB medium at human body temperature (37°C) until mid-

exponential phase then shifted to 15°C or 25°C for 1h. RNA was harvested just before shift and 1h post-shift. Transcriptional profiling was done using microarrays and data were analyzed using SAM software, with a >2-fold change in gene expression and an FDR of <3%. A total of 595 and 254 genes were significantly differentially expressed upon shift to 15°C and 25°C, respectively, when compared with pre-shift (Supplementary Table S1). There were 98 genes differentially expressed at both 15°C and 25°C; 50 of these were upregulated (Supplementary Table S1). These genes included ones predicted to encode proteins involved in amino acid biosynthesis, energy metabolism, transport, and binding (Supplementary Table S1). Additionally the cold shock protein *cspV* (VCA0933) was up-regulated under both conditions, with a 2.6-fold increase at 25°C and a 51.2-fold increase at 15°C (Supplementary Table S1). 48 genes were down-regulated in a similar manner upon shifts to both 15°C and 25°C. These genes are predicted to encode proteins involved pathogenesis, heat shock, carbohydrate transport and binding, and transcriptional regulation (Supplementary Table S1). Several genes were differentially regulated between 15°C and 25°C post-shift. These genes included ones involved in regulating biofilm formation (Figure 1), which were up-regulated at 15°C but not at 25°C, and the T6SS genes (Figure 1), which were down-regulated at 15°C but up-regulated at 25°C. We From the many differentially expressed genes, we focused the remainder of our studies on several genes that are predicted to impact the

behavior of *V. cholerae* after their transition from the human host into the environment. including genes encoding proteins involved in biofilm formation/regulation, T6SS, and cold shock response.

Figure 1 *V. cholerae* transcriptome is altered by temperature down shift. Expression profiles of *V. cholerae* cells grown at 37°C to those shifted to 15°C. or 25°C for 1 h. Induced expression is represented in yellow; repressed expression is represented in blue. Differential expression of genes involved in (a) virulence, (b) biofilm formation, (c) T6SS, and (d) cold shock was observed upon cold-shift. Color scale shown at the bottom of the panels. The details of expression data are in Supplementary Table S1.

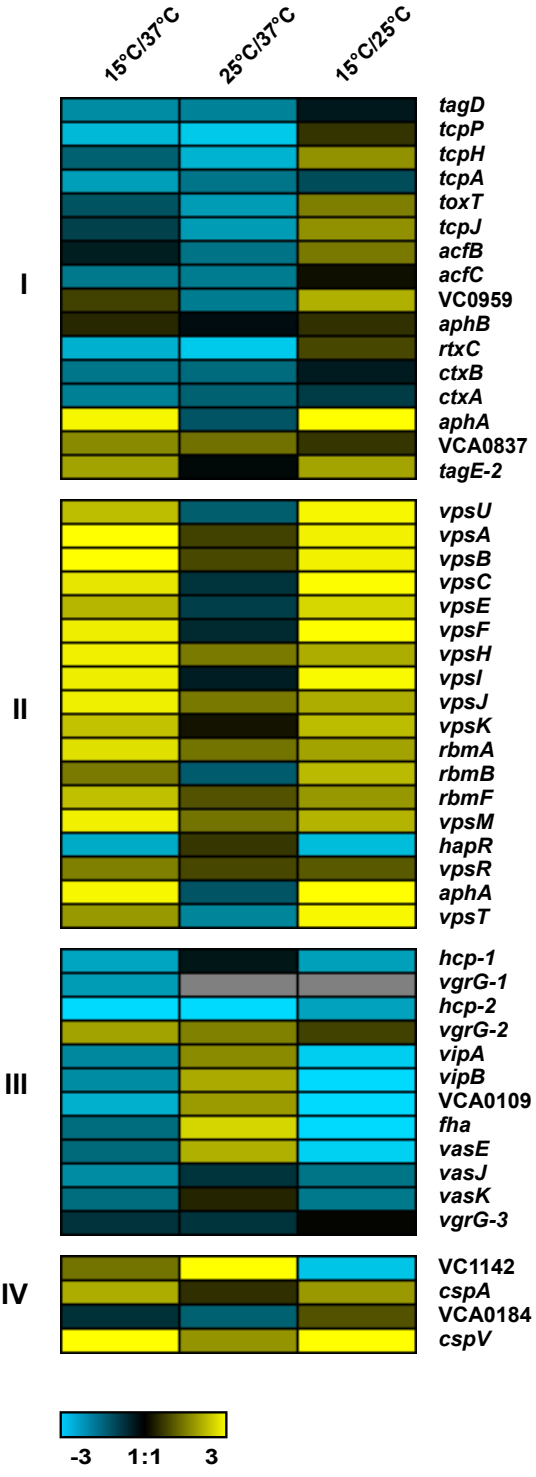
15°C/37°C
25°C/37°C
15°C/25°C
I
tagD
tcpP
tcpH
tcpA
toxT
tcpJ
acfB
acfC
VC0959
aphB
rtxC
ctxB
ctxA
aphA
VCA0837
tagE-2
II
vpsU
vpsA
vpsB
vpsC
vpsE
vpsF
vpsH
vpsI
vpsJ
vpsK
rbmA
rbmB
rbmF
vpsM
hapR
vpsR
aphA
vpsT
III
hcp-1
vgrG-1
hcp-2
vgrG-2
vipA
vipB
VCA0109
fha
vasE
vasJ
vasK
vgrG-3
IV
VC1142
cspA
VCA0184
cspV
-3
1:1
3

Biofilm gene expression is modulated by temperature

Numerous biofilm-related genes were differentially expressed at low temperatures. Specifically, expression of major biofilm regulators, *aphA*, *vpsR* and *vpsT,* and genes encoding the VPS structural components, *vps*-I, *vps*-II and *rbmA*, were up-regulated, while the negative regulator of biofilm formation, *hapR* was down-regulated upon shift from 37°C to 15°C (Figure 1 and Supplementary Table S1). We performed real-time PCR to confirm these observations. We found that *aphA, vpsL*, *vpsR,* and *vpsT* mRNA message abundance was increased 8.3, 2.2, 4.3, and 5.3-fold, respectively, while *hapR* message abundance was decreased 7.1-fold 1 h after a shift from 37°C to 15°C (Figure 2a). This analysis thus supports our microarray findings that positive biofilm regulators show increased expression and negative biofilm regulators show decreased expression at low temperature.

Since biofilm gene expression was affected by low temperatures, we wanted to determine if the major biofilm regulators were responsible for modulating biofilm gene expression at low temperatures. To this end, Δ*aphA* ,Δ*vpsR,* and Δ*vpsT* mutants were grown at 15°C, 25°C, and 37°C in static chambers for 24 h and biofilms were imaged using confocal laser scanning microscopy (CLSM) and compared to wild-type *V. cholerae*. As shown previously (Townsley and Yildiz, 2015), biofilm formation is enhanced at 15°C and 25°C when compared to 37°C (Figure 2b, Table 1). We found that Δ*vpsR*

and Δ*vpsT* mutants exhibit markedly lower biomass and thickness when compared to wild type at both 15°C and 25°C (Figure 2, Table 1). The Δ*aphA* mutant exhibited a small but reproducible decrease in biomass and thickness (Figure 2, Table 1) at low temperatures. These results suggest that temperature affects biofilm formation through modulation of known biofilm regulators *vpsR*, *vpsT*, and *aphA.*

Figure 2 Biofilm formation is modulated by temperature. (a) Analysis of biofilm gene expression in response to low-temperature shift by real-time PCR. Error bars indicate standard deviations of three biological replicates. The Pfaffl method was used to compare expression levels of each gene-of-interest to that of 16s rRNA. All genes exhibited a statistically significant difference between 15°C and 37°C ($P < 0.05$). (b) Three-dimensional biofilm structures of wild-type *V. cholerae* formed at 37°C, 25°C, and 15°C after 24 h incubation. Images shown are from one representative experiment of three independent experiments. Scale bars represent 40 μm.

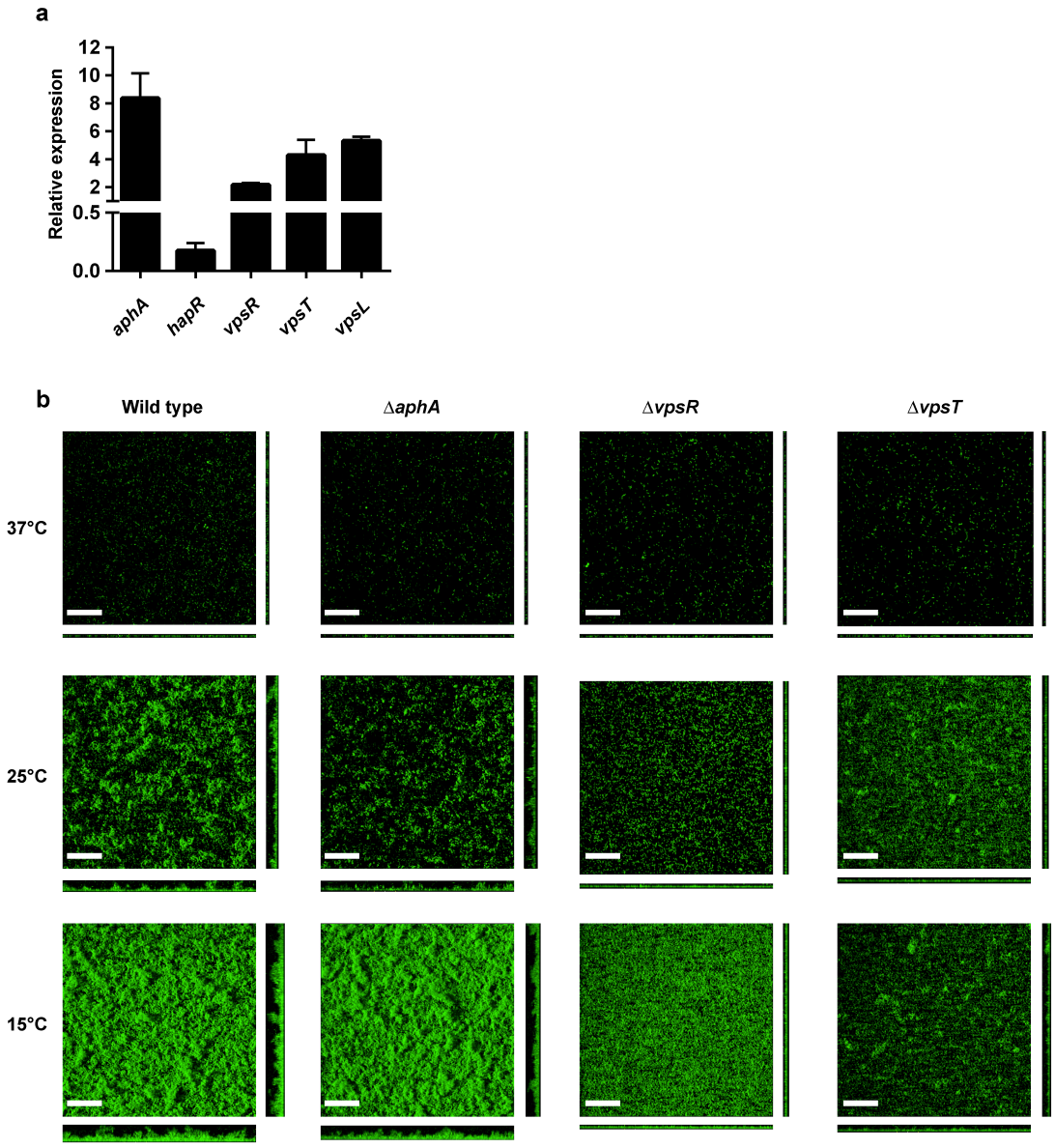
a
Relative expression
12
10
8
6
4
2
0.5
0.0
aphA
hapR
vpsR
vpsT
vpsL
b
Wild type
ΔaphA
ΔvpsR
ΔvpsT
37°C
25°C
15°C

Table 1. COMSTAT analysis of biofilm regulator mutants grown at 15°C, 25°C, and 37°C in static chambers in LB for 24 h.

Strain	Temperature (°C)	Biomass ($\mu m^3/\mu m^2$)	Thickness (μm)		Roughness coefficient
			Average	Maximum	
Wild type	37	0.22 (0.02)	0.30 (0.09)	5.57 (1.02)	1.83 (0.04)
	25	1.64 (0.25)	1.89 (0.15)	15.55 (1.02)	1.19 (0.05)
	15	6.64 (0.23)	7.33 (0.24)	22.00 (2.33)	0.43 (0.02)
Δ*aphA*	37	0.12 (0.02)	0.13 (0.02)	7.63 (4.06)	1.92 (0.02)
	25	2.71 (0.28)	3.35 (0.12)	18.77 (3.09)	0.78 (0.06)
	15	7.41 (0.37)	7.73 (0.42)	23.17 (1.02)	0.40 (0.01)
Δ*vpsR*	37	0.17 (0.03)	0.19 (0.02)	5.87 (0.51)	1.89 (0.02)
	25	1.17 (0.18)	1.22 (0.07)	6.45 (1.02)	1.30 (0.05)
	15	3.25 (0.28)	3.09 (0.31)	6.16 (0.88)	0.30 (0.05)
Δ*vpsT*	37	0.16 (0.01)	0.17 (0.03)	5.28 (0.88)	1.89 (0.01)
	25	0.87 (0.47)	1.17 (0.47)	7.33 (0.51)	1.40 (0.25)
	15	2.37 (0.36)	2.62 (0.27)	9.68 (0.88)	0.54 (0.06)

Type VI secretion *gene expression is modulated by temperature*

The microarray analysis revealed that genes involved in type VI secretion were down-regulated at 15°C, but not at 25°C. We further confirmed this finding by analyzing levels of mRNA for a gene that encodes the main T6SS pilus, *hcp*, using Real-Time PCR and observed that *hcp* mRNA abundance was decreased nearly 1.5-fold 1 h after shift from 37°C to 15°C and increased 6.0-fold 1 h after shift from 37°C to 25°C, (Figure 3a). Cultures maintained at 37°C for 1 h were included for comparison. To further evaluate the affect of temperature on the T6SS we performed a western analysis to compare Hcp production in whole cells and secretion into the media before and 1 h after shift from 37°C to 15°C or 25°C. We found that Hcp production was low and no secretion was observed in 15°C grown cells. In contrast, Hcp production and secretion were high at 25°C (Figure 3b) corroborating results from both the array and Real-Time PCR data.

Figure 3 T6SS is modulated by temperature. (a) Analysis of *hcp* gene expression by real-time PCR. Error bars indicate standard deviations of three biological replicates. The Pfaffl method was used to compare expression levels of each gene-of-interest to that of 16s rRNA ($P < 0.05$) (b) Hcp production levels by western blot analysis response to low-temperature shift. (c) T6SS-mediated killing of *E. coli* at 37°C, 25°C, 15°C. Error bars indicate standard deviations of three biological replicates. *$P < 0.05$, n.s., $P > 0.05$.

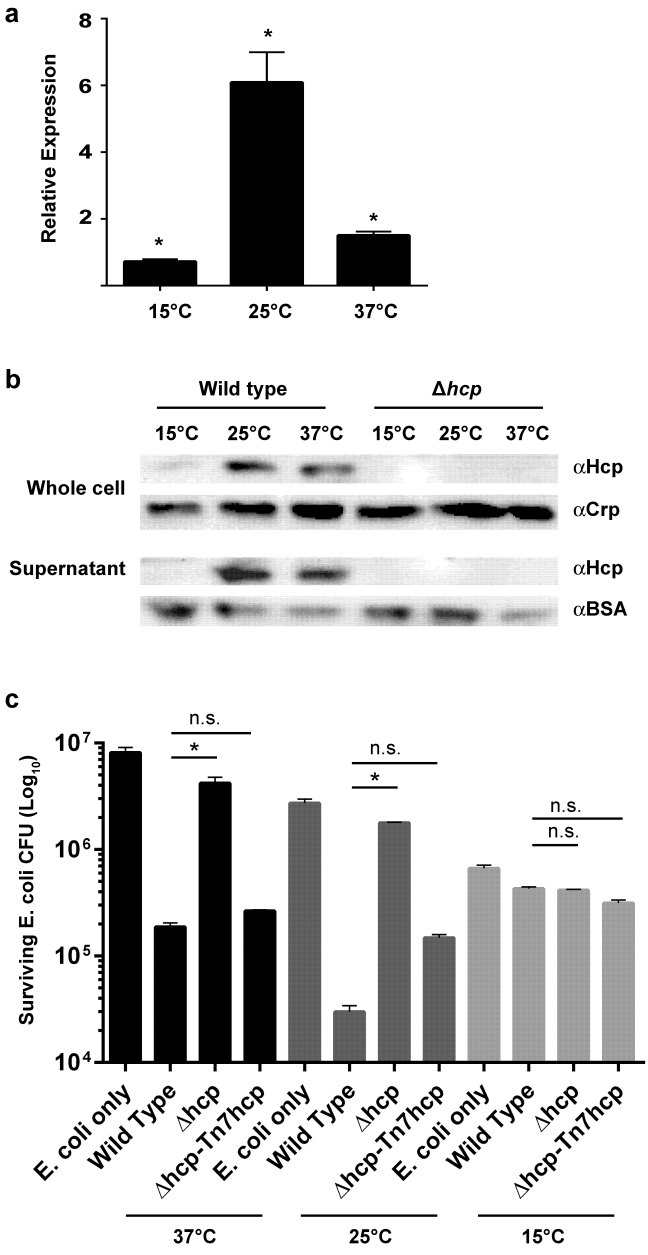
a
Relative Expression
8
6
4
2
*
*
*
15°C
25°C
37°C
b
Wild type
Δhcp
15°C
25°C
37°C
15°C
25°C
37°C
Whole cell
αHcp
αCrp
Supernatant
αHcp
αBSA
c
Surviving E. coli CFU (Log10)
10^7
10^6
10^5
10^4
n.s.
*
n.s.
*
n.s.
n.s.
E. coli only
Wild Type
Δhcp
Δhcp-Tn7hcp
E. coli only
Wild Type
Δhcp
Δhcp-Tn7hcp
E. coli only
Wild Type
Δhcp
Δhcp-Tn7hcp
37°C
25°C
15°C

To further investigate the impact that temperature has on the T6SS in *V. cholerae*, we performed T6SS-mediated killing assays using *E. coli* K-12 MC4100 as a prey strain. We observed a 5-fold reduction in number of *E. coli (*colony forming units, CFUs) after incubation with wild-type *V. cholerae* at 37°C (Figure 3c) and an 16-fold reduction in *E. coli* CFUs when incubated with wild-type *V. cholerae* at 25°C (Figure 3c). However, when we incubated *E. coli* with *V. cholerae* at 15°C we saw no significant decrease (1.1-fold) in *E. coli* CFUs, indicating that under the conditions tested, wild-type *V. cholerae* does not use its T6SS to kill *E. coli* when incubated at 15°C (Figure 3c).

Expression of cold shock genes is modulated by temperature

We next evaluated mRNA levels for another set of genes that was temperature regulated in our microarray analysis, the cold shock genes. Real-Time PCR was used to quantify mRNA message abundance of each of the four putative cold shock genes in *V. cholerae* before and 1 h after shift to 15°C and 25°C. We found that message abundance of *cspA, cspV,* VC1142, and VCA0184 was increased 21.9, 60.9, 2.5, and 1.2-fold respectively upon shift to 15°C (Figure 4a) and increased 4.7, 2.0, 4.5, and decreased 1.8-fold respectively upon shift to 25°C (Figure 4b).

Figure 4 Expression of cold shock genes is differentially regulated by temperature and cold shock proteins impact biofilm formation. Analysis of cold shock gene expression in response to shift from 37°C to 15°C (a) and 37°C to 25°C (b) by real-time PCR . Error bars indicate standard deviations of three biological replicates. The Pfaffl method was used to compare expression levels of each gene-of-interest to that of 16s rRNA ($P < 0.05$)

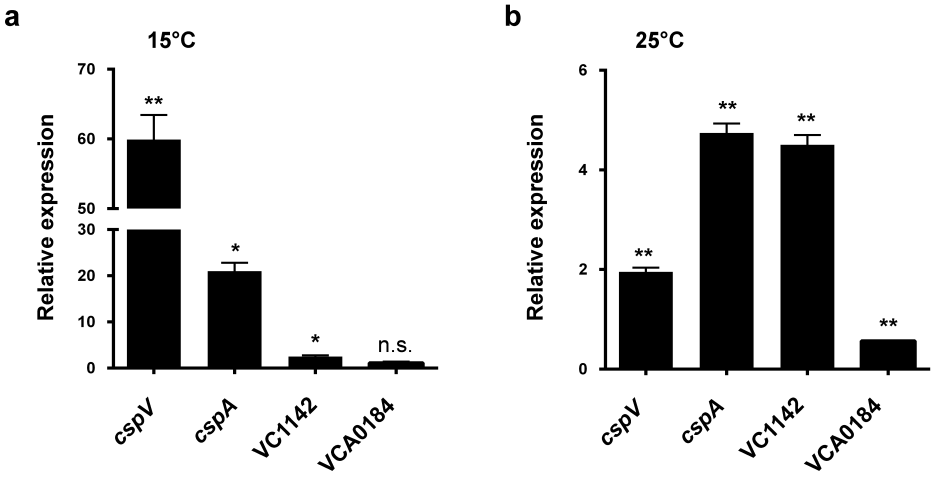

Transcriptional profile of ΔcspV *upon cold-shift*

The most highly induced gene was cspV, which encodes a protein with XX domain and thus is predicted to regulate gene expression. We therefore tested whether *cspV* regulates gene expression upon low-temperature shift. We compared the transcriptional profile of a Δ*cspV* null mutant to that of an isogenic wild type before and 1h after a shift from 37°C to 15°C using WHAT METHOD. We found that a total of 92 genes were significantly differentially regulated upon shift to 15°C when compared to wild type respectively (Supplementary Table S2). We also found that 24 genes were differentially regulated before the shift when compared to wild type (Supplementary Table S2), indicating that *cspV* plays a role in gene regulation at both temperatures, but affects more genes at 15°C. Differentially regulated genes included those involved in biofilm formation and T6SS (Supplementary Table S2).

CpsV regulates biofilm gene expression, biofilm formation, and cellular c-di-GMP levels

We next examined several of the genes that had altered expression in the cspV mutant. First, we confirmed that biofilm gene expression is decreased in the *cspV* mutant (Figure? Where is data?). Then we examined biofilm formation directly in strains lacking these cold shock genes and compared to that of wild-type *V. cholerae* incubated at 15°C, 25°C, and 37°C for 24 h using

CLSM. When grown at 15°C the *cspV* mutant showed lower biofilm formation when compared to wild type, as measured by multiple parameters (Fig. 5A). Specifically, we measured a 1.8, 2.4, and 3.7-fold decrease in biomass, average thickness, and maximum thickness respectively when compared with wild type (Figure 5a, Table 2). At 25°C the *cspV* mutant did not show significant change in any biofilm parameters when compared with wild type (Figure 5a, Table 2). These results indicate that *cspV* affects biofilm formation more dramatically at 15°C under the conditions tested in this study. We also found that Δ*cspA*, ΔVC1142, and ΔVCA0184 had biofilm defects at 15°C, although less dramatic than the Δ*cspV* strain, whereas all three strains looked similar to wild type at 25°C (Figure 5a, Table 2).

Figure 5 *cspV* regulates biofilm gene expression and cellular c-di-GMP levels. (a) Three-dimensional biofilm structures of wild-type *V. cholerae* and strains lacking *cspV, cspA,* VC1142, or VCA0184 formed at 37, 25, and 15°C after 24 h incubation. *$P < 0.05$, ** $P < 0.005$, n.s., $P > 0.05$. Images shown are from one representative experiment of three independent experiments. Scale bars represent 40 μm. (b) Biofilm gene expression in Δ*cspV* compared with wild-type *V. cholerae* upon shift from 37°C to 15°C by real-time PCR. All genes exhibited a statistically significant difference between Δ*cspV* and wild type at 15°C ($P < 0.05$). Error bars indicate standard deviations of four biological replicates (c) c-di-GMP levels in Δ*cspV* and wild-type *V. cholerae* grown at 37°C, then shifted to 15°C for 1h. Error bars indicate standard deviations of four biological replicates *$P < 0.05$, n.s., $P > 0.05$

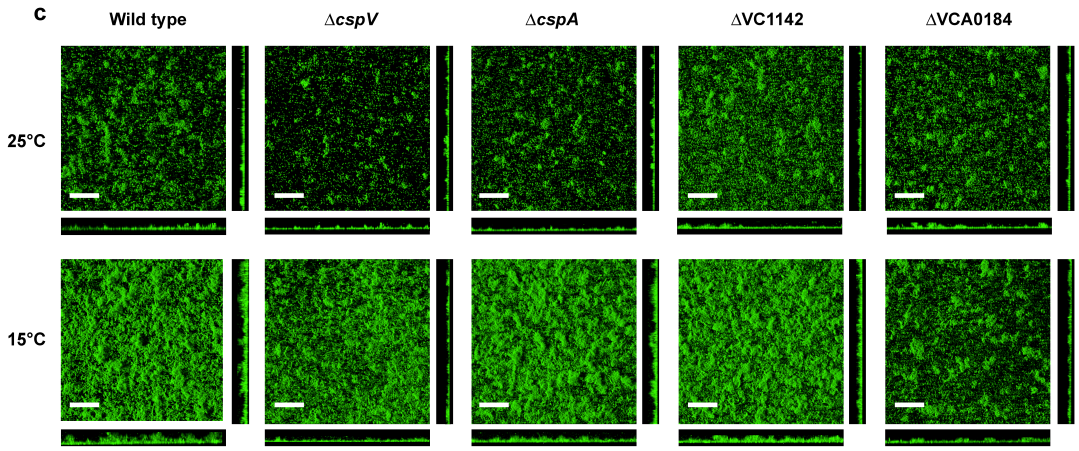
c
Wild type
ΔcspV
ΔcspA
ΔVC1142
ΔVCA0184
25°C
15°C

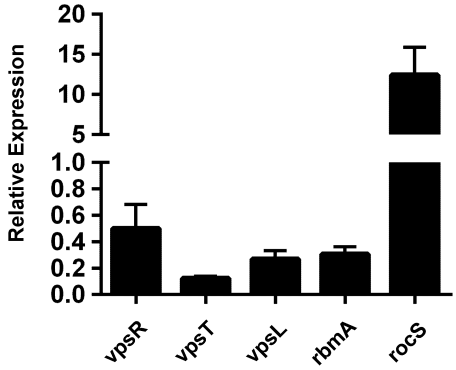
Relative Expression
20
15
10
5
1.0
0.8
0.6
0.4
0.2
0.0
vpsR
vpsT
vpsL
rbmA
rocS

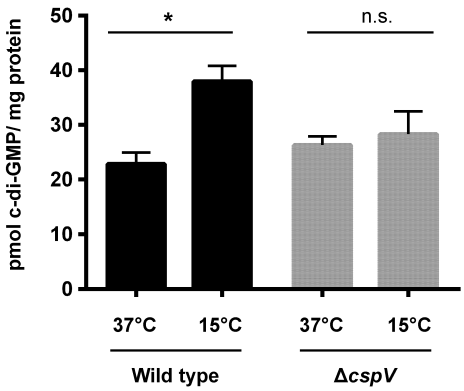
pmol c-di-GMP/ mg protein
50
40
30
20
10
0
*
n.s.
37°C
15°C
37°C
15°C
Wild type
ΔcspV

Table 2. COMSTAT analysis of cold shock protein mutants grown at 15°C and 25°C in static chambers in LB for 24 h.

Strain	Temperature (°C)	Biomass ($\mu m^3/\mu m^2$)	Thickness (μm)		Roughness coefficient
			Average	Maximum	
Wild type	25	1.84 (0.76)	1.78 (0.64)	10.07 (3.22)	1.05 (0.33)
	15	4.61 (1.24)	5.10 (1.55)	15.64 (3.01)	0.53 (0.10)
Δ*cspA*	25	1.97 (0.36)	1.89 (0.35)	9.78 (3.77)	0.95 (0.28)
	15	4.06 (1.39)	3.88 (0.96)	12.61 (0.59)	0.58 (0.30)
Δ*cspV*	25	1.40 (0.92)	1.17 (0.74)	7.33 (2.69)	1.16 (0.50)
	15	2.26 (0.89)	1.90 (0.53)	5.67 (2.85)	0.51 (0.35)
ΔVC1142	25	2.26 (0.04)	2.49 (0.52)	10.95 (4.05)	0.83 (0.20)
	15	5.12 (1.7)	5.23 (2.75)	11.73 (2.56)	0.49 (0.09)
ΔVCA0184	25	2.71 (0.35)	2.67 (0.48)	10.76 (2.39)	0.78 (0.17)
	15	3.86 (0.96)	3.68 (1.07)	11.34 (3.05)	0.52 (0.12)

Biofilm formation is regulated by the second messenger cyclic diguanylate (c-di-GMP) (Tischler et al., 2004) and c-di-GMP levels are increased at low temperatures (Townsley & Yildiz, 2015). We observed that the expression of one phosphodiesterase responsible for degrading c-di-GMP, *rocS*, was up-regulated in Δ*cspV.* We therefore hypothesized that *cspV* might act via c-di-GMP to regulate the expression of genes required for biofilm formation. Thus, cellular levels of c-di-GMP were quantified in Δ*cspV* before and 1 h post-shift from 37°C to 15°C and compared to wild type. In agreement with previously published findings (Townsley and Yildiz, 2015) we found that c-di-GMP levels were over 1.5-fold higher ($P < 0.005$) at 15°C (post-shift) when compared to 37°C (pre-shift) in wild-type *V. cholerae* (Figure 5). However, there was no significant increase in cellular levels of c-di-GMP at 15°C (post-shift) when compared to 37°C (pre-shift) ($P > 0.05$) in the Δ*cspV* mutant (Figure 5). This outcome suggests that *cspV* affects biofilm formation through modulation of c-di-GMP.

Type VI secretion system is altered in ΔcspV

We observed decreased expression of two important T6SS genes, *hcp*-1 and *hcp*-2, in Δ*cspV* when compared to wild type at both 15°C and 37°C (Figure 3a). To confirm the role *cspV* in the regulation of the T6SS, we first compared *hcp* mRNA message abundance, 1 h after a shift from 37°C to 15°C and 25°C using Real-Time PCR. We observed no difference (1.04-fold)

in Hcp expression when Δ*cspV* was compared to wild type at 15°C (Figure 6a); however, a 14.0-fold decrease in Hcp expression when Δ*cspV* was compared to wild type at 25°C (Figure 6a). Next we performed a western analysis to observe Hcp production and secretion in Δ*cspV* grown at 25°C. We found that Δ*cspV* produced no Hcp similar to the Δ*hcp* control (Figure 6b). Finally, we compared T6SS-mediated killing of *E. coli* between Δ*cspV* and wild-type *V. cholerae.* The Δ*cspV* strain exhibited a significant decrease in T6SS-mediated killing of *E. coli,* comparable to that of the Δ*hcp* mutant, at 37°C and 25°C, while no killing was observed at 15°C similar to both wild type and the Δ*hcp* mutant (Figure 6c). This strongly indicates that *cspV* is required for T6SS-mediated killing under the conditions tested.

Figure 6. *cspV* impacts T6SS Analysis of *hcp* expression by real-time PCR in Δ*cspV* and wild-type *V. cholerae* upon shift from 37°C to 15°C (a) or to 25°C (b). Error bars indicate standard deviations of four biological replicates, (c) Hcp production levels by western blot analysis in *cspV* at 25°C. (d) T6SS-mediated killing of *E. coli* at 37°C, 25°C, 15°C. Error bars indicate standard deviations of three biological replicates *P< 0.5., n.s., P > 0.05.

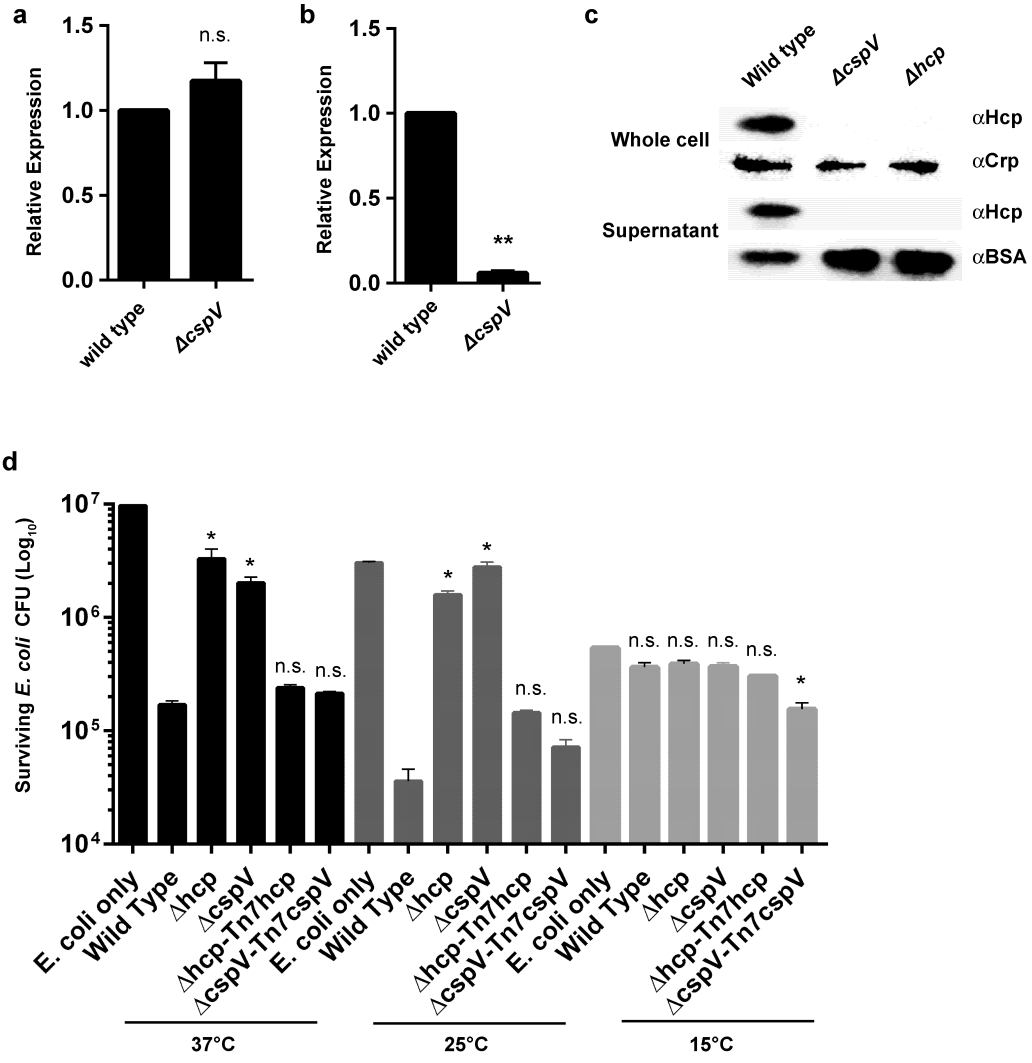

Daphnia colonization

It is well established that *V. cholerae* demonstrate a strong association with the seasonal occurrence of plankton blooms in the aquatic environment (Baker-Austin et al., 2012; Constantin de Magny et al., 2008; Huq et al., 2005b; Turner et al., 2014). Because we observed that *cspV* affects biofilm formation and type VI secretion-mediated interspecies killing, we hypothesized that *cspV* could be important for both attachment to chitinous zooplankton and competition with the native microbiome that colonize the plankton surface (Sison-Mangus & Ebert, 2014). To further investigate the impact of *cspV* on plankton association, we analyzed the ability of both wild-type *V. cholerae* and the *cspV* deletion mutant to colonize *Daphnia magna* by individually infecting *D. magna* with each strain and enumerating the surviving bacteria after 24 h. We also infected *D. magna* with an *mshA* deletion mutant as a control since it was previously established that this mutant has an attachment defect on the surface of *Daphnia* (Chiavelli & Taylor, 2001). We found that Δ*cspV* attached to *Daphnia* 9.8-fold less compared with wild type (Figure 7a), a reduction that was statistically significant and similar to the Δ*mshA* control (Figure 7a). We corroborated this observation using scanning electron microscopy analysis to visualize wild type, Δ*cspV,* and Δ*mshA* attached to the *D. magna* under the same conditions as described above (Figure 7b). We found clusters of wild-type *V. cholerae* attached to the surface of *D. magna,* however we found very few attached cells in *Daphnia*

colonized with the strain lacking *cspV* (Figure 7b) or with the *mshA* mutant (data not shown). This indicates *V. cholerae* is able to attach to the surface of *Daphnia* and that *cspV* is important for this attachment.

Figure 7. *cspV* impacts attachment to *D. magna* (a) Analysis of wild-type *V. cholerae* and Δ*mshA,* Δ*cspV* to colonize *D. magna.* (b) survival in ADaM. (c) Images showing wild-type and *cspV* attached to *D. magna.* Error bars indicate standard deviations of eight biological replicates *P< 0.5., n.s., P > 0.05.

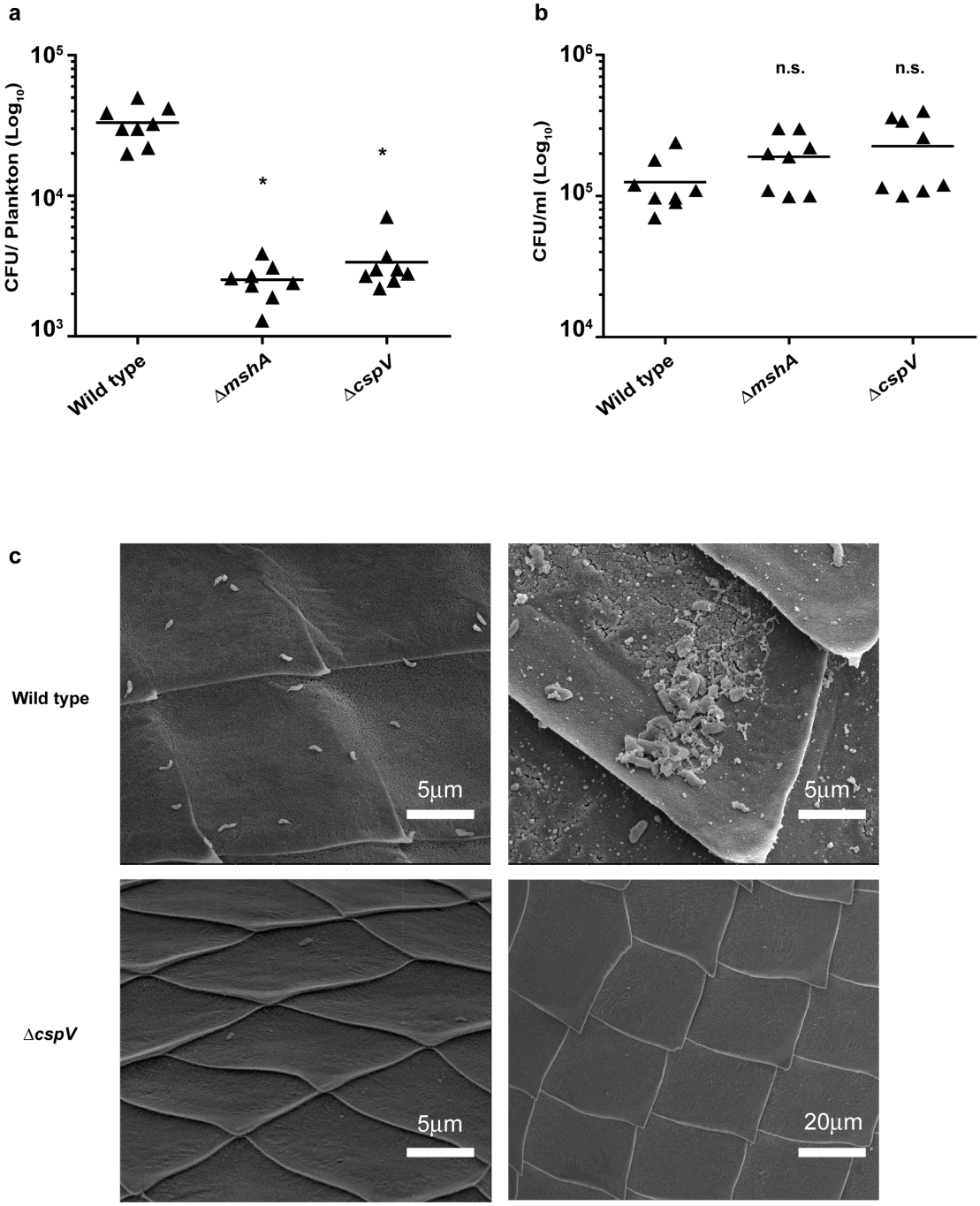
a
b
c
CFU/ Plankton (Log10)
CFU/ml (Log10)
10^5
10^4
10^3
10^6
10^5
10^4
*
*
n.s.
n.s.
Wild type
ΔmshA
ΔcspV
Wild type
ΔcspV
5µm
5µm
5µm
20µm

Next, we determined whether *V. cholerae* uses T6SS-mediated interspecies killing to compete with the surface microbiome of *D. magna.* We first focused on single member of the *D. magna* surface microbial community, an Aeromonas species that was isolated from D magna (REF). We compared T6SS-mediated killing of this *Aeromonas sp.,* between Δ*cspV* and wild-type *V. cholerae* using in vitro killing assays. We observed a nearly 44-fold reduction in CFUs of *Aeromonas sp.* after incubation with wild-type *V. cholerae* at 25°C (Figure 8a); however, there was only a slight decrease in *Aeromonas sp.* when incubated with Δ*cspV* or the mutant lacking T6SS (Δ*hcp)* control (3.2 and 1.8-fold respectively) (Figure 8a). Introduction of a wild-type copy of either *cspV* at a neutral site, expressed from their native promoters, restored interbacterial killing ability. This finding supports that cspV is responsible for the deficit. We then performed the killing assays using live *D. magna* as an attachment surface. We found that there was an 23-fold decrease in *Aeromonas sp.* when incubated with wild-type *V. cholerae* on *D. magna* (Figure 8b) and only a 1.2 and 1.4-fold change when incubated with Δ*cspV* or the Δ*hcp* control (Figure 8b). Complemented strains phenocopied interbacterial killing ability of the wild type strain. Collectively, these results indicate that *cspV* is important for association with live chitinous zooplankton.

Figure 8. *cspV* contributes to interspecies killing on the surface of *D. magna* (a) T6SS-mediated killing of *Aeromonas* in vitro and (b) on the surface of *D. magna.* (c) Error bars indicate standard deviations of eight biological replicates *P< 0.5., n.s., P > 0.05.

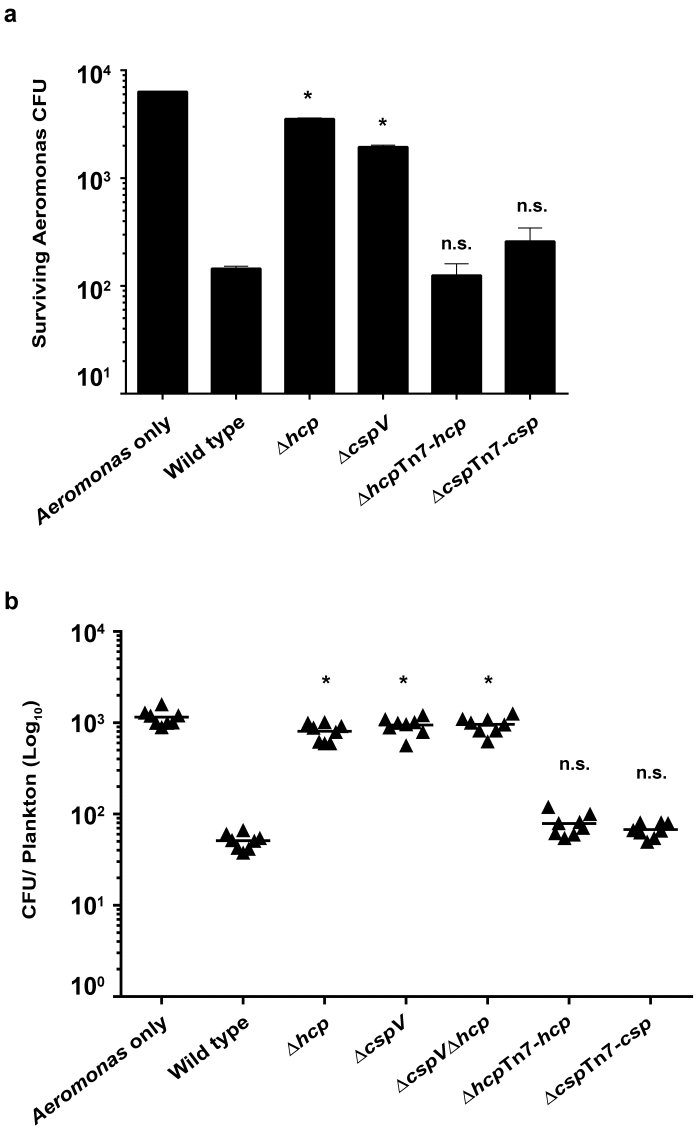

DISCUSSION

Temperature adaptation is crucial for the survival of *V*. *cholerae* in the environment and upon entering and exiting the human host, and thereby facilitates the continuation of its infectious cycle. We used whole genome expression profiling to gain an insight into cellular process regulated by temperature in *V. cholerae*. We determined that expression of genes involved in biofilm formation, T6SS, and cold shock adaptation are controlled by temperature.

We recently reported that low temperature growth induces biofilm formation though modulation of c-di-GMP signaling in *V. cholerae* (Townsley & Yildiz, 2015). Growth in biofilms enhances the ability of bacteria to resist stress and thus it may by important for surviving low-temperature stress. Here we have demonstrated that low-temperature biofilm formation is controlled by the modulation of biofilm gene transcription of *aphA*, *hapR*, *vpsR* and *vpsT* (Figure 2a). Both VpsR and VpsT have been demonstrated as receptors of c-di-GMP (Krasteva et al., 2010; Srivastava et al., 2011) therefore they could be the receptors responsible for relaying increased c-di-GMP signals to downstream processes at low temperatures, however future studies will be needed address this. It was previously determined that *aphA* is not significantly affected by temperature (Skorupski & Taylor, 1999); however

only 37°C and 30°C were tested, while here we saw mRNA abundance of *aphA* was significantly increased at 15°C (Figure 2a). To our knowledge this is the first report of the modulation of this virulence regulator at 15°C, suggesting that this virulence regulator may be important for controlling biofilm formation outside the human host.

In our study we determined that temperature has a dramatic impact on the T6SS. We found that *hcp* message abundance, and protein production and secretion were highest at 25°C (Figure 3ab). It was previously reported that Hcp is increased in cells grown at 23°C when compared to 37°C (Ishikawa et al., 2012) consistent with the results reported here. In agreement with our real-time qPCR and western analysis we saw little to no killing of *E. coli* at 15°C. At this time we do now know what is responsible for modulating *hcp* at low temperatures, however, it has been established that HapR positively regulates Hcp expression (Ishikawa et al., 2009; Tsou et al., 2009) and we have observed that *hapR* message abundance is significantly decreased at low temperatures (Figure 2a).

There are four predicted cold shock protein (CSP) homologues in *V. cholerae*, and one study determined that two that are cold inducible, CspA and CspV (Datta et al., 2003). Transcriptional profiling of human-shed *V. cholerae* found the region of *cspV* to be highly induced (Merrell et al., 2002) suggesting that cold shock genes may play an important role in the infectious cycle of *V.*

cholerae by promoting survival and persistence in the environment after dissemination from the human host. Other transcriptional profiling studies have found *cspV* transcript levels are high in the presence of bile (Cerda-Maira et al., 2008) and high c-di-GMP (Beyhan et al., 2006). Previous work on *cspV* has indicated that *cspV* contains a cold-inducible promoter that lacks a long 5' un-translated region in its mRNA transcript, an unusual exception amongst cold shock genes who are traditionally post-transcriptionaly regulated (Datta & Bhadra, 2003). In our microarray analysis we identified *cspV* to be highly expressed at low temperatures (Supplementary Table S1). We found that deletion of this gene causes a significant defect in biofilm formation and type VI secretion in *V. cholerae* (Figures 5 and 7). The molecular details of how *cspV* controls these processes remains unclear; however, data from the *cspV* microarray indicate that *cspV* regulates genes involved in biofilm formation and type VI secretion (Supplementary Table S2). Further studies are needed to determine the molecular details of this regulation.

Environmental temperature is an important factor that affects the prevalence of *V. cholerae* in the environment and also impacts *V. cholerae*/plankton interactions, In the current study we have demonstrated that *cspV* is important for the attachment to live zooplankton and competition with other plankton-attached bacteria, suggesting that *cspV* could have an immense impact on not only the survival of *V. cholerae* but its transmission as well. It is

well established that surface water temperature and abundance of zooplankton covary with *V. cholerae* prevalence in the aquatic environment (Gil et al., 2004; Turner et al., 2014). The survival of *V. cholerae* is extended at low temperatures with the addition of chitin alone (Amakoet al., 1987); however, the survival of *V. cholerae* has been shown to be 100-fold greater in the presence of live zooplankton when compared to dead ones (a Huq et al., 1983). In addition, the ingestion of untreated water containing a small number of plankton-attached *V. cholerae* can easily provide the required infective dose 10^9 ml^1 to cause disease (Constantin de Magny et al., 2008). A filtration procedure using sari material to reduce the number *Vibrios* attached to plankton from raw pond and river water used for drinking yielded an amazing 48% reduction in cases of cholera in Bangladesh (Colwell et al., 2003). These studies clearly demonstrate the importance of *V. cholerae* attachment to plankton in promoting environmental survival and perpetuating the infectious cycle of this pathogen.

Our studies have provided insight into alterations to the transcriptome that aid in the survival of *V. cholerae* upon shift from high to low temperatures. We have identified cellular processes, biofilm formation and type VI secretion, which are modulated by temperature through the cold shock gene *cspV.* Furthermore we have demonstrated that *cspV* is crucial for attachment to live zooplankton and T6SS-mediated killing of bacteria attached to live

zooplankton. Collectively these findings support that temperature adaptation and the cold shock gene *cspV* are important for the environmental survival and transmission of *V. cholerae.*

EXPERIMENTAL PROCEDURES

Bacterial strains and growth conditions

V. cholerae O1 El Tor A1552 was used as our wild-type strain. *E. coli* CC118λ*pir* and S17-1λ*pir* were used for cloning and conjugation, respectively. Luria Bertani (LB) medium (1% tryptone, 0.5% yeast extract, 0.2M NaCl; pH 7.5) was used to grow all strains. Temperature-shift experiments were performed by inoculating overnight-grown cultures of *V. cholerae* in a 1:200 dilution in LB and incubating at 37°C until exponential phase (OD_{600}=0.4); cultures were then shifted to 15°C and 25°C for the time indicated. Constant temperature experiments were performed by inoculating overnight-grown cultures in a 1:200 dilution in LB followed by incubation at 15°C, 25°C, or 37°C for 24 hours. When needed ampicillin and rifampicin were used at 100 μg/ml, except for biofilm complementation analysis where ampicillin was used at 25 μg/ml, and streptomycin was used at 50 μg/ml.

Generation of in-frame deletion mutants

Deletion mutants were generated using previously published protocols (Fong et al., 2006). Briefly, approximately 500 bp up and downstream of the gene of interest was amplified by PCR using two sets of deletion primers. These two PCR products were then joined via splicing by overlap extension PCR (Fong et al., 2006) and cloned into a pGP704-sacB28 suicide plasmid. The deletion

plasmids were maintained in *E. coli* CC118 (λ pir). Biparental matings were carried out with *V. cholerae* A1552 and the conjugative strain *E. coli* S17-1 (λ pir) harboring the deletion plasmid. Ampicillin- and rifampin-resistant transconjugants, resulting from single homologous recombinations, were selected and subjected to sucrose-based selection. Ampicillin-sensitive and sucrose-resistant *V. cholerae* deletion strains, which had undergone double homologous recombinations, were selected and verified by PCR.

Gene expression profiling

Microarrays used were composed of spotted 70-mer oligonucleotides representing the open reading frames of the *V. cholerae* strain N16961 genome and were printed at the University of California, Santa Cruz (Beyhan et al., 2006). A common reference RNA sample was used for all whole-genome expression analyses. Reference RNA was sampled from *V. cholerae* grown overnight in LB supplemented with 0.2 M NaCl, then diluted 1:200 in fresh medium, and harvested at mid-exponential phase at an OD_{600} of 0.4. Experimental RNA samples were isolated from *V. cholerae* cells that were exposed to cold-shift. For this experiment overnight-grown cultures of *V. cholerae* were diluted 1:200 in LB and incubated at 37°C until exponential phase (OD_{600}=0.4); cultures were then shifted to 15°C, 25°C or maintained at 37°C for one hour. 2 ml aliquots were collected by centrifugation, immediately resuspended in 1 ml of Trizol reagent (Invitrogen) and 0.2 ml of

chloroform was added into each tube. RNA preparation and microarray hybridization and scanning was performed as described previously (Beyhan et al., 2006a) Normalized signal ratios were obtained with LOWESS print-tip normalization, using the Bioconductor packages (Gentleman et al., 2004) in the R environment. Differentially regulated genes were determined using three biological replicates and two technical replicates for each treatment (six data points for each spot), using the Significance Analysis of Microarrays (SAM) program (Tusher et al., 2001) with a 2-fold difference in gene expression and a 3% false discovery rate (FDR) as cutoff values.

Expression analysis - Real Time PCR

RNA was harvested as described above. To remove contaminating DNA, total RNA was incubated with TURBO DNase (Ambion), and the RNeasy Mini kit (QIAGEN) was used to clean up the RNA after DNase digestion. cDNA was synthesized using iScript cDNG Synthesis Kit (Bio-Rad) from 1 µg of total RNA. Real-time PCR was performed using a Bio-Rad CFX1000 thermal cycler and Bio-Rad CFX96 real-time imager with specific primer pairs (designed within the coding region of the target genes) and SsoAdvanced SYBR green supermix (Bio-Rad). Results are from two independent experiments performed in triplicate. All samples were normalized to the expression of the housekeeping gene 16S using the Pfaffl method (Pfaffl, 2004). Relative expression was calculated by normalizing expression at 15°C

or 25°C by that at 37°C. Statistical analysis was performed using two-tailed student's *t* test.

Generation of GFP-tagged strains.

V. cholerae strains were tagged with green fluorescent protein (GFP) according to the procedure previously described (Fong et al., 2006). Briefly, triparental matings were carried out with donor *E. coli* S17-1 (λ pir) carrying pMCM11, helper *E. coli* S17-1 (λ pir) harboring pUX-BF13, and various *V. cholerae* strains. Transconjugants were selected on thiosulfate-citrate-bile salts-sucrose (Difco) agar medium containing gentamicin at 37°C. GFP-tagged *V. cholerae* strains were verified by PCR.

Biofilm Imaging

GFP-expressing *V. cholerae* from overnight-grown cultures were diluted into LB broth to an OD_{600} of about 0.02, then 3 ml were inoculated into glass chambers (Lab-Tek) and incubated statically at 15°C, 25°C, or 37°C. After 24 hours, planktonic bacteria were removed by gently inverting the chambers and washed gently twice with LB. Biofilm formation was visualized using confocal laser-scanning microscopy (CLSM) with an LSM 5 Pascal laser-scanning microscope (Zeiss). Three-dimensional images were reconstructed using Imaris 7.6 and analyzed using COMSTAT (Heydorn et al., 2000). Each

experiment included three independent biological replicates and three images were taken for each replicate.

Determination of intracellular c-di-GMP levels

Overnight grown *V. cholerae* strains diluted 1:200 and grown to an OD_{600} of 4.0, at which time cultures were harvested and remaining culture was shifted to 15°C for 1 h then sampled. c-di-GMP extraction was performed as described previously (Liu et al., 2010; Townsley et al., 2015). Briefly, 40 ml of culture was centrifuged at 3220 *g* for 30 min. Cell pellets were allowed to dry briefly then re-suspended in 1 ml extraction solution (40% acetonitrile, 40% methanol, 0.1% formic acid, 19.9% water), and incubated on ice for 5 min. Samples were then centrifuged at 16,100 *g* for 5 min and 800 µl of supernatant was dried under vacuum and then lyophilized. Samples were re-suspended in 50 µl of 184 mM NaCl and analyzed by liquid chromatography-tandem mass spectrometry (LC-MS/MS) on a Thermo-Electron Finnigan LTQ mass spectrometer coupled to a surveyor HPLC.

To determine protein concentration, 4 ml from each culture was pelleted, the supernatant was removed, and cells were lysed in 1 ml of 2% sodium dodecyl sulfate. Total protein in the samples was estimated with BCA assay (Thermo Fisher) using bovine serum albumin (BSA) as standards. Each c-di-GMP quantification experiment was performed with four biological replicates.

Levels of c-di-GMP were compared between temperatures using a two-tailed student's *t* test.

Hcp Western Blot Analysis

Overnight grown *V. cholerae* strains diluted 1:200 and grown to an OD_{600} of 4.0, at which time cultures were sampled and remaining culture was shifted to 15°C, 25°C or maintained at 37°C for 1 h then sampled. Sample preparation and western blotting was performed as previously described (Cheng et al., 2015). Briefly, samples (25 ml) were centrifuged to obtain whole cell pellets. Culture supernatants containing secreted proteins were filtered and secreted proteins were precipitated with 13% trichloroacetic acid (TCA) overnight at 4°C, pelleted by centrifugation, washed with ice cold acetone, then resuspended in 1x PBS containing Complete protease inhibitor (Roche). Bovine serum albumin (BSA, 100 μg/ml) was added to the culture supernatant prior to TCA precipitation as a control. Protein pellets from whole cell were suspended in 2% sodium dodecyl sulfate (SDS) and protein concentrations were estimated using a Pierce BCA protein assay kit (Thermo Scientific). Equal amounts of total protein (20 μg) were loaded onto a SDS 13% polyacrylamide gel electrophoresis (SDS-PAGE). Western blot analyses were performed using anti-Hcp polyclonal antiserum provided by the Wai lab (Ishikawa et al., 2009), anti-CRP (Neoclone Inc.), and anti-BSA (Santa Cruz Biotech). These experiments were conducted with three biological replicates.

Bacterial killing assay

Killing assays were performed as described previously (Zheng et al., 2011) with slight alterations. Bacterial strains were grown overnight on LB plates and resuspended in LB broth containing 0.2 M NaCl. *V. cholerae* and *E. coli* MC4100 or *Aeromonas sp.* were mixed at a 10:1 ratio and 25 µl was spotted onto LB agar plates containing 0.2 M NaCl and incubated for 4 hours. *E. coli* diluted 10:1 in LB was plated and incubated under the same conditions as above for comparison. All spots were harvested, serially diluted in LB, and plated onto LB plates containing 50 µg/ml of streptomycin to enumerate surviving prey cells.

Growth of Daphnia

Bacteria-free and gnotobiotic *Daphnia* containing only one bacterial strain *Aeromonas* were produced following methods previously described (Sison-Mangus et al., 2014). Briefly, pregnant *Daphnia magna* (HU-H02 clone) were washed three times with 0.2 µm filtered artificial *Daphnia* medium (ADaM). Eggs were carefully removed from the brood chamber and washed three times with sterile ADaM. Eggs were exposed to double antibiotic solution (1 mg/ml ampicillin and 50 µg/ml kanamycin) for 48 hours until eggs developed into hatchlings in a 20°C environmental room with 16:8 light dark photoperiod. Bacteria-free animals were transferred in 80-ml sterile ADAM and fed axenic or autoclaved *Scenedesmus obliquus* green algae. For gnotobiotic Daphnia,

the strain *Aeromonas* previously cultured in LB and resuspended in sterile ADaM, were introduced to bacteria-free hatchlings and grown in the same environmental condition as the bacteria-free *Daphnia* until further experimentation.

Daphnia attachment assays

V. cholerae from overnight-grown cultures incubated at 37°C in LB broth were washed twice using 1X PBS and a serial dilution was performed to ensure input amount was equal for each culture. Cultures were then diluted to an OD_{600} of 0.02 in 5 ml ADaM media in a 14 ml round-bottom tube (BD Falcon), gently vortexed, then a single *Daphnia* was added to each culture tube and incubated statically at 25°C, with no lid. After 24 h culture was plated to enumerate the planktonic population while *Daphnia* were removed and added to fresh ADaM, then homogenized and plated to enumerate the attached population. A two-tailed student's *t* test was used to determine statistical significance. For live-*Daphnia* T6SS mediated-killing assays overnight-grown cultures of *V. cholerae* and *Aeromonas sp.* were washed twice using 1X PBS, at which time cultures were normalized to the same OD_{600}, mixed at a 10:1 ratio, then diluted and added to *Daphnia* as described above. After 4 h *Daphnia* were removed and added to fresh ADaM, then homogenized and plated onto LB plates containing 50 μg/m Streptomycin to enumerate the surviving prey cells.

Acknowledgements

This work was supported by a NIH grant AI102584 to F.H.Y. L. T. was supported in part by the National Human Genome Research Institute (NHGRI) funded Research Mentoring Institute (RMI) at UC Santa Cruz and the Eugene Cota-Robles (ECR) Fellowship. c-di-GMP quantification was performed at the UCSC Mass Spectrometry Facility, which is funded by NIH grant S10-RR20939 (MS equipment grant). We kindly thank Q. Zhang for help with the HPLC/MS-MS experiments and analysis. B. Abrams at the UCSC Microscopy center for help with confocal microscopy. T. Yuzvinsky for assistance with sample preparation and electron microscopy and the W.M. Keck Center for Nanoscale Optofluidics for use of the FEI Quanta 3D Dualbeam microscope.

REFERENCES

Alam, M., Alam, M., Sultana, M., Sultana, M., Nair, G. B., Nair, G. B., Colwell, R. R. (2006). *Vibrio cholerae*. *Society*, *72*(4), 2849–2855.

Amako, K., Shimodori, S., Imoto, T., Miake, S., & Umeda, A. (1987). Effects of Chitin and Its Soluble Derivatives on Survival of *Vibrio cholerae* 01 at Low Temperature, *53*(3), 603–605.

Baffone, W., Tarsi, R., Pane, L., Campana, R., Repetto, B., Mariottini, G. L., & Pruzzo, C. (2006). Detection of free-living and plankton-bound vibrios in coastal waters of the Adriatic Sea (Italy) and study of their pathogenicity-associated properties. *Environmental Microbiology*, *8*(7), 1299–1305.

Baker-Austin, C., Trinanes, J. a., Taylor, N. G. H., Hartnell, R., Siitonen, A., & Martinez-Urtaza, J. (2012). Emerging Vibrio risk at high latitudes in response to ocean warming. *Nature Climate Change*, *3*(1), 73–77.

Basler, M., Ho, B. T., & Mekalanos, J. J. (2013). Tit-for-tat: Type VI secretion system counterattack during bacterial cell-cell interactions. *Cell*, *152*(4), 884–894.

Basler, M., Pilhofer, M., Henderson, G. P., Jensen, G. J., & Mekalanos, J. J. (2012). Type VI secretion requires a dynamic contractile phage tail-like structure. *Nature*, *483*(7388), 182–186.

Beyhan, S., Tischler, A. D., Camilli, A., & Yildiz, F. H. (2006a). Differences in gene expression between the classical and El Tor biotypes of *Vibrio cholerae* O1. *Infection and Immunity*, *74*(6), 3633–3642.

Beyhan, S., Tischler, A. D., Camilli, A., & Yildiz, F. H. (2006b). Transcriptome and phenotypic responses of *Vibrio cholerae* to increased cyclic di-GMP level. *Journal of Bacteriology*, *188*(10), 3600–3613.

Borgeaud, S., Metzger, L. C., Scrignari, T., & Blokesch, M. (2015). The type VI secretion system of Vibrio cholerae fosters horizontal gene transfer. *Science*, *347*(6217), 63–67.

Brooks, T. M., Unterweger, D., Bachmann, V., Kostiuk, B., & Pukatzki, S. (2013). Lytic activity of the *Vibrio cholerae* type VI secretion toxin VgrG-3 is inhibited by the antitoxin TsaB. *Journal of Biological Chemistry*, *288*(11), 7618–7625.

Broza, M., Gancz, H., & Kashi, Y. (2008). The association between non-biting midges and Vibrio cholerae. *Environmental Microbiology*, *10*(12), 3193–3200.

Cerda-Maira, F. A., Ringelberg, C. S., & Taylor, R. K. (2008). The bile response repressor BreR regulates expression of the *Vibrio cholerae* breAB efflux system operon. *Journal of Bacteriology*, *190*(22), 7441–7452.

Chen, P., & Shakhnovich, E. I. (2010). Thermal adaptation of viruses and bacteria. *Biophysical Journal*, *98*(7), 1109–18.

Cheng, A. T., Ottemann, K. M., & Yildiz, F. H. (2015). *Vibrio cholerae* Response Regulator VxrB Controls Colonization and Regulates the Type VI Secretion System. *PLOS Pathogens*, *11*(5), e1004933.

Chiavelli, D. a., Marsh, J. W., & Taylor, R. K. (2001). The Mannose-Sensitive Hemagglutinin of *Vibrio cholerae* Promotes Adherence to Zooplankton. *Applied and Environmental Microbiology*, *67*(7), 3220–3225.

Colwell, R. R., Huq, A., Islam, M. S., Aziz, K. M. a, Yunus, M., Khan, N. H., Russek-Cohen, E. (2003). Reduction of cholera in Bangladeshi villages by simple filtration. *Proceedings of the National Academy of Sciences of the United States of America*, *100*(3), 1051–1055.

Constantin de Magny, G., Murtugudde, R., Sapiano, M. R. P., Nizam, A., Brown, C. W., Busalacchi, A. J., Colwell, R. R. (2008). Environmental signatures associated with cholera epidemics. *Proceedings of the National Academy of Sciences of the United States of America*, *105*(46), 17676–17681.

Datta, P. P., & Bhadra, R. K. (2003). Cold Shock Response and Major Cold Shock Proteins of *Vibrio cholerae*. *Society*, *69*(11), 6361–6369.

Dong, T. G., Ho, B. T., Yoder-Himes, D. R., & Mekalanos, J. J. (2013). Identification of T6SS-dependent effector and immunity proteins by Tn-seq in *Vibrio cholerae*. *Proceedings of the National Academy of Sciences of the United States of America*, *110*(7), 2623–8.

Faruque, S. M., Albert, M. J., & Mekalanos, J. J. (1998). Epidemiology, Genetics, and Ecology of Toxigenic *Vibrio cholerae* Epidemiology , Genetics , and Ecology of Toxigenic *Vibrio cholerae*. *Microbiology and Molecular Biology Reviews*, *62*(4), 1301–1314.

Faruque, S. M., Biswas, K., Udden, S. M. N., Ahmad, Q. S., Sack, D. a, Nair, G. B., & Mekalanos, J. J. (2006). Transmissibility of cholera: in vivo-formed

biofilms and their relationship to infectivity and persistence in the environment. *Proceedings of the National Academy of Sciences of the United States of America*, *103*(16), 6350–5.

Fong, J. C. N., Karplus, K., Schoolnik, G. K., & Yildiz, F. H. (2006). Identification and Characterization of RbmA , a Novel Protein Required for the Development of Rugose Colony Morphology and Biofilm Structure in *Vibrio cholerae*. *Journal of Bac*, *188*(3), 1049–1059.

Fong, J. C. N., Syed, K. a., Klose, K. E., & Yildiz, F. H. (2010). Role of *Vibrio* polysaccharide (vps) genes in VPS production, biofilm formation and *Vibrio cholerae* pathogenesis. *Microbiology*, *156*(9), 2757–2769.

Fong, J. C. N., & Yildiz, F. H. (2007). The rbmBCDEF gene cluster modulates development of rugose colony morphology and biofilm formation in *Vibrio cholerae*. *Journal of Bacteriology*, *189*(6), 2319–30.

Gentleman, R. C., Gentleman, R. C., Carey, V. J., Carey, V. J., Bates, D. M., Bates, D. M., Zhang, J. (2004). Bioconductor: open software development for computational biology and bioinformatics. *Genome Biology*, *5*(10), R80.

Gil, A. I., Louis, V. R., Rivera, I. N. G., Lipp, E., Huq, A., Lanata, C. F., Colwell, R. R. (2004). Occurrence and distribution of *Vibrio cholerae* in the coastal environment of Peru. *Environmental Microbiology*, *6*(7), 699–706.

Hébraud, M., & Potier, P. (1999). Cold shock response and low temperature adaptation in psychrotrophic bacteria. *Journal of Molecular Microbiology and Biotechnology*, *1*(2), 211–9.

Heydorn, a, Nielsen, a T., Hentzer, M., Sternberg, C., Givskov, M., Ersbøll, B. K., & Molin, S. (2000). Quantification of biofilm structures by the novel computer program COMSTAT. *Microbiology (Reading, England)*, *146 (Pt 1*, 2395–407.

Ho, B. T., Dong, T. G., & Mekalanos, J. J. (2014). A view to a kill: The bacterial type VI secretion system. *Cell Host and Microbe*, *15*(1), 9–21.

Huq, a, Small, E. B., West, P. a, Huq, M. I., & Colwell, R. R. (1983). Ecological relationships between *Vibrio cholerae* and planktonic crustacean Ecological Relationships Between *Vibrio cholerae* and Planktonic Crustacean Copepods, *45*(1), 275–283.

Huq, A., Sack, R. B., Nizam, A., Longini, I. M., Nair, G. B., Ali, A., Albert, M. J. (2005). Critical Factors Influencing the Occurrence of *Vibrio cholerae* in the

Environment of Bangladesh *Applied and Environmental Microbiology*, *71*(8), 4645-4654,

Ishikawa, T., Rompikuntal, P. K., Lindmark, B., Milton, D. L., & Wai, S. N. (2009). Quorum sensing regulation of the two *hcp* alleles in *Vibrio cholerae* O1 strains. *PLoS ONE*, *4*(8).

Ishikawa, T., Sabharwal, D., Bröms, J., Milton, D. L., Sjöstedt, A., Uhlin, B. E., & Wai, S. N. (2012). Pathoadaptive conditional regulation of the type VI secretion system in vibrio cholerae O1 strains. *Infection and Immunity*, *80*, 575–584.

Kitaoka, M., Miyata, S. T., Brooks, T. M., Unterweger, D., & Pukatzki, S. (2011). VasH is a transcriptional regulator of the type VI secretion system functional in endemic and pandemic *Vibrio cholerae*. *Journal of Bacteriology*, *193*(23), 6471–6482.

Krasteva, P. V, Fong, J. C. N., Shikuma, N. J., Beyhan, S., Navarro, M. V. a S., Yildiz, F. H., & Sondermann, H. (2010). *Vibrio cholerae* VpsT regulates matrix production and motility by directly sensing cyclic di-GMP. *Science (New York, N.Y.)*, *327*(5967), 866–868.

Lipp, E. K., Huq, A., & Colwell, R. R. (2002). Effects of Global Climate on Infectious Disease : the Cholera Model Effects of Global Climate on Infectious Disease : the Cholera Model, *15*(4).

Lipp, E. K., Rivera, I. N. G., Gil, A. I., Espeland, E. M., Choopun, N., Louis, V. R., … Louis, R. (2003). Direct Detection of Vibrio cholerae and ctxA in Peruvian Coastal Water and Plankton by PCR Direct Detection of *Vibrio cholerae* and ctxA in Peruvian Coastal Water and Plankton by PCR, *69*(6), 3676–3680.

Liu, X., Beyhan, S., Lim, B., Linington, R. G., & Yildiz, F. H. (2010). Identification and characterization of a phosphodiesterase that inversely regulates motility and biofilm formation in *Vibrio cholerae*. *Journal of Bacteriology*, *192*(18), 4541–4552.

Louis, V. R., Russek-cohen, E., Choopun, N., Rivera, I. N. G., Gangle, B., Jiang, S. C., Colwell, R. R. (2003). Predictability of *Vibrio cholerae* in Chesapeake Bay. *Applied and Environmental Microbiology*, *69*(5), 2773–2785.

Ma, A. T., McAuley, S., Pukatzki, S., & Mekalanos, J. J. (2009). Translocation of a *Vibrio cholerae* Type VI Secretion Effector Requires Bacterial Endocytosis by Host Cells. *Cell Host and Microbe*, *5*(3), 234–243.

Merrell, D. S., Butler, S. M., Qadri, F., Dolganov, N. a, Alam, A., Cohen, M. B., Camilli, A. (2002). Host-induced epidemic spread of the cholera bacterium. *Nature*, *417*(6889), 642–5.

Miyata, S. T., Unterweger, D., Rudko, S. P., & Pukatzki, S. (2013). Dual Expression Profile of Type VI Secretion System Immunity Genes Protects Pandemic *Vibrio cholerae*. *PLoS Pathogens*, *9*(12), 1–18.

Nahar, S., Sultana, M., Naser, M. N., Nair, G. B., Watanabe, H., Ohnishi, M., Alam, M. (2012). Role of shrimp chitin in the ecology of toxigenic *Vibrio cholerae* and cholera transmission. *Frontiers in Microbiology*, *2*(JAN), 1–8.

Parsot, C., & Mekalanos, J. J. (1990). Expression of ToxR, the transcriptional activator of the virulence factors in *Vibrio cholerae*, is modulated by the heat shock response. *Proceedings of the National Academy of Sciences of the United States of America*, *87*(24), 9898–902.

Pfaffl, M. W. (2004). Quantification strategies in real-time PCR Michael W . Pfaffl. In *A-Z of quantitative PCR* (pp. 87–112).

Phadtare, S. (2004). Recent developments in bacterial cold-shock response. *Current Issues in Molecular Biology*, *6*(2), 125–36.

Phadtare, S., & Inouye, M. (2004). Genome-Wide Transcriptional Analysis of the Cold Shock Response in. *Society*, *186*(20), 7007–7014.

Phadtare, S., & Severinov, K. (2010). RNA remodeling and gene regulation by cold shock proteins. *RNA Biology*, *7*(6), 788–95. Retrieved from

Pukatzki, S., Ma, A. T., Revel, A. T., Sturtevant, D., & Mekalanos, J. J. (2007). Type VI secretion system translocates a phage tail spike-like protein into target cells where it cross-links actin. *Proceedings of the National Academy of Sciences of the United States of America*, *104*, 15508–15513.

Pukatzki, S., Ma, A. T., Sturtevant, D., Krastins, B., Sarracino, D., Nelson, W. C., Mekalanos, J. J. (2006). Identification of a conserved bacterial protein secretion system in *Vibrio cholerae* using the Dictyostelium host model system. *Proceedings of the National Academy of Sciences of the United States of America*, *103*(5), 1528–1533.

Rodrigues, D. F., & Tiedje, J. M. (2008). Coping with our cold planet. *Applied and Environmental Microbiology*, *74*(6), 1677–86.

Russell, A. B., LeRoux, M., Hathazi, K., Agnello, D. M., Ishikawa, T., Wiggins, P. a, Mougous, J. D. (2013). Diverse type VI secretion phospholipases are functionally plastic antibacterial effectors. *Nature*, *496*(7446), 508–12.

Schindelin, H., Jiang, W., Inouye, M., & Heinemann, U. (1994). Crystal structure of CspA, the major cold shock protein of Escherichia coli. *Proceedings of the National Academy of Sciences of the United States of America*, *91*(11), 5119–5123.

Silverman, J., & Brunet, Y. (2012). Structure and regulation of the type VI secretion system. *Annual Review*, 453–472.

Sison-Mangus, M. P., Mushegian, A. a, & Ebert, D. (2014). Water fleas require microbiota for survival, growth and reproduction. *The ISME Journal*, *9*(1), 59–67.

Skorupski, K., & Taylor, R. K. (1999). A new level in the Vibrio cholerae ToxR virulence cascade: AphA is required for transcriptional activation of the *tcpPH* operon. *Molecular Microbiology*, *31*(3), 763–771.

Srivastava, D., Harris, R. C., & Waters, C. M. (2011). Integration of cyclic di-GMP and quorum sensing in the control of *vpsT* and *aphA* in *Vibrio cholerae*. *Journal of Bacteriology*, *193*(22), 6331–41.

Tamayo, R., Patimalla, B., & Camilli, A. (2010). Growth in a biofilm induces a hyperinfectious phenotype in *Vibrio cholerae*. *Infection and Immunity*, *78*(8), 3560–9.

Tischler, A. D., & Camilli, A. (2004). Cyclic diguanylate (c-di-GMP) regulates *Vibrio cholerae* biofilm formation. *Molecular Microbiology*, *53*(3), 857–69.

Tinoco, I., & Bustamante, C. (1999). How RNA folds. *Journal of molecular biology*, *293*(2), 271-281.

Townsley, L., & Yildiz, F. H. (2015). Temperature affects c-di-GMP signaling and biofilm formation in *Vibrio cholerae*. *Environmental Microbiology*,

Tsou, A. M., Cai, T., Liu, Z., Zhu, J., & Kulkarni, R. V. (2009). Regulatory targets of quorum sensing in *Vibrio cholerae*: Evidence for two distinct HapR-binding motifs. *Nucleic Acids Research*, *37*(8), 2747–2756.

Turner, J. W., Good, B., Cole, D., & Lipp, E. K. (2009). Plankton composition and environmental factors contribute to *Vibrio* seasonality. *The ISME Journal*, *3*(9), 1082–1092.

Turner, J. W., Malayil, L., Guadagnoli, D., Cole, D., & Lipp, E. K. (2014). Detection of *Vibrio parahaemolyticus, Vibrio vulnificus* and *Vibrio cholerae* with respect to seasonal fluctuations in temperature and plankton abundance. *Environmental Microbiology*, *16*(4), 1019–1028.

Tusher, V. G., Tibshirani, R., & Chu, G. (2001). Significance analysis of microarrays applied to the ionizing radiation response. *Proceedings of the National Academy of Sciences of the United States of America*, *98*(9), 5116–5121.

Unterweger, D., Miyata, S. T., Bachmann, V., Brooks, T. M., Mullins, T., Kostiuk, B., Pukatzki, S. (2014). The *Vibrio cholerae* type VI secretion system employs diverse effector modules for intraspecific competition. *Nature Communications*, *5*, 3549.

Wang, N., Yamanaka, K., & Inouye, M. (1999). CspI, the ninth member of the CspA family of *Escherichia coli*, is induced upon cold shock. *Journal of Bacteriology*, *181*(5), 1603–1609.

Waters, C. M., Lu, W., Rabinowitz, J. D., & Bassler, B. L. (2008). Quorum sensing controls biofilm formation in *Vibrio cholerae* through modulation of cyclic Di-GMP levels and repression of vpsT. *Journal of Bacteriology*, *190*(7), 2527–2536.

Weber, G. G., Kortmann, J., Narberhaus, F., & Klose, K. E. (2014). RNA thermometer controls temperature-dependent virulence factor expression in *Vibrio cholerae*. *Proceedings of the National Academy of Sciences*, *111*(39), 14241–14246.

Yang, M., Frey, E. M., Liu, Z., Bishar, R., & Zhu, J. (2010). The virulence transcriptional activator *aphA* enhances biofilm formation by *Vibrio cholerae* by activating expression of the biofilm regulator VpsT. *Infection and Immunity*, *78*(2), 697–703. h

Yildiz, F. H., & Schoolnik, G. K. (1999). *Vibrio cholerae* O1 El Tor: identification of a gene cluster required for the rugose colony type, exopolysaccharide production, chlorine resistance, and biofilm formation. *Proceedings of the National Academy of Sciences of the United States of America*, *96*(7), 4028–4033.

Zamorano-Sánchez, D., Fong, J. C. N., Kilic, S., Erill, I., & Yildiz, F. H. (2015). Identification and Characterization of VpsR and VpsT Binding Sites in *Vibrio cholerae*. *Journal of Bacteriology*, *197*(7), 1221–1235.

Zheng, J., Ho, B., & Mekalanos, J. J. (2011). Genetic analysis of anti-amoebae and anti-bacterial activities of the type vi secretion system in *Vibrio cholerae*. *PLoS ONE*, *6*(8).

Zheng, J., Shin, O. S., Cameron, D. E., & Mekalanos, J. J. (2010). Quorum sensing and a global regulator TsrA control expression of type VI secretion and virulence in *Vibrio cholerae*. *Pnas*, *107*(49), 21128–21133.

Supplementary Figure S1

Gene ID	Gene Name	FUNCTIONS	Fold Change 15°C / 37°C	Fold Change 25°C / 37°C
Biofilm Formation				
VC0916	vpsU	*Vibrio* polysaccharide gene U	3.9	
VC0917	vpsA	*Vibrio* polysaccharide gene A	7.2	
VC0918	vpsB	*Vibrio* polysaccharide gene B	8.6	
VC0919	vpsC	*Vibrio* polysaccharide gene C	6.0	
VC0921	vpsE	*Vibrio* polysaccharide gene E	3.8	
VC0922	vpsF	*Vibrio* polysaccharide gene F	7.2	
VC0924	vpsH	*Vibrio* polysaccharide gene H	4.8	
VC0925	vpsI	*Vibrio* polysaccharide gene I	6.6	
VC0926	vpsJ	*Vibrio* polysaccharide gene J	6.8	
VC0927	vpsK	*Vibrio* polysaccharide gene K	4.0	
VC0928	rbmA	Rugosity and biofilm structure modulator A	5.6	
VC0929	rbmB	Rugosity and biofilm structure modulator B	2.0	
VC0933	rbmF	Rugosity and biofilm structure modulator F	3.9	
VC0935	vpsM	*Vibrio* polysaccharide gene M	6.0	
Amino Acid Biosynthesis				
VC0019	avtA	Valine-pyruvate aminotransferase, avtA	2.0	
VC0030	ilvM	Acetolactate synthase II small subunit, ilvM	0.3	
VC0390	metH	5-methyltetrahydrofolate--homocysteine methyltransferase, metH		2.3
VC0391	lysC	Aspartokinase III lysine-sensitive, lysC	3.6	4.6
VC0941	glyA-1	Serine hydroxymethyltransferase, glyA-1		4.6
VC0991	asnB	Asparagine synthetase B glutamine-hydrolyzing, asnB		2.8
VC1061		Cysteine synthase/cystathionine beta-synthase family protein	4.1	
VC1137	hisA	Isomerase, hisA		3.2
VC1169	trpA	Tryptophan synthase alpha subunit, trpA		2.3
VC1293	aspC	Aspartate aminotransferase, aspC		4.0
VC1671	metC	Cystathionine beta-lyase, metC		3.2
VC2036	asd	Aspartate-semialdehyde dehydrogenase, asd		2.7
VC2116	aroC	Chorismate synthase, aroC		2.5
VC2152	dapE	Succinyl-diaminopimelate desuccinylase, dapE		3.3
VC2273	proA	Gamma-glutamyl phosphate reductase, proA	0.5	
VC2329	dapD	2345-tetrahydropyridine-26-dicarboxylate N-succinyltransferase, dapD	0.6	
VC2362	thrC	Threonine synthase, thrC	0.5	
VC2373	gltB-1	Glutamate synthase large subunit, gltB-1		5.3
VC2376	gltB-2	Glutamate synthase large subunit, gltB-2	2.0	
VC2481	serA	D-3-phosphoglycerate dehydrogenase, serA		11.0
VC2493	leuD	3-isopropylmalate dehydratase small subunit, leuD	0.5	
VC2618	argD	Acetylornithine aminotransferase, argD	10.2	6.2
VC2746	glnA	Glutamate ammonia ligase, glnA		2.9

VCA0278	glyA-2	Serine hydroxymethyltransferase, glyA-2	2.5	3.3
Biosynthesis of cofactors prosthetic groups and carriers				
VC0064	thiS	ThiS protein, thiS	2.1	
VC0065	thiG	ThiG protein, thiG	2.2	
VC0468	gshB	Glutathione synthetase, gshB	0.4	
VC0472	metK	S-adenosylmethionine synthase, metK	0.2	
VC0626	hemL	Heme porphyrin and cobalamin, hemL	0.3	
VC0889	dxs	1-deoxyxylulose-5-phosphate synthase, dxs	0.5	
VC0943	lipA	Lipoic acid synthetase, lipA	0.5	
VC0944	lipB	Lipoate-protein ligase B, lipB	0.3	
VC1112	bioB	Biotin synthase, bioB	0.4	
VC1114	bioC	Biotin synthesis protein BioC, bioC	0.6	
VC1296	thiD	Thiamine, phosphomethylpyrimidine kinase, thiD	3.1	
VC1299		6-pyruvoyl tetrahydrobiopterin synthase putative	0.5	0.3
VC1509	cobB	Heme porphyrin and cobalamin, cobB	2.1	
VC1942	folD	Folic acid, folD		6.6
VC1973	menB	Naphthoate synthase, menB	0.5	
VC2180	hemA	Glutamyl-tRNA reductase, hemA	0.3	
VC2308	thiJ	Thiamine, thiJ	0.5	
VC2422	nadC	Pyridine nucleotides, nadC	0.5	
VCA0723	hmgA	3-hydroxy-3-methylglutaryl CoA reductase, hmgA	0.5	
VCA0827	phhB	pterin-4-alpha-carbinolamine dehydratase, phhB	3.3	
Cell envelope				
VC0212	msbB	Biosynthesis/ degradation of surface polysaccharides, msbB	0.4	
VC0259	rfbV	Biosynthesis/ degradation of surface polysaccharides, rfbV	0.5	0.3
VC0344	amiB	N-acetylmuramoyl-L-alanine amidase, amiB	0.4	
VC0430		Immunogenic protein		2.5
VC0533	nlpD	Lipoprotein NlpD, nlpD		3.0
VC0700	slt	Soluble lytic murein transglycosylase, slt	0.3	
VC0905	yaeC	Lipoprotein YaeC, yaeC		2.3
VC1195		Lipoprotein putative	0.2	
VC1312		Alanine racemase putative		0.3
VC1537	nlpC	Lipoprotein NlpC, nlpC	4.0	
VC2635	mrcA	Penicillin-binding protein 1A, mrcA	0.4	
VC2762	glmU	Biosynthesis/ degradation of surface polysaccharides, glmU	0.2	
VCA0572	ddlA	D-alanine--D-alanine ligase, ddlA	2.0	
VCA0867	ompW	Outer membrane protein OmpW, ompW	2.5	5.0
Chemotaxis and motility				
VC0216		Methyl-accepting chemotaxis protein		2.2
VC1313		Methyl-accepting chemotaxis protein		0.3
VC1413		Methyl-accepting chemotaxis protein		8.9
VC1898		Methyl-accepting chemotaxis protein	4.2	

VC2161		Methyl-accepting chemotaxis protein		2.4
VC2187	flaC	Flagellin FlaC, flaC	2.9	3.4
VC2203		Flagellar protein putative		2.6
VCA0658		Methyl-accepting chemotaxis protein	0.3	
VCA0663		Methyl-accepting chemotaxis protein	0.4	
VCA0974		Methyl-accepting chemotaxis protein	0.5	
VCA1031		Methyl-accepting chemotaxis protein		0.1
Central intermediary metabolism				
VC0238		Transferase hexapeptide repeat family	0.3	
VC0392		Aminotransferase class V		3.8
VC0454		Glutaminase family protein	0.5	
VC0487	glmS	Aminotransferase (isomerizing), glmS	0.5	
VC0586		Carbonic anhydrase putative	0.4	
VC0667		Oxidoreductase Tas aldo/keto reductase family	2.3	3.6
VC0723	ppk	Phosphorus compounds, polyphosphate kinase, ppk	0.2	
VC0748		Aminotransferase NifS class V	2.0	
VC0979		Oxidoreductase short-chain dehydrogenase/reductase family	2.0	
VC1119		Oxidoreductase short-chain dehydrogenase/reductase family	8.9	
VC1184		NifS-related protein	2.0	
VC2309		Aminotransferase class V	0.4	
VC2545	ppa	Phosphorus compounds, inorganic pyrophosphatase, ppa	0.5	
VC2559	cysN	Sulfur metabolism, sulfate adenylate transferase subunit 1, cysN	0.4	
VCA0102		CbbY family protein	2.0	
VCA0316		Acetyltransferase putative		2.2
VCA0496		Glutathione S-transferase putative	2.2	
VCA0523		Aminotransferase class II	0.5	
VCA0614	fhs	Formate--tetrahydrofolate ligase, fhs	0.6	
VCA0783		Arylesterase	2.0	
VCA0798		CbbY family protein	3.4	
VCA0947	speG	Spermidine n1-acetyltransferase, speG	0.4	0.4
DNA metabolism				
VC0167	rep	ATP-dependent DNA helicase Rep, rep	0.3	
VC0215	dfp	DNA/pantothenate metabolism flavoprotein, dfp	0.2	
VC0394	uvrA	Excinuclease ABC subunit A, uvrA	2.1	
VC0535	mutS	DNA mismatch repair protein MutS, mutS	0.4	
VC0971	ligA-1	DNA ligase, ligA-1	0.4	
VC1011	nth	Endonuclease III, nth	0.4	
VC1056	recR	Recombination protein RecR, recR	0.5	
VC1765		Restriction/modification, type I restriction enzyme HsdR putative	0.3	
VC1846	ruvA	Holliday junction DNA helicase RuvA, ruvA		2.3
VC1886	mfd	Transcription-repair coupling factor, mfd	0.4	
VC2360	nfo	Endonuclease IV, nfo	0.2	0.3

VC2430	parC	Topoisomerase IV subunit A, parC	0.5	
VC2431	parE	Topoisomerase IV subunit B, parE	0.5	
VC2435		MutT/nudix family protein	0.3	
VC2459	recO	DNA repair protein RecO, recO	4.6	
VC2502	holC	DNA polymerase III chi subunit, holC	0.4	
Energy metabolism				
VC1242	astE	Succinylglutamate desuccinylase, astE		2.2
VC1284	celF	6-phospho-beta-glucosidase, celF	3.2	3.1
VC1300	sdaA-1	L-serine dehydratase 1, sdaA-1	0.5	
VC1512	fdhB	Formate dehydrogenase iron-sulfur subunit, fdhB	3.6	5.1
VC1513		Formate dehydrogenase alpha subunit putative authentic frameshift	2.0	
VC1558	bglA	6-phospho-beta-glucosidase, bglA		2.2
VC1726	glgA	Glycogen synthase, glgA		3.0
VC1727	glgC-1	Glucose-1-phosphate adenylyltransferase, glgC-1		3.7
VC1905	ald	Alanine dehydrogenase, ald		3.8
VC2616	aruD	Succinylglutamate 5-semialdehyde dehydrogenase, aruD	11.3	
VC2698	aspA	Aspartate ammonia-lyase, aspA		0.3
VCA0014	malQ	4-alpha-glucanotransferase, malQ		7.3
VCA0276	gcvP	Glycine cleavage system P protein, gcvP	4.3	11.7
VCA0277	gcvH	Glycine cleavage system H protein, gcvH	3.1	6.0
VCA0280	gcvT	Glycine cleavage system T protein, gcvT	2.4	2.6
VCA0875	dsdA	D-serine dehydratase, dsdA		2.3
VCA0886	kbl	2-amino-3-ketobutyrate coenzyme A ligase, kbl		3.1
Electron transport				
VC0002	mioC	Electron transport, mioC protein, mioC	0.2	
VC0306	trxA	Thioredoxin, trxA	0.5	0.4
VC1013		RnfG-related protein		0.4
VC1182	trxB	Thioredoxin reductase, trxB	0.4	
VC1254		Iron-sulfur cluster-binding protein putative	0.4	
VC1516		Iron-sulfur cluster-binding protein	4.9	5.3
VC1844	cydA-1	Cytochrome d ubiquinol oxidase subunit I, cydA-1	0.4	
VCA0538		Cytochrome b561 putative	8.5	
VCA0676	napF	Iron-sulfur cluster-binding protein NapF, napF	0.4	
VCA0677	napD	NapD protein, napD	0.4	
VCA0678	napA	Periplasmic nitrate reductase, napA	0.3	
VCA0679	napB	Periplasmic nitrate reductase cytochrome c-type protein, napB	0.3	
VCA0680	napC	Periplasmic nitrate reductase cytochrome c-type protein, napC	0.3	
VCA0752	trxC	Thioredoxin 2, trxC	0.1	0.4
Fatty acid and phospholipid metabolism				
VC0295	accC	Acetyl-CoA carboxylase biotin carboxylase, accC	0.4	
VC0296	accB	Acetyl-CoA carboxylase biotin carboxyl carrier protein, accB	0.5	

VC0745		Inositol monophosphate family protein	0.1	
VC1000	accD	Acetyl-CoA carboxylase carboxyl transferase beta subunit, accD	0.5	
VC1046	hadHB	Degradation, fatty oxidation complex beta subunit, hadHB	2.7	
VC1122	cfa	Cyclopropane-fatty-acyl-phospholipid synthase, cfa	2.9	2.6
VC1483	fabA	3-hydroxydecanoyl-(acyl-carrier-protein) dehydratase, fabA	0.4	
VC2020	acp	Acyl carrier protein, acp	0.4	
VC2109	fabB	3-oxoacyl-(acyl-carrier-protein) synthase I authentic frameshift, fabB	0.5	
VCA0751	fabH-2	3-oxoacyl-(acyl-carrier-protein) synthase III, fabH-2	2.6	
Fermentation				
VC0551	oadB-1	Oxaloacetate decarboxylase beta subunit, oadB-1		3.0
VC0819	aldA-1	Aldehyde dehydrogenase, aldA-1	4.1	
VC1097	pta	Phosphate acetyltransferase, pta	0.2	
VC1098	ackA-1	Acetate kinase, ackA-1	0.1	
VCA0235	ackA-2	Acetate kinase, ackA-2	0.4	
Glycolysis				
VC0336	yibO	Phosphoglycerate mutase 23-bisphosphoglycerate-independent, yibO	0.5	
VC0478	fbaA	Fructose-bisphosphate aldolase class II, fbaA		2.8
VC2544	fbp	Fructose-16-bisphosphatase, fbp		4.3
VC2738	pckA	Phosphoenolpyruvate carboxykinase, pckA		3.1
VCA0843	gapA-2	Glyceraldehyde 3-phosphate dehydrogenase, gapA-2		3.1
VCA0987	ppsA	Phosphoenolpyruvate synthase, ppsA		2.3
TCA cycle				
VC0432	mdh	Malate dehydrogenase, mdh		3.8
VC0604	acnB	Aconitate hydratase 2, acnB		5.1
VC1141	icd	Isocitrate dehydrogenase NADP-dependent monomeric type, icd		2.7
VC2084	sucD	Succinyl-CoA synthase alpha subunit, sucD		6.6
VC2085	sucC	Succinyl-CoA synthase beta subunit, sucC		7.2
VC2086	sucB	2-oxoglutarate dehydrogenase E2 component, sucB		4.3
VC2087	sucA	2-oxoglutarate dehydrogenase E1 component, sucA		4.0
VC2088	sdhB	Succinate dehydrogenase iron-sulfur protein, sdhB		2.6
VC2089	sdhA	Succinate dehydrogenase flavoprotein subunit, sdhA		2.3
VC2091	sdhC	Succinate dehydrogenase cytochrome b556 subunit, sdhC	2.4	2.6
VC2092	gltA	Citrate synthase, gltA	3.5	4.3
Other metabolism				
VC0473	tktA-1	Pentose phosphate pathway, transketolase 1, tktA-1		2.6
VC1188	sfcA	Malate oxidoreductase, sfcA	0.3	
VC1725		Beta-ketoadipate enol-lactone hydrolase putative	2.9	
VC2350	deoC	Deoxyribose-phosphate aldolase, deoC	0.4	0.1

VC2413	aceF	Pyruvate dehydrogenase E2 component, aceF	0.2	
VC2414	aceE	Pyruvate dehydrogenase E1 component, aceE	0.2	
VC2613	prkB	Phosphoribulokinase, prkB		2.8
VC2669		5-carboxymethyl-2-hydroxymuconate delta isomerase putative		2.5
VC2681		Malate oxidoreductase putative	0.3	0.2
VCA0007		3-hydroxyisobutyrate dehydrogenase putative		2.7
VCA0623	talB	Transaldolase B, talB	0.4	0.3
VCA0657	glpD	Aerobic glycerol-3-phosphate dehydrogenase, glpD	13.0	
VCA0744	gplK	Glycerol kinase, gplK	5.6	4.9
Pathogenesis				
VC0824	tagD	TagD protein, tagD	0.3	
VC0826	tcpP	Toxin co-regulated pilus biosynthesis protein P, tcpP	0.2	0.2
VC0827	tcpH	Toxin co-regulated pilus biosynthesis protein H, tcpH		0.3
VC0828	tcpA	Toxin co-regulated pilin, tcpA	0.3	
VC0838	toxT	TCP pilus virulence regulatory protein, toxT		0.3
VC0839	tcpJ	Leader peptidase TcpJ, tcpJ		0.3
VC0840	acfB	Accessory colonization factor AcfB, acfB		0.4
VC0841	acfC	Accessory colonization factor AcfC, acfC	0.4	0.3
VC0959		Hemolysin putative		0.4
VC1450	rtxC	RTX toxin activating protein, rtxC	0.2	0.2
VC1456	ctxB	Cholera enterotoxin B subunit, ctxB	0.5	
VC1457	ctxA	Cholera enterotoxin A subunit, ctxA	0.4	
VCA0837		Hemolysin putative	2.4	
VCA1043	tagE-2	TagE protein, tagE-2	2.8	
Protein fate				
VC0018	ibpA	16 kDa heat shock protein A, ibpA	0.2	
VC0034	tpcG	Thiol:disulfide interchange protein, tpcG	0.3	
VC0046	def-1	Polypeptide deformylase, def-1	0.5	
VC0067		Aminopeptidase P		2.2
VC0157		Alkaline serine protease	2.4	
VC0188	prlC	Oligopeptidase A, prlC	0.3	
VC0566	htrA	Protease DO, htrA	0.5	0.3
VC0711	clpB-1	ClpB protein, clpB-1	0.2	0.3
VC0717		Protease putative	0.4	
VC0854	grpE	Heat shock protein GrpE, grpE	0.2	
VC0855	dnaK	DnaK protein, dnaK	0.0	0.2
VC0856	dnaJ	DnaJ protein, dnaJ	0.1	
VC0985	htpG	Heat shock protein HtpG, htpG	0.1	0.1
VC1039	asmA	AsmA protein, asmA	0.4	
VC1414		Thermostable carboxypeptidase 1		2.7
VC1494	pepN	Aminopeptidase N, pepN	2.3	2.4
VC1735	aat	Leucyl/phenylalanyl-tRNA protein transferase, aat	0.2	
VC1756		Periplasmic linker protein putative	0.2	
VC1920	lon	ATP-dependent protease LA, lon	0.2	

VC1983		Peptidase putative		10.6
VC2445	exeA	General secretion pathway protein A, exeA	2.4	
VC2664	groEL-1	Chaperonin 60 Kd subunit, groEL-1	0.0	0.1
VC2665	groES-1	Chaperonin 10 Kd subunit, groES-1	0.0	0.1
VC2674	hslU	Protease HslVU ATPase subunit HslU, hslU	0.3	
VC2675	hslV	Protease HslVU subunit HslV, hslV	0.3	
VCA0150	def-2	Polypeptide deformylase, def-2	0.1	0.2
VCA0661		Peptidyl-prolyl cis-trans isomerase-related protein	0.4	
Protein synthesis				
VC0663		Peptide chain release factor 2 , prfB	0.4	
VC0631	tyrS-2	Tyrosyl-tRNA synthetase, tyrS-2	0.4	
VC0643	infB	Initiation factor IF-2, infB	2.4	
VC0645	truB	tRNA pseudouridine 55 synthase, truB	4.3	
VC0659	prfC	Peptide chain release factor 3, prfC	0.4	
VC0664	lysU	Lysyl-tRNA synthetase heat inducible, lysU	0.4	
VC0875	proS	Prolyl-tRNA synthetase, proS	0.3	
VC0999	truA	tRNA pseudouridine synthase A, truA	0.5	
VC1036	metG	Methionyl-tRNA synthetase, metG	0.4	
VC1110	serS	Seryl-tRNA synthetase, serS	0.4	
VC1209		Elongation factor P family protein	0.2	
VC1220	pheT	Phenylalanyl-tRNA synthetase beta chain, pheT	0.5	
VC1297	asnS	Asparaginyl-tRNA synthetase, asnS	0.5	
VC1374		DnaK-related protein	0.3	
VC1737	infA	Initiation factor IF-1, infA	0.2	0.1
VC1910	miaE	tRNA-(MS[2]IO[6]A)-hydroxylase, miaE		0.4
VC2028	rluC	Ribosomal large subunit pseudouridine synthase C, rluC		0.3
VC2214	gltX	Glutamyl-tRNA synthetase, gltX	0.3	
VC2503	valS	Valyl-tRNA synthetase, valS	0.3	
VC2623	trpS	Tryptophanyl-tRNA synthetase, trpS	0.5	
VC2660	efp	Elongation factor P, efp	0.5	0.4
VCA0287	thrS	Threonyl-tRNA synthetase, thrS	2.7	
Purines, pyrimidines, nucleosides, and nucleotides				
VC0052	purE	Purine ribonucleotide biosynthesis, purE	4.3	13.1
VC0275	purD	Glycine ligase, purD		7.9
VC0276	purH	Purine ribonucleotide biosynthesis, purH		11.4
VC0441	apaH	Bis(5-nucleosyl)-tetraphosphatase, apaH	2.7	
VC0585	hpt	Salvage of nucleosides and nucleotides, hpt	0.5	
VC0767	guaB	Inosine-5-monophosphate dehydrogenase, guaB		2.8
VC0768	guaA	GMP synthase, guaA		3.4
VC0869	purL	Purine ribonucleotide biosynthesis, purL		16.4
VC0986	adk	Adenylate kinase, adk	0.3	0.4
VC1004	purF	Amidophosphoribosyltransferase, purF		2.0
VC1126	purB	Adenylosuccinate lyase, purB		2.8
VC1129	gsk-1	Inosine-guanosine kinase, gsk-1	0.2	0.2

VC1167	tdk	Thymidine kinase, tdk	0.3	
VC1228	purT	Purine ribonucleotide biosynthesis, purT		8.0
VC1255	nrdB	2-Deoxyribonucleotide metabolism, nrdB	0.4	
VC1256	nrdA	2-Deoxyribonucleotide metabolism, nrdA	0.4	
VC1992	purU	Formyltetrahydrofolate deformylase, purU	2.6	
VC2016	tmk	Thymidylate kinase, tmk	0.4	
VC2183	prsA	Ribose-phosphate pyrophosphokinase, prsA	0.2	
VC2225	upp	Salvage of nucleosides and nucleotides, upp	0.4	
VC2226	purM	Purine ribonucleotide biosynthesis, purM	3.0	17.7
VC2227	purN	Purine ribonucleotide biosynthesis, purN		26.9
VC2277	gpt	Salvage of nucleosides and nucleotides, gpt	0.5	
VC2347	deoD-1	Purine nucleoside phosphorylase, deoD-1	0.3	0.3
VC2348	deoB	Phosphopentomutase, deoB	0.5	0.3
VC2349	deoA	Thymidine phosphorylase, deoA	0.4	0.3
VC2390	carA	Pyrimidine ribonucleotide biosynthesis, carA		2.7
VC2510	pyrB	Pyrimidine ribonucleotide biosynthesis, pyrB	2.4	14.7
VC2511	pyrI	Pyrimidine ribonucleotide biosynthesis, pyrI		7.6
VCA0053	deoD-2	Purine nucleoside phosphorylase, deoD-2	0.5	0.3
VCA0197	guaC	GMP reductase, guaC	0.4	
VCA0801	gsk-2	Inosine-guanosine kinase, gsk-2		0.3
VCA0925	pyrC	Dihydroorotase, pyrC		2.7
Regulatory functions				
VC0290	fis	Factor-for-inversion stimulation protein, fis	0.1	0.1
VC0307	rho	Transcription termination factor Rho, rho	0.4	
VC0328	rpoB	DNA-directed RNA polymerase beta subunit, rpoB	0.4	
VC03291	rpoC	DNA-directed RNA polymerase beta subunit, rpoC	0.3	
VC03292	rpoC	DNA-directed RNA polymerase beta subunit, rpoC	0.4	
VC0330	rsd	Regulator of sigma D, rsd	2.9	2.6
VC0347		RNA-binding protein, hfq	2.3	
VC0594	pcnB	PolyA polymerase, pcnB	0.6	
VC0601	hrpB	ATP-dependent helicase HrpB, hrpB	0.5	
VC0644	rbfA	RNA processing, ribosome-binding factor A, rbfA	4.6	
VC0647	pnp	Polyribonucleotide nucleotidyltransferase, pnp	3.8	
VC0693		Response regulator		2.4
VC0706		Sigma-54 modulation protein putative	0.3	
VC0812		Helicase-related protein	0.6	
VC1021	luxO	LuxO repressor protein, luxO	0.2	
VC1142	cspD	Cold shock-like protein CspD, cspD		11.7
VC1222	himA	Integration host factor alpha subunit, himA	2.2	
VC1320		DNA-binding response regulator	0.5	
VC1796		Middle operon regulator-related protein	2.6	
VC1904	lrp	Leucine-responsive regulatory protein, lrp	2.7	
VC1907	cysB	Cys regulon Transcriptional activator, cysB	2.1	
VC2302		RNA polymerase sigma-70 factor ECF subfamily	2.0	2.2
VC2415	pdhR	Pyruvate dehydrogenase complex repressor, pdhR	0.3	
VC2433	cpdA	Cyclic AMP phosphodiesterase, cpdA	0.4	

VC2466	rseA	Sigma-E factor negative regulatory protein RseA, rseA	2.0	
VC2530		Sigma-54 modulation protein putative		2.4
VC2533	ptsO	Phosphocarrier protein NPr, ptsO	0.2	
VC2709	rpoZ	DNA-directed RNA polymerase omega subunit, rpoZ		0.5
VC2744	typA	GTP-binding protein TypA, typA	0.5	
VCA0166	cspA	Cold shock Transcriptional regulator CspA, cspA	2.9	
VCA0519	fruR	Fructose repressor, fruR	0.4	0.2
VCA0607		Regulator of nucleoside diphosphate kinase	0.6	
VCA0709	torS	Sensor protein TorS, torS	0.4	
VCA0804	deaD	ATP-dependent RNA helicase DeaD, deaD	6.5	
VCA0933	cspV	Cold shock domain family protein	51.2	2.6
VCA0990		ATP-dependent RNA helicase DEAD box family		8.3
VCA1087		Anti-sigma F factor antagonist putative	0.5	
Transcriptional regulators				
VC0166		Transcriptional regulator, TetR family	0.3	
VC0278		Transcriptional regulator, CadC putative	0.3	
VC0583	hapR	Transcription factor, hapR	0.2	
VC0649		Transcriptional regulator, MarR family	2.0	
VC0665	vpsR	Transcriptional regulator, sigma-54 dependent vpsR	2.2	
VC0677	nhaR	Transcriptional activator protein NhaR, nhaR	2.0	
VC0701		trp operon repressor putative	0.3	
VC1213		Transcriptional regulator, LuxR family	2.1	
VC1968		Transcriptional regulator, HTH3 family	2.3	
VC2485		Transcriptional regulator, LysR family	0.4	0.3
VC2636		Transcriptional regulator, LysR family	2.0	
VC2647	aphA	Transcriptional regulator, PadR N-terminal-like, aphA	7.3	
VC2702		Transcriptional regulator, LuxR family	2.4	5.3
VCA0542		Transcriptional regulator, LysR family	0.5	
VCA0575		Transcriptional regulator, LysR family	2.2	
VCA0642		Transcriptional regulator, ArsR family		3.0
VCA0888		Transcriptional regulator, LuxR family	2.8	
VCA0952	vpsT	Transcriptional regulator, LuxR family, vpsT	2.4	0.3
Amino Acid transport and binding				
VC0171		Peptide ABC transporter periplasmic peptide-binding protein		2.6
VC1091	oppA	Oligopeptide ABC transporter, oppA		4.8
VC1092	oppB	Oligopeptide ABC transporter permease protein, oppB		4.1
VC1093	oppC	Oligopeptide ABC transporter permease protein, oppC		4.4
VC1094	oppD	Oligopeptide ABC transporter ATP-binding protein, oppD		4.4
VC1095	oppF	Oligopeptide ABC transporter ATP-binding protein, oppF		6.6
VC1362		Amino acid ABC transporter periplasmic amino acid-binding protein	5.4	4.5
VC1422		Sodium/alanine symporter	2.8	
VC1658	sdaC-2	Serine transporter, sdaC-2		0.4

VC1680	sapA	Peptide ABC transporter periplasmic peptide-binding protein, sapA	0.4	
VC1863		Amino acid ABC transporter periplasmic amino acid-binding protein	2.7	2.3
VC1864		Amino acid ABC transporter ATP-binding protein	4.7	5.0
VC2537		Thiamine ABC transporter ATP-binding protein putative	0.5	
VC2538		Thiamine ABC transporter permease protein putative	0.4	
VCA0759	artI	Arginine ABC transporter periplasmic arginine-binding protein, artI	3.6	8.8
VCA0978		Amino acid ABC transporter periplasmic amino acid-binding protein	2.0	
Anion/ cation transport and binding				
VC0475	irgA	Enterobactin receptor, irgA	0.4	
VC0608		Iron(III) ABC transporter periplasmic iron-compound-binding protein		2.2
VC0724	pstC-1	Phosphate ABC transporter permease protein, pstC-1	0.5	
VC1264		Iron-regulated protein A putative	0.4	
VC1437		Cation transport ATPase E1-E2 family	2.2	
VC1544	tonB2	TonB2 protein, tonB2	0.3	
VC1545	exbD2	TonB system transport protein ExbD2, exbD2	0.3	
VC1546	exbB2	TonB system transport protein ExbB2, exbB2	0.5	
VC1547		Biopolymer transport protein ExbB-related protein	0.3	
VC1627	nhaA	Na+/H+ antiporter protein, nhaA	2.2	
VC1655	mgtE-1	Magnesium transporter, mgtE-1	0.3	0.1
VC1757		Transporter AcrB/D/F family	0.5	
VC2082	znuC	Zinc ABC transporter ATP-binding protein, znuC	3.1	
VC2442		pho4 family protein	0.5	
VCA0227	vctP	Vibriobactin and enterobactin ABC transporter, vctP	0.3	
VCA0576	hutA	Heme transport protein HutA, hutA	0.4	
Carbohydrate transport and binding				
VC0910	treB	PTS system trehalose-specific IIBC component, treB		2.4
VC1235		sodium/dicarboxylate symporter	0.2	0.1
VC1695		Formate transporter 1 putative	0.2	
VC1779	dctP-1	C4-dicarboxylate-binding periplasmic protein, dctP-1	6.1	
VC1823	frwB	PTS system fructose-specific IIB component, frwB	2.6	4.6
VC2013	ptsG	PTS system glucose-specific IIBC component, ptsG	0.5	
VCA0516	fruA-2	PTS system fructose-specific IIBC component, fruA-2	0.2	0.1
VCA0518	fruB	PTS system fructose-specific IIA/FPR component, fruB	0.3	0.3
VCA0943	malG	Maltose ABC transporter permease protein, malG	0.5	4.3
VCA0945	malE	Maltose ABC transporter, malE	0.4	5.0
VCA0946	malK	Maltose/maltodextrin ABC transporter , malK	0.4	
VCA1028	ompS	Maltoporin, ompS		3.0
Spermidine/putrescine transport and binding				
VC1424	potD-1	Spermidine/putrescine ABC transporter, potD-1	0.4	

VC1425	potD-2	Spermidine/putrescine ABC transporter, potD-2	0.1	
VC1426	potC	Spermidine/putrescine ABC transporter permease protein, potC	0.3	
VC1427	potB	Spermidine/putrescine ABC transporter permease protein, potB	0.2	
VC1428	potA	Spermidine/putrescine ABC transporter ATP-binding protein, potA	0.3	
Other transport and binding				
VC0589		ABC transporter ATP-binding protein	0.2	
VC0590		Permease putative	0.5	
VC0698		ABC transporter ATP-binding protein	0.4	
VC0972		Porins, porin putative	2.8	
VC1103		ABC transporter ATP-binding protein	3.4	
VC1168	gltP-1	Proton/glutamate symporter, gltP-1	2.0	3.0
VC1180	cydC	Transport ATP-binding protein CydC, cydC	0.5	
VC1447	rtxD	RTX toxin transporter, rtxD	0.4	
VC1630		ABC transporter ATP-binding protein		0.3
VC1660		ABC transporter ATP-binding protein putative		2.6
VC1854	ompT	OmpT protein, ompT		6.1
VC1878	msbA	Transport ATP-binding protein MsbA, msbA	0.5	
VC2162		Permease PerM putative	3.2	
VC2171	uraA	Uracil permease, uraA	0.4	
VC2305	ompK	Outer membrane protein OmpK, ompK	0.5	
VC2761		Multidrug resistance protein		0.4
VCA0179		Nucleosides purines and pyrimidines, NupC family protein	0.4	0.3
VCA0214	emrD-2	Multidrug resistance protein D, emrD-2	5.1	2.6
VCA0782		ABC transporter ATP-binding protein	2.3	
VCA0807		ABC transporter periplasmic substrate-binding protein		4.2
VCA0904		Permease	3.0	
Type VI secretion				
VC1415	hcp-1	Hemolysin-coregulated protein, hcp-1	0.2	
VCA0017	hcp2	Hemolysin-coregulated protein, hcp-2	0.0	
VCA0107	vipA	Hypothetical, vipA	0.3	2.4
VCA0108	vipB	Hypothetical, vipB	0.3	2.6
VCA0109		Hypothetical	0.2	2.9
VCA0112	fha	Hypothetical, fha	0.4	3.4
VCA0114	vasE	Hypothetical, vasE	0.5	2.9
VCA0119	vasJ	Hypothetical, vasJ	0.3	
VCA0120	vasK	Hypothetical, vasK	0.5	
Other functions				
VC0003	thdF	Thiophene and furan oxidation protein ThdF, thdF	0.6	
VC0036		FixG-related protein		2.2
VC0039		SpoOM-related protein	2.0	
VC0049	smg	Smg protein, smg	2.0	

VC0255		rfbT-related protein	2.8	
VC0258	rfbT	rfbT protein, rfbT	3.1	
VC0291		NifR3/Smm1 family protein	0.3	0.3
VC0348	hflX	GTP-binding protein HflX, hflX	2.0	
VC0437		GTP1/Obg family protein	3.1	
VC0446	imp	Organic solvent tolerance protein, imp	0.2	
VC0627		HesB family protein	0.5	
VC0687		Carbon starvation protein A putative	4.1	
VC0731		Detoxification, antioxidant AhpC/Tsa family	0.2	
VC0750		HesB family protein	2.5	
VC0763		GTP-binding protein	2.9	
VC0851	smpA	Small protein A, smpA	3.1	
VC0864	yfhC	YfhC protein, yfhC	0.5	
VC0870	tnpA	IS1004 transposase, tnpA	2.7	
VC1003		Bacteriocin production protein		4.6
VC1022	luxU	Phosphorelay protein, luxU	0.2	
VC1037	mrp	Mrp protein, mrp	0.4	
VC1455	rstR-1	Transcriptional repressor RstR, rstR-1	3.3	
VC1470	tlcR-1	TlcR protein, tlcR-1	0.4	
VC1532		ROK family protein		2.2
VC1579		Enterobactin synthetase component F-related protein	0.2	0.3
VC1599		GGDEF family protein		5.2
VC1676	pspC	Phage shock protein C, pspC	0.3	
VC1677	pspB	Phage shock protein B, pspB	0.5	
VC1696		DNA-binding protein inhibitor Id-2-related protein		2.9
VC1736		Arginyl-tRNA-protein transferase-related protein	0.4	
VC1998		PilB-related protein	0.3	
VC2153		DD-carboxypeptidase-related protein		3.7
VC2160	bcp	Dacterioferritin comigratory protein, bcp	0.4	
VC2361		Formate acetyl transferase-related protein	0.3	
VC2774	gidB	Glucose inhibited division protein B, gidB	0.5	
VCA0175		MoxR-related protein	0.4	
VCA0308		Eeoxyguanosinetriphosphate triphosphohydrolase-related protein	0.5	
VCA0324	dinJ	DNA-damage-inducible protein J, dinJ	0.5	
VCA0337	mccF-1	Microcin immunity protein MccF, mccF-1	2.3	
VCA0387		Toxin resistance protein	2.0	
VCA0439	mccF-2	Microcin immunity protein MccF, mccF-2	2.0	
VCA0493	tnpA	IS1004 transposase, tnpA	2.7	
VCA0549	phnA	PhnA protein, phnA	0.4	
VCA0628		SecA-related protein		2.3
VCA0633	glpM	GlpM protein glpM		7.2
VCA1006		Organic hydroperoxide resistance protein putative	3.8	
Hypothetical				
VC0025		Hypothetical protein	14.7	3.9
VC0038		Hypothetical protein	2.2	2.6

VC0184	Hypothetical protein	3.3	
VC0292	Hypothetical protein	0.5	
VC0343	Hypothetical protein	0.4	
VC0491	Hypothetical protein	0.4	
VC0549	Hypothetical protein		4.6
VC0600	Hypothetical protein	0.5	
VC0712	Hypothetical protein	2.1	
VC0714	Hypothetical protein	2.8	
VC0764	Hypothetical protein	4.4	
VC0823	Hypothetical protein	2.0	
VC0862	Hypothetical protein	0.5	
VC0886	Hypothetical protein	0.2	
VC0901	Hypothetical protein	0.5	
VC0922	Hypothetical protein	7.2	
VC0926	Hypothetical protein	6.8	
VC0928	Hypothetical protein	5.6	
VC0933	Hypothetical protein	3.9	
VC0935	Hypothetical protein	6.0	
VC1077	Hypothetical protein	0.4	
VC1078	Hypothetical protein	0.4	
VC1125	Hypothetical protein	3.4	3.1
VC1158	Hypothetical protein	2.6	3.9
VC1183	Hypothetical protein	2.0	
VC1191	Hypothetical protein	3.1	
VC1224	Hypothetical protein	3.0	
VC1246	Hypothetical protein	0.5	
VC1247	Hypothetical protein	2.2	
VC1266	Hypothetical protein	0.4	
VC1272	Hypothetical protein	0.1	0.3
VC1368	Hypothetical protein	2.4	
VC1371	Hypothetical protein	3.6	
VC1380	Hypothetical protein	0.5	
VC1438	Hypothetical protein	2.0	
VC1449	Hypothetical protein	0.2	0.2
VC1471	Hypothetical protein	5.8	
VC1479	Hypothetical protein	2.8	
VC1480	Hypothetical protein	2.4	
VC1493	Hypothetical protein	6.5	
VC1510	Hypothetical protein	2.1	
VC1514	Hypothetical protein	3.1	
VC1517	Hypothetical protein	6.1	3.1
VC1518	Hypothetical protein	6.2	
VC1543	Hypothetical protein	0.2	
VC1548	Hypothetical protein	0.2	
VC1559	Hypothetical protein	0.5	
VC1564	Hypothetical protein	0.4	
VC1577	Hypothetical protein	0.2	0.3

VC1578	Hypothetical protein	0.1	0.3
VC1642	Hypothetical protein	0.2	
VC1654	Hypothetical protein	0.3	
VC1738	Hypothetical protein	0.4	
VC1743	Hypothetical protein	2.0	
VC1780	Hypothetical protein	3.4	
VC1808	Hypothetical protein		2.2
VC1810	Hypothetical protein	2.6	
VC1943	Hypothetical protein		11.0
VC1964	Hypothetical protein	4.9	
VC1999	Hypothetical protein	0.2	
VC2002	Hypothetical protein		8.3
VC2010	Hypothetical protein	2.0	
VC2011	Hypothetical protein		5.4
VC2149	Hypothetical protein	0.3	
VC2154	Hypothetical protein	2.1	3.1
VC2155	Hypothetical protein	5.6	
VC2221	Hypothetical protein	0.3	
VC2357	Hypothetical protein		3.0
VC2388	Hypothetical protein	3.2	
VC2395	Hypothetical protein	2.0	
VC2486	Hypothetical protein	0.4	
VC2509	Hypothetical protein		5.5
VC2543	Hypothetical protein		3.4
VC2605	Hypothetical protein	2.2	
VC2663	Hypothetical protein	0.3	0.3
VC2737	Hypothetical protein	0.4	
VCA0005	Hypothetical protein	0.2	0.2
VCA0052	Hypothetical protein	0.4	
VCA0078	Hypothetical protein		3.5
VCA0125	Hypothetical protein	2.7	
VCA0139	Hypothetical protein	2.8	0.5
VCA0169	Hypothetical protein	0.6	
VCA0170	Hypothetical protein	0.3	
VCA0190	Hypothetical protein	2.1	
VCA0236	Hypothetical protein	0.2	
VCA0240	Hypothetical protein	2.1	
VCA0252	Hypothetical protein		0.4
VCA0259	Hypothetical protein	2.1	
VCA0260	Hypothetical protein	2.2	2.5
VCA0261	Hypothetical protein	5.0	5.9
VCA0271	Hypothetical protein	2.4	
VCA0285	Hypothetical protein	2.0	
VCA0297	Hypothetical protein	2.5	
VCA0303	Hypothetical protein	2.0	2.2
VCA0312	Hypothetical protein	2.4	
VCA0331	Hypothetical protein	4.7	5.5

VCA0333	Hypothetical protein	2.9	
VCA0358	Hypothetical protein	2.2	2.4
VCA0375	Hypothetical protein	2.5	
VCA0390	Hypothetical protein	2.2	
VCA0408	Hypothetical protein	2.3	
VCA0425	Hypothetical protein	2.0	
VCA0448	Hypothetical protein	2.4	2.3
VCA0450	Hypothetical protein	6.2	
VCA0452	Hypothetical protein	3.2	
VCA0457	Hypothetical protein	2.1	
VCA0458	Hypothetical protein	2.6	2.5
VCA0460	Hypothetical protein	2.3	
VCA0462	Hypothetical protein	2.6	
VCA0465	Hypothetical protein		3.0
VCA0486	Hypothetical protein	0.5	
VCA0535	Hypothetical protein	5.3	
VCA0537	Hypothetical protein		2.3
VCA0556	Hypothetical protein	0.4	
VCA0593	Hypothetical protein	3.2	
VCA0652	Hypothetical protein	0.4	
VCA0670	Hypothetical protein		2.6
VCA0721	Hypothetical protein	0.2	
VCA0722	Hypothetical protein		0.4
VCA0742	Hypothetical protein	2.2	
VCA0770	Hypothetical protein	9.0	
VCA0771	Hypothetical protein	8.6	
VCA0796	Hypothetical protein	0.5	
VCA0799	Hypothetical protein	2.5	
VCA0806	Hypothetical protein	2.1	
VCA0821	Hypothetical protein	0.2	0.1
VCA0842	Hypothetical protein		2.8
VCA0849_1	Hypothetical protein	3.8	
VCA0849_2	Hypothetical protein	3.6	
VCA0849_3	Hypothetical protein	3.7	
VCA0874	Hypothetical protein	43.1	5.5
VCA0881	Hypothetical protein	0.5	
VCA0882	Hypothetical protein	0.5	
VCA0883	Hypothetical protein	0.4	2.4
VCA0920	Hypothetical protein	4.1	
VCA0921	Hypothetical protein	0.4	
VCA0997	Hypothetical protein	0.3	
VCA1035	Hypothetical protein	0.5	
Hypothetical conserved			
VC0131	Hypothetical protein, conserved	0.3	

VC0134	Hypothetical protein, conserved	0.3	
VC0153	Hypothetical protein, conserved		2.9
VC0163	Hypothetical protein, conserved	0.3	
VC0239	Hypothetical protein, conserved	0.4	
VC0254	Hypothetical protein, conserved	2.9	
VC0264	Hypothetical protein, conserved	2.7	
VC0265	Hypothetical protein, conserved	0.4	
VC0428	Hypothetical protein, conserved	0.4	
VC0438	Hypothetical protein, conserved	2.9	
VC0519	Hypothetical protein, conserved		0.4
VC0648	Hypothetical protein, conserved	2.4	
VC0661	Hypothetical protein, conserved	0.6	
VC0708	Hypothetical protein, conserved	2.2	
VC0710	Hypothetical protein, conserved	2.5	
VC0718	Hypothetical protein, conserved		2.9
VC0747	Hypothetical protein, conserved	2.8	
VC0757	Hypothetical protein, conserved	0.4	
VC0765	Hypothetical protein, conserved	2.3	
VC0770	Hypothetical protein, conserved	0.1	0.3
VC0845	Hypothetical protein, conserved	2.4	
VC0876	Hypothetical protein, conserved	2.0	
VC0882	Hypothetical protein, conserved	2.0	
VC0902	Hypothetical protein, conserved	0.4	
VC0913	Hypothetical protein, conserved	2.1	
VC0945	Hypothetical protein, conserved	0.2	
VC0962	Hypothetical protein, conserved	0.4	
VC0975	Hypothetical protein, conserved		3.4
VC0976	Hypothetical protein, conserved		2.5
VC0977	Hypothetical protein, conserved	0.2	
VC0981	Hypothetical protein, conserved	0.6	
VC1048	Hypothetical protein, conserved	2.2	
VC1055	Hypothetical protein, conserved	0.2	
VC1101	Hypothetical protein, conserved	2.2	
VC1121	Hypothetical protein, conserved	2.1	
VC1151	Hypothetical protein, conserved	2.9	
VC1153	Hypothetical protein, conserved	2.2	
VC1163	Hypothetical protein, conserved	0.5	
VC1198	Hypothetical protein, conserved	2.0	3.7
VC1208	Hypothetical protein, conserved	0.3	
VC1217	Hypothetical protein, conserved	0.5	
VC1249	Hypothetical protein, conserved	0.3	
VC1259	Hypothetical protein, conserved	0.2	
VC1317	Hypothetical protein, conserved	0.5	
VC1364	Hypothetical protein, conserved	2.1	
VC1432	Hypothetical protein, conserved	0.3	
VC1433	Hypothetical protein, conserved	2.8	2.2
VC1498	Hypothetical protein, conserved	0.4	

VC1523	Hypothetical protein, conserved		3.5
VC1606	Hypothetical protein, conserved	0.4	
VC1628	Hypothetical protein, conserved		0.3
VC1645	Hypothetical protein, conserved		3.5
VC1647	Hypothetical protein, conserved	0.4	
VC1722	Hypothetical protein, conserved	3.1	
VC1731	Hypothetical protein, conserved	2.9	
VC1755	Hypothetical protein, conserved	0.4	
VC1766	Hypothetical protein, conserved	0.4	
VC1767	Hypothetical protein, conserved	0.6	
VC1811	Hypothetical protein, conserved	2.4	
VC1841	Hypothetical protein, conserved	0.4	
VC1842	Hypothetical protein, conserved	0.4	
VC1871	Hypothetical protein, conserved	0.1	
VC1893	Hypothetical protein, conserved	2.1	2.4
VC1931	Hypothetical protein, conserved	4.4	3.6
VC1938	Hypothetical protein, conserved	2.9	
VC1939	Hypothetical protein, conserved	5.3	4.7
VC1989	Hypothetical protein, conserved	0.3	
VC2001	Hypothetical protein, conserved		2.5
VC2014	Hypothetical protein, conserved	0.3	0.3
VC2017	Hypothetical protein, conserved	0.5	
VC2039	Hypothetical protein, conserved	0.5	
VC2110	Hypothetical protein, conserved	0.2	
VC2112	Hypothetical protein, conserved	0.4	
VC2113	Hypothetical protein, conserved	0.5	
VC2146	Hypothetical protein, conserved	2.6	
VC2163	Hypothetical protein, conserved	2.2	
VC2172	Hypothetical protein, conserved	0.5	
VC2303	Hypothetical protein, conserved	0.5	
VC2378	Hypothetical protein, conserved	3.1	
VC2429	Hypothetical protein, conserved	0.5	
VC2434	Hypothetical protein, conserved	0.4	
VC2443	Hypothetical protein, conserved	0.4	
VC2498	Hypothetical protein, conserved	0.6	
VC2507	Hypothetical protein, conserved	3.3	
VC2512	Hypothetical protein, conserved	0.4	
VC2527	Hypothetical protein, conserved	0.5	
VC2546	Hypothetical protein, conserved	2.1	2.2
VC2615	Hypothetical protein, conserved	10.0	5.9
VC2620	Hypothetical protein, conserved	0.4	
VC2647	Hypothetical protein, conserved	7.3	
VC2686	Hypothetical protein, conserved		0.3
VC2720	Hypothetical protein, conserved	2.0	
VCA0006	Hypothetical protein, conserved	0.2	0.3
VCA0037	Hypothetical protein, conserved		2.4
VCA0040	Hypothetical protein, conserved	0.5	

VCA0048	Hypothetical protein, conserved	0.3	
VCA0076	Hypothetical protein, conserved	0.3	
VCA0079	Hypothetical protein, conserved	0.5	
VCA0097	Hypothetical protein, conserved	0.4	
VCA0159	Hypothetical protein, conserved	2.7	
VCA0163	Hypothetical protein, conserved	2.8	
VCA0171	Hypothetical protein, conserved	0.2	
VCA0172	Hypothetical protein, conserved	0.3	0.3
VCA0323	Hypothetical protein, conserved	0.5	
VCA0338	Hypothetical protein, conserved	2.0	2.6
VCA0345	Hypothetical protein, conserved		2.5
VCA0487	Hypothetical protein, conserved	0.3	
VCA0488	Hypothetical protein, conserved	0.5	
VCA0527	Hypothetical protein, conserved		2.4
VCA0544	Hypothetical protein, conserved	2.0	
VCA0569	Hypothetical protein, conserved		3.0
VCA0586	Hypothetical protein, conserved	2.5	
VCA0689	Hypothetical protein, conserved		15.0
VCA0732	Hypothetical protein, conserved	0.3	
VCA0743	Hypothetical protein, conserved		0.3
VCA0763	Hypothetical protein, conserved	0.3	
VCA0769	Hypothetical protein, conserved	9.7	
VCA0789	Hypothetical protein, conserved	2.2	
VCA0838	Hypothetical protein, conserved	2.3	
VCA0903	Hypothetical protein, conserved	6.2	
VCA0907	Hypothetical protein, conserved	0.5	
VCA0931	Hypothetical protein, conserved	2.4	
VCA0986	Hypothetical protein, conserved		6.2
VCA1004	Hypothetical protein, conserved	2.4	
VCA1042	Hypothetical protein, conserved	2.3	
VCA1072	Hypothetical protein, conserved	2.2	
VCA1085	Hypothetical protein, conserved		2.6

Supplementary Figure S2

Gene ID	Gene Name	FUNCTIONS	Fold Change (Δ*cspV*/wt) 37°C	15°C
Biofilm formation				
VC0928	rbmA	Rugosity and biofilm structure modulator A	0.19	0.25
VC0932	rbmE	Rugosity and biofilm structure modulator E		0.27
VC0933	rbmF	Rugosity and biofilm structure modulator F		0.23
Cell envelope				
VC0263		Galactosyl-transferase putative		2.19
VCA0867	ompW	Outer membrane protein OmpW, ompW	4.12	
Chemotaxis and motility				
VC1313		Methyl-accepting chemotaxis protein		2.75
VC2191	flgM	Flagellar hook-associated protein FlgM, flgM		2.50
VC2193	flgI	Flagellar P-ring protein FlgI, flgI		3.33
VC2195	flgG	Flagellar basal-body rod protein FlgG, flgG		3.21
VC2601	motX	Sodium-type flagellar protein MotX, motX		2.00
Central intermediary metabolism				
VC0238		transferase hexapeptide repeat family		3.10
VC1114	bioC	Biotin synthesis protein BioC, bioC		
VCA0637		oxygen-insensitive NAD(P)H nitroreductase		0.39
DNA metabolism				
VC0482	iciA	Chromosome initiation inhibitor, iciA		2.07
VC2385		RNA-directed DNA polymerase		2.30
Energy metabolism				
VC1069	gap	Glyceraldehyde 3-phosphate dehydrogenase, gap		4.88
VC1300	sdaA-1	L-serine dehydratase 1, sdaA-1		0.44
VC1616		Glutaredoxin_ putative ||	0.07	
VC1905	ald	Alanine dehydrogenase, ald		0.45
VC2033	adhE	Alcohol dehydrogenase/acetaldehyde dehydrogenase, adhE	5.72	
VC2544	fbp	Fructose-1 6-bisphosphatase, fbp		0.38
VC2698	aspA	Aspartate ammonia-lyase, aspA		0.40
VCA0235	ackA-2	Acetate kinase, ackA-2		0.29
VCA0656	cscK	Fructokinase, cscK		0.34
VCA0677	napD	NapD protein || napD	3.93	
VCA0749	glpC	Anaerobic glycerol-3-phosphate dehydrogenase subunit C, glpC		3.39
VCA082	phhA	Phenylalanine-4-hydroxylase, phhA		2.70

8				
VCA0875	dsdA	D-serine dehydratase, dsdA		5.43
Pathogenesis				
VC0827	tcpH	Toxin co-regulated pilus biosynthesis protein H, tcpH		2.20
VC0828	tcpA	Toxin co-regulated pilin, tcpA		2.98
VC1451	rtxA	RTX toxin RtxA , rtxA	4.08	
VCA0594	hlx	Hemolysin, hlx		0.47
Protein fate				
VC0566	htrA	Protease, htrA		1.94
VC1343		Peptidase M20A family		0.25
VC1920	lon	ATP-dependent protease LA, lon	3.75	
Protein synthesis				
VC0878		Ribosomal protein L31P family		0.40
VC0879		Ribosomal protein L36, putative		0.44
VCA0104	rluA-2	Ribosomal large subunit pseudouridine synthase A, rluA-2		2.25
Purines, pyrimidines, nucleosides, and nucleotides				
VC0052	purE	Phosphoribosylaminoimidazole carboxylase catalytic subunit, purE		0.27
VC2448	pyrG	Pyrimidine ribonucleotide biosynthesis CTP synthase, pyrG	3.07	
VCA0053	deoD-2	Purine nucleoside phosphorylase, deoD-2		0.40
VCA0511	nrdD	Anaerobic ribonucleoside-triphosphate reductase, nrdD	3.28	
Regulatory functions				
VC0290	fis	Factor-for-inversion stimulation protein, fis		2.41
VC1070		phosphatase putative		2.68
VC1445	vpsS	Sensor histidine kinase/response regulator		2.94
VC2302		RNA polymerase sigma-70 factor ECF subfamily		0.42
VC2464	rseC	Sigma-E factor regulatory protein RseC, rseC		2.04
VC2709	rpoZ	DNA-directed RNA polymerase omega subunit, rpoZ		0.49
VCA0189		response regulator		2.39
VCA0519	fruR	Fructose repressor, fruR		0.18
VCA0531		Sensor histidine kinase	3.51	
VCA0675	narQ	Nitrate/nitrite sensor protein NarQ, narQ	3.05	
VCA0768		ATP-dependent RNA helicase DEAD box family		3.57
VCA0933	cspV	cold shock domain family protein, cspV	0.11	0.00
VCA093		Sensory box/GGDEF family protein		2.26

9				
Transcriptional regulators				
VC0176		Transcriptional regulator putative		3.52
VC1049		Transcriptional regulator, LysR family	3.68	
VC1068		Transcriptional regulator, ArsR family		8.32
VC1679	pspF	Psp operon transcriptional activator, pspF		0.45
Amino acid transport and binding				
VCA1071	putP	Amino acids, peptides, amines sodium/proline symporter, putP		0.51
Anion/cation transport and binding				
VC0475	irgA	Enterobactin receptor, irgA		0.07
VC2081	znuA	Zinc ABC transporter periplasmic zinc-binding protein, znuA		0.40
VCA0912	exbD1	TonB system transport protein ExbD1, exbD1		0.44
Carbohydrate transport and binding				
VC1325	mglB	Periplasmic D-galactose/D-glucose-binding protein, mglB		0.37
VC1695		Formate transporter 1 putative		2.41
VC2699	dcuA	C4-dicarboxylate transporter anaerobic, dcuA		0.51
VCA0518	fruB	PTS system fructose-specific IIA/FPR component, fruB		0.22
VCA0945	malE	Periplasmic maltose-binding protein, malE		0.29
VCA0946	malK	Maltose/maltodextrin ABC transporter ATP-binding protein, malK		0.33
VCA1028	ompS	Maltoporin, ompS	0.10	0.21
VCA1045	mtlA	PTS system mannitol-specific IIABC component, mtlA		2.98
Type VI secretion				
VC1415	hcp-1	Hemolysin-coregulatred protein, hcp-1	0.11	0.23
VCA0017	hcp-2	Hemolysin-coregulatred protein, hcp-2	0.02	0.19
Other functions				
VC0653	rocS	c-di-GMP phosphodiesterase A-related protein, rocS		2.26
VC0870	tnpA	IS1004 transposase, tnpA	0.29	
VC1329		opacity protein-related protein	0.29	
VCA0558		Gamma-glutamyltranspeptidase putative		3.29
VCA0808		NodN-related protein		3.12
VCA1060	ribB	3 4-dihydroxy-2-butanone 4-phosphate synthase, ribB		3.59
Hypothetical				

VC0074		Hypothetical protein		2.43
VC0177	vspR	Hypothetical protein		3.45
VC0179	dncV	Hypothetical protein		2.27
VC0220		Hypothetical protein		2.18
VC0316		Hypothetical protein		3.15
VC0885		Hypothetical protein		0.45
VC1078		Hypothetical protein		2.15
VC1444	vpsV	Hypothetical protein		3.29
VC1577	almG	Hypothetical protein		3.11
VC1578	almF	Hypothetical protein		3.22
VC1601		Hypothetical protein		3.32
VC1865		Hypothetical protein	4.27	
VC1943		Hypothetical protein		0.34
VC1964		Hypothetical protein		0.36
VC2189		Hypothetical protein		2.42
VC2667		Hypothetical protein		2.25
VCA0004		Hypothetical protein		7.07
VCA0087		Hypothetical protein		0.40
VCA0169		Hypothetical protein		3.26
VCA0170		Hypothetical protein		2.11
VCA0457		Hypothetical protein		3.29
VCA0559		Hypothetical protein		2.00
VCA0874		Hypothetical protein	0.31	0.42
Hypothetical conserved				
VC0180		Hypothetical protein, conserved		2.85
VC0181		Hypothetical protein, conserved		2.43
VC0641		Hypothetical protein, conserved		2.15
VC0654		Hypothetical protein, conserved	7.18	
VC0977		Hypothetical protein, conserved	4.74	
VC1433		Hypothetical protein, conserved		0.41
VC1567		Hypothetical protein, conserved		3.55
VC2334		Hypothetical protein, conserved	3.37	
VC2736		Hypothetical protein, conserved	3.49	
VCA0527		Hypothetical protein, conserved		0.44
VCA0907	hutZ	Hypothetical protein, conserved		0.40
VCA0908	hutX	Hypothetical protein, conserved		0.30

CHAPTER 4: Cyclic diguanylate-binding protein VCA1082-3 and large adhesion protein VCA0849 are important for low-temperature biofilm formation in *V. cholerae*

Loni Townsley and Fitnat H. Yildiz

ABSTRACT

In *Vibrio cholerae* temperature is an important environmental signal that controls biofilm formation through modulation of the second messenger cyclic diguanylate (c-di-GMP). During low temperature growth cellular levels of c-di-GMP are high and expression of two putative large adhesins, VCA0849 and VC1620 are differentially regulated. These adhesins are putative substrates for a predicted c-di-GMP receptor VCA1082-3, which is thought to promote biofilm formation by inhibiting the activity of a periplasmic protease VCA1081 and thereby releasing VCA0849 and VC1620 from the cell surface. In this study we provide evidence in support this model by demonstrating a biofilm defect in strains lacking the putative receptor and substrate, VCA1082-3 and VCA0849 and enhanced biofilm formation in a strain lacking the putative protease, VCA1081. We observed no biofilm defect in ΔVC1620; however we observed a significant defect in biofilm formation in a ΔVC1620ΔVCA0849 double deletion strain. Furthermore we observed the ΔVCA1082-3 and ΔVCA0849, ΔVC1620ΔVCA0849 have a decreased ability to bind the surfaces of equine erythrocytes when compared with wild-type *V. cholerae.* Mutations in residues of VCA1082-3 predicted to be important for c-di-GMP binding and VCA1081 interactions impacted the ability of a plasmid harboring VCA1082-3 to complement biofilm formation in a strain lacking VCA1082-3 indicating these interactions are important for the function of this protein. These results support that this system is functionally analogous to the

LapD/G system in *Pseudomonas fluorescens* in which biofilm formation is controlled through an inside-out signal transduction mechanism that controls production of a large adhesion through inhibition of a periplasmic protease. Our findings provide more information on the molecular mechanism of low-temperature signal sensing and how it affects biofilm formation in *V. cholerae*.

INTRODUCTION

Vibrio cholerae is the causative agent of the diarrheal disease cholera. Seasonality of cholera outbreaks in areas where the disease is endemic are linked to environmental conditions that affect the population dynamics of *V. cholerae* in aquatic reservoirs (Lipp et al., 2002). Biofilms are structurally complex, dynamic bacterial accretions that can adhere to almost any surface. These matrix-enclosed communities provide protection to their bacterial constituents from adverse conditions, facilitating resistance to environmental stress (Matz & Kjelleberg, 2005; Yildiz & Schoolnik, 1999). In *V. cholerae* biofilm formation has been shown to facilitate environmental survival, transmission, and infectivity (Alam et al., 2006; Charles & Ryan, 2011; Faruque et al., 1998; Nelson et al., 2009; Tamayo, et al. 2010). Yet the molecular details of how environmental signals are integrated into the biofilm formation regulatory network are poorly understood.

Cyclic diguanylate (c-di-GMP) is a second messenger that relays environmental signals to downstream receptors that control cellular processes such as biofilm formation, motility, and virulence (Römling et al., 2013). c-di-GMP is produced by diguanylate cyclases (DGCs) which contain GGDEF domains and degraded by phosphodiesterases (PDEs) that contain either EAL or HD-GYP domains (Ryjenkov et al., 2005; Schmidt et la., 2005). These proteins often contain additional sensing domains such as REC, PAS, and GAF domains that likely to integrate environmental signals into the activity of c-di-GMP signaling proteins (Römling et al., 2013). Environmental signals that impact c-di-GMP levels identified in *V. cholerae* thus far include anaerobic conditions (Schaller et al., 2012), polyamine norspermidine levels (Karatan et al., 2005), bile and bicarbonate levels (Koestler & Waters, 2014), and temperature (Townsley & Yildiz, 2015). Temperature is a critical environmental signal that governs the occurrence of *V. cholerae* in the environment, and cholera outbreaks are highly correlated with sea surface temperature (Lipp et al., 2002). Furthermore *V. cholerae* must survive cold stress after it has been expelled from the human host into the environment. At low temperatures levels of c-di-GMP are increased, which in turn enhances biofilm formation, however the receptors responsible for relaying low temperature signals to affect biofilm formation remain unidentified.

In *Pseudomonas fluorescens* LapD has been identified as a c-di-GMP effector protein that controls biofilm formation via an inside-out signal transduction pathway (Chatterjee et al., 2014; Hinsa & O'Toole, 2006; Newell et al., 2011). LapD contains degenerate GGDEF and EAL domains that are inactive, however, the degenerate EAL domain is able to bind c-di-GMP generated in response to high inorganic phosphate levels (Newell et al., 2009). The binding of c-di-GMP by LapD promotes surface attachment through the retention of a large adhesin called LapA (Newell et al., 2009). c-di-GMP-bound LapD controls LapA localization by engaging the periplasmic protease LapG through its PAS-like domain, thus preventing LapG from cleaving the N-terminus of LapA, retaining LapA on the surface and facilitating biofilm attachment (Navarro et al., 2011; Newell et al., 2011). When c-di-GMP levels are low, in cells are grown under low inorganic phosphate conditions, the periplasmic domain of LapD cannot bind LapG. Then, LapA is proteolytically cleaved by free LapG and released from the cell surface; causing disrupting surface attachment (Boyd et al., 2014; Boyd et al., 2012). In *V. cholerae* homologues of the LapD/G system have been bioinformatically predicted; VCA1081 (LapG-like), VCA1082-3 (LapD-like), VCA0849 and VC1620 (putative substrates) (Navarro et al., 2011). Here we elucidate the function of these proteins and examine their effect on low temperature biofilm formation.

RESULTS AND DISCUSSION

VCA0849 and VC1620 *mRNA abundance is affected by temperature*

To determine if temperature plays a role in modulating gene expression of LapDG-like system in *V. cholerae*, we used Real Time PCR to compare mRNA abundance of the putative substrates between wild-type *V. cholerae* cells grown at 37°C to those shifted to 15°C for 1h. We observed an over 4-fold increase in VCA0849 and a 3-fold decrease in VC1620 (Figure 1) indicating that the expression of these genes is modulated by temperature in an opposite manner. Next we wanted to determine if temperature affects expression of the *lapD, lapG* homologues, VCA1082-3 and VCA1081 respectively. These genes are located in a predicted operon with a putative HlyD family, type I secretion membrane fusion protein, VCA1080 and 14 nucleotides upstream of a predicted type I secretion system ATPase, VCA1084. We compared the mRNA message abundance of each gene in the VCA1080-1084 region under the same conditions. We found no significant difference in the expression of the VCA1080, VCA1081, VCA1082-3, or VCA1084 in respect to growth temperature (Figure 1). These results indicate that expression of the putative substrates is modulated in a temperature-dependent manner, while the VC1080-84 operon is not affected by temperature.

Figure 1. Temperature affects VCA0849 and VC1620 expression.

Analysis of expression by real-time PCR in wild-type *V. cholerae* upon shift from 37°C to 15°C for 1h. Error bars indicate standard deviations of three biological replicates. Statistical significance was determined by a two tailed students *t* test. **P*< 0.5., n.s., *P* > 0.05.

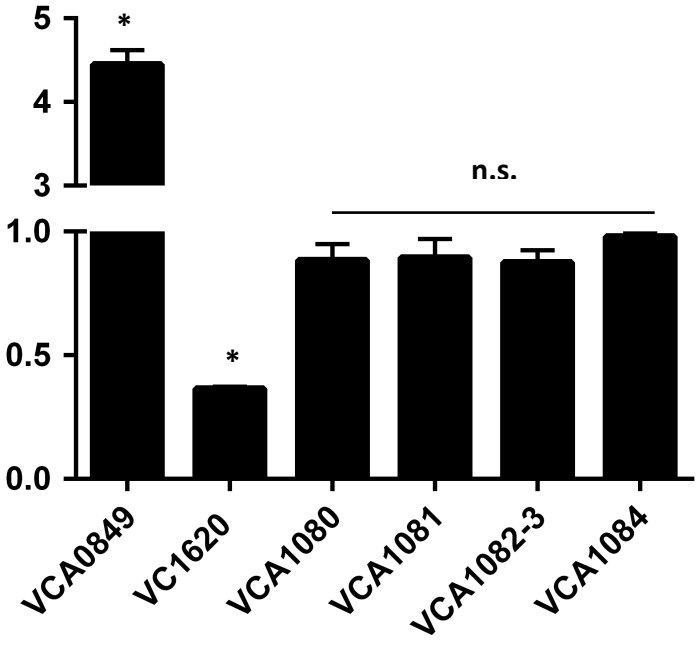

VCA0849 and VC1620 *promoter activity is modulated by c-di-GMP and biofilm regulators VpsR and VpsT*

Next, we compared VCA0849 and VC1620 promoter activity under varying levels of c-di-GMP in order to determine if their expression was affected by c-di-GMP levels using a luciferase transcriptional reporter construct. Δ6 DGC was used as a low c-di-GMP background strain, and Δ3 PDE was used as a high c-di-GMP strain as previous studies have demonstrated that these strains have low and high respective cellular c-di-GMP levels (Townsley & Yildiz. 2015). For VCA0849 promoter activity, we saw a 140-fold decrease in Δ6 DGC and 1.5-fold increase in Δ3 PDE when compared with wild type (Figure 2A), indicating that this gene is highly expressed concurrently with high levels of c-di-GMP. We found VC1620 promoter activity was decreased 3-fold in Δ3 PDE when compared with wild type (Figure 2B) suggesting that this gene is decreased when levels of cellular c-di-GMP are high. There was no significant difference in VC1620 promoter activity in Δ6 DGC compared with wild type ($P>0.05$) (Figure 2B), possibly indicating that factors other than c-di-GMP are important for controlling VC1620 expression. Previous whole genome expression studies found that biofilm regulators VpsR and VpsT modulate transcription of both VCA0849 and VC1620 (Beyhan et al., 2007). Therefore, we compared promoter activity of each gene in strains lacking *vpsR* or *vpsT*. For VCA0849 promoter activity we found an approximately 190-fold decrease in Δ*vpsR*, 4-fold decrease in Δ*vpsT* (Figure 2A) and for

VC1620 promoter activity we found a 2.7-fold increase in Δ*vpsR* and a 2.9-fold increase in Δ*vpsT* (Figure 2B) indicating these genes are oppositely regulated by the biofilm regulators VpsR and VpsT.

Figure 2. c-di-GMP levels affect VCA0849 and VC1620 promoter activity

Promoter activity of (A) VCA0849 and (B) VC1620 in wild-type *V. cholerae* and strains that harbor in-frame deletions of six DGCs, three PDEs, *vpsR, vpsT*. *V. cholerae* cells were grown at 30°C to OD_{600} of 0.4. Expression is reported in luminescence counts min^{-1} ml^{-1}/OD_{600}. Error bars indicate standard deviations of three biological replicates. Statistical significance was determined by a two tailed students *t* test. **P*< 0.5., n.s., *P* > 0.05.

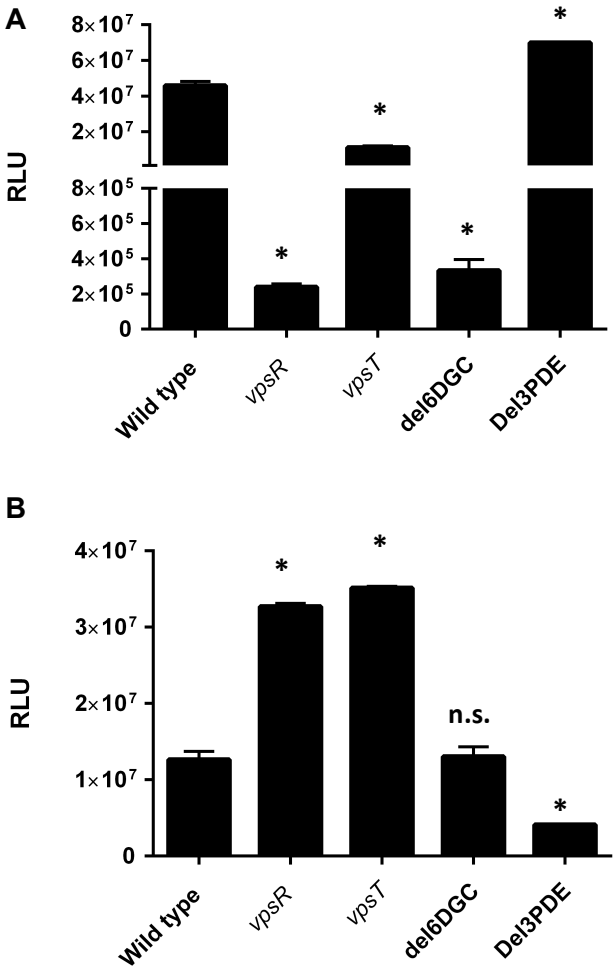

Colony morphology and pellicle formation of mutants

Next we wanted to perform a phenotypic analysis of strains lacking VCA0849 and VC1620 to determine if they have any effect on c-di-GMP-regulated phenotypes. Enhanced biofilm matrix production can impact both colony morphology and pellicle formation in strains with high levels of c-di-GMP. Thus we observed colony morphology and pellicle formation in both the wild type (smooth) and rugose genetic backgrounds of *V. cholerae* strains lacking VCA0849 and VC1620. We found no difference in colony morphology or pellicle formation between any of the mutants when compared to wild type in either the smooth or rugose background (Figure 3A). Next we observed these phenotypes in smooth and rugose backgrounds lacking genes VCA1080, VCA1081, VCA1082-3, and VCA1084. We found that ΔVCA1082-3 had a defect in pellicle formation at 25°C in the wild-type genetic background (Figure 3B), all other mutants looked comparable to wild type in respect to both colony morphology and pellicle formation (Figure 3B). We did not see any significant phenotypic differences in any of the mutants in the rugose background. We think that high basal levels of c-di-GMP in the rugose strain is leading to activation of biofilm formation thus masking any subtle biofilm defects. In addition, we found that these strains were unable to from pellicles at 15C despite enhanced surface attachment at low temperatures, suggesting low-temperature biofilm formation may prefer the liquid-surface as opposed to the air-liquid interface.

Figure 3. Pellicle formation and colony morphology Wild-type *V. cholerae* and strains lacking VCA0849, VCA1081, and VCA1082-3 were grown in LB for 1 week at 37°C, 25°C, and 15°C (from top to bottom) and colonies were formed on LB plates and imaged after 3 days in (A) Rugose-variant and (B) Smooth wild type backgrounds.

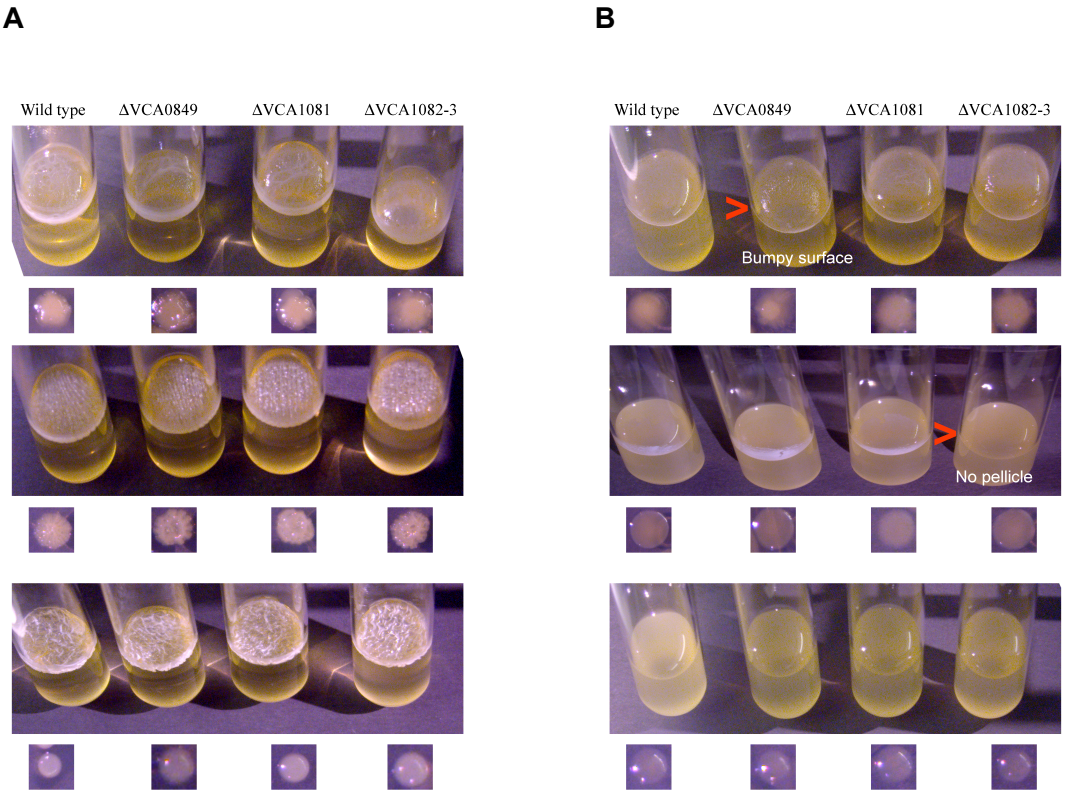

Hemagglutination phenotypes of mutants

Adhesins on the bacterial surface have been shown to bind the surfaces of equine erythrocytes causing hemagglutination. To determine if these mutants have an effect on binding to the surfaces of erythrocytes we analyzed their ability to agglutinate equine erythrocytes using a hemagglutination assay. We found that ΔVCA0849 was defective for hemagglutination (Figure 4) suggesting that this putative adhesion could act at a hemagglutinin. We did not observe a defect for hemagglutination in ΔVC1620 (Figure 4). This is contradictory to a study done by Syed et al. in which they observed a hemagglutination defect in a *V. cholerae* strain lacking VC1620 (Syed et al., 2009). The discrepancy could be due to the fact that the strains used in that study were isogenic with O1 classical strain O395 as opposed to the O1 El Tor A1552 strain used in this study, or due to the fact that human erythrocytes were used. We did observe a decrease in hemagglutination in the ΔVC1620ΔVCA0849 strain, although it was less severe than the ΔVCA0849 single deletion strain indicating that the lack of VC1620 may indeed enhance hemagglutination (Figure 4). Next we observed the hemagglutination phenotypes of the LapD/G-like operon mutants. We found that ΔVCA1082-3 exhibited a hemagglutination defect similar to that of the ΔVCA0849 mutation. This suggests that VCA1082-3 could affect hemagglutination through modulation of VCA0849 or an unidentified adhesion. We observed no hemagglutination defects in ΔVCA1080, ΔVCA1081, or ΔVCA1084.

Figure 4. Hemagglutination phenotypes of mutants Hemagglutination assays were performed with wild-type *V. cholerae* and strains lacking VC1620, VCA0849, VCA1081, and VCA1082-3 grown at 37°C.

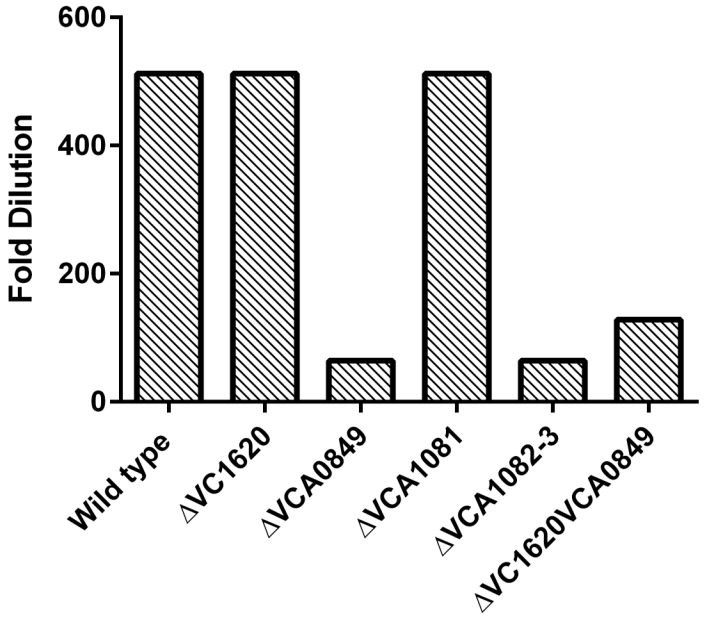

Biofilm formation phenotypes of mutants

We next analyzed the ability of each mutant to form biofilm at 15°C at 6, 24, 48, and 72-h using a confocal laser scanning microscopy (CLSM). CLSM is a much more sensitive method of analyzing biofilm formation than colony morphology or pellicle formation that is able to detect more slight defects. We observed a significant biofilm defect in ΔVCA0849 but not in the ΔVC1620 (Figure 5). However we did see a significant decrease in biofilm formation in a ΔVC1620ΔVCA0849 double mutant (Figure 5) that was more severe than the ΔVCA0849 single deletion, suggesting that VCA0849 expression may be able to compensate for a VC1620 deletion with respect to biofilm formation. We also compared biofilm formation in the VCA1081 and VCA1082-3 deletion mutants to determine if they affected biofilm formation in a similar manner to that in *P. fluoresces.* In agreement with the LapG/D model, the predicted protease mutation ΔVCA1081 had an increase in biofilm thickness, and the predicted c-di-GMP receptor mutant ΔVCA1082-3 had a defect in biofilm thickness and surface coverage (Figure 5).

Figure 5. Biofilm formation phenotypes of mutants. Three-dimensional biofilm structures of (A) wild-type *V. cholerae* and ΔVCA0849, ΔVCA1081, and ΔVCA1082-3 formed at 15°C after 6, 24, 48. and 72 h incubation and (B) ΔVC1620, ΔVCA0849, and ΔVC1620ΔVCA0849 at 15°C after 24 h. Images shown are from one representative experiment of three independent experiments. Scale bars represent 40 μm.

A

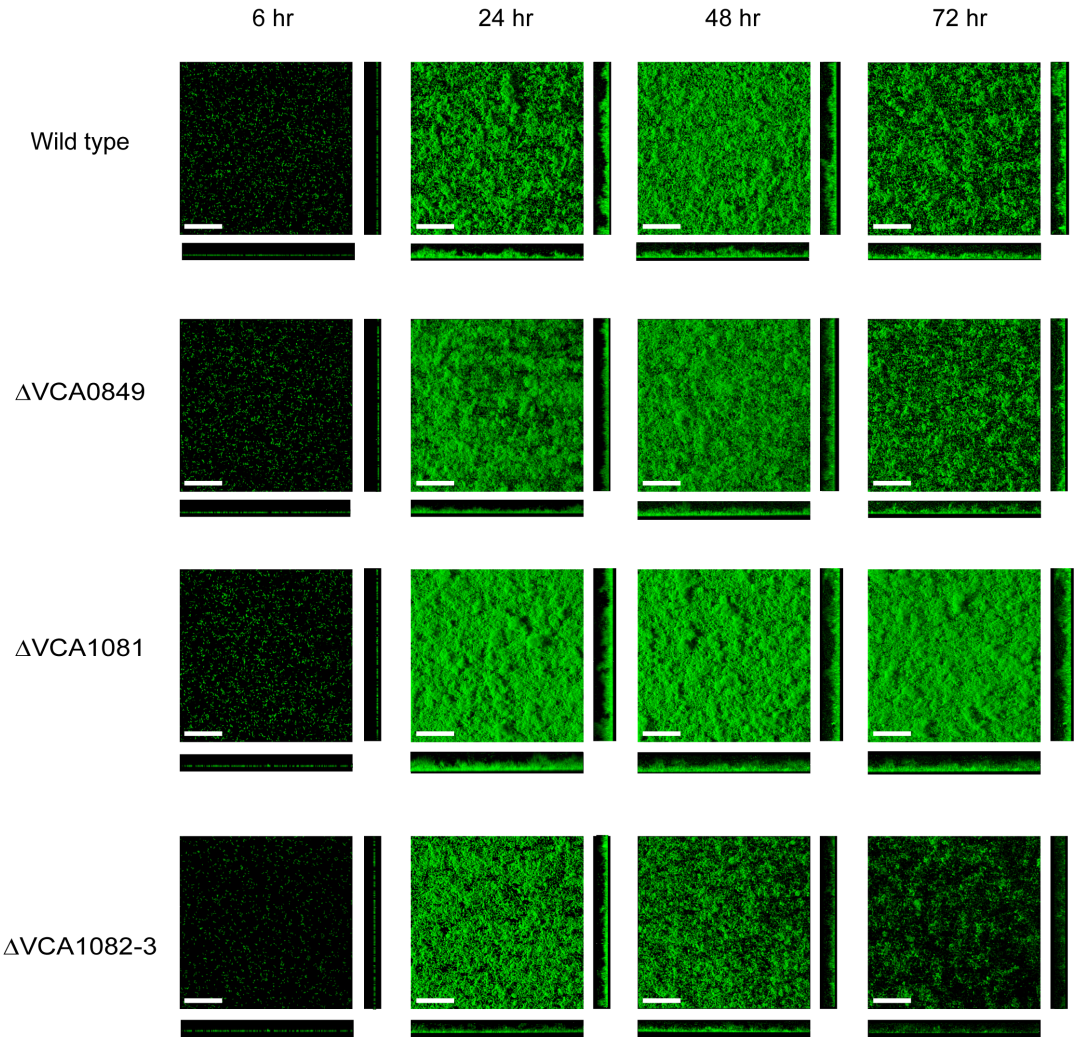

B

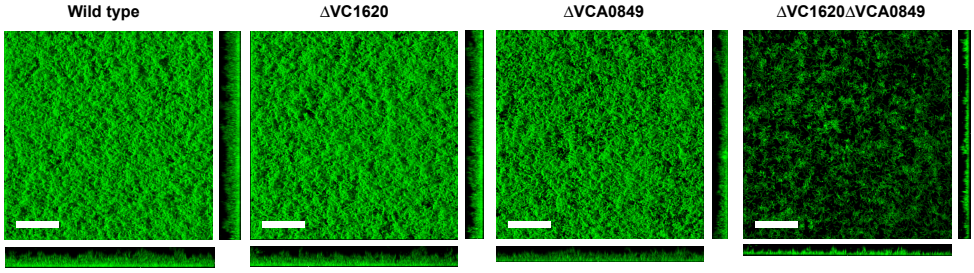

VCA1082-3 point mutations affect biofilm formation

In order to elucidate the molecular details of how VCA1082-3 affects attachment we performed mutagenesis of residues predicted to be important for VCA1082-3 functions. W126 is in the periplasmic domain of VCA1082-3 and is important for binding VCA1081; F223, Q231, and R234 are located within the S-helix of VCA1082-3 and appear to be important for auto inhibition interaction with EAL domain; R248, R423 and R611 are in the c-di-GMP binding site; and T314 is a site that may bind an unidentified substrate. We analyzed the ability of plasmids harboring VCA1082-3 with aforementioned point mutations and evaluated complemention biofilm defect in the VCA1082-3 strain. As mentioned above we saw a decrease in biofilm formation in the VCA1082-3 when compared with wild type (Figure 6). We observed that strains harboring plasmids mutated version of VCA1082-83 with Q231A and R611E alterations formed biofilms similar to wild type (Figure 6), indicating that these mutated versions were still able to complement, F223D, R234D, R248D, R423D and W126E formed less biofilm than wild type, meaning these mutations did not complement the biofilm defect, and T314R formed more biofilm than wild type, signifying this mutations complements even better than wild type (Figure 6).

Figure 6. Biofilm formation is affected by point mutations in VCA1082-3

Three-dimensional biofilm structures of wild-type *V. cholerae* harboring pBAD and ΔVCA1082-3 harboring pBAD, pVCA1082-3, or pVCA1082-3 point mutantions as indicated. Images shown are from one representative experiment of three independent experiments. Scale bars represent 40 μm.

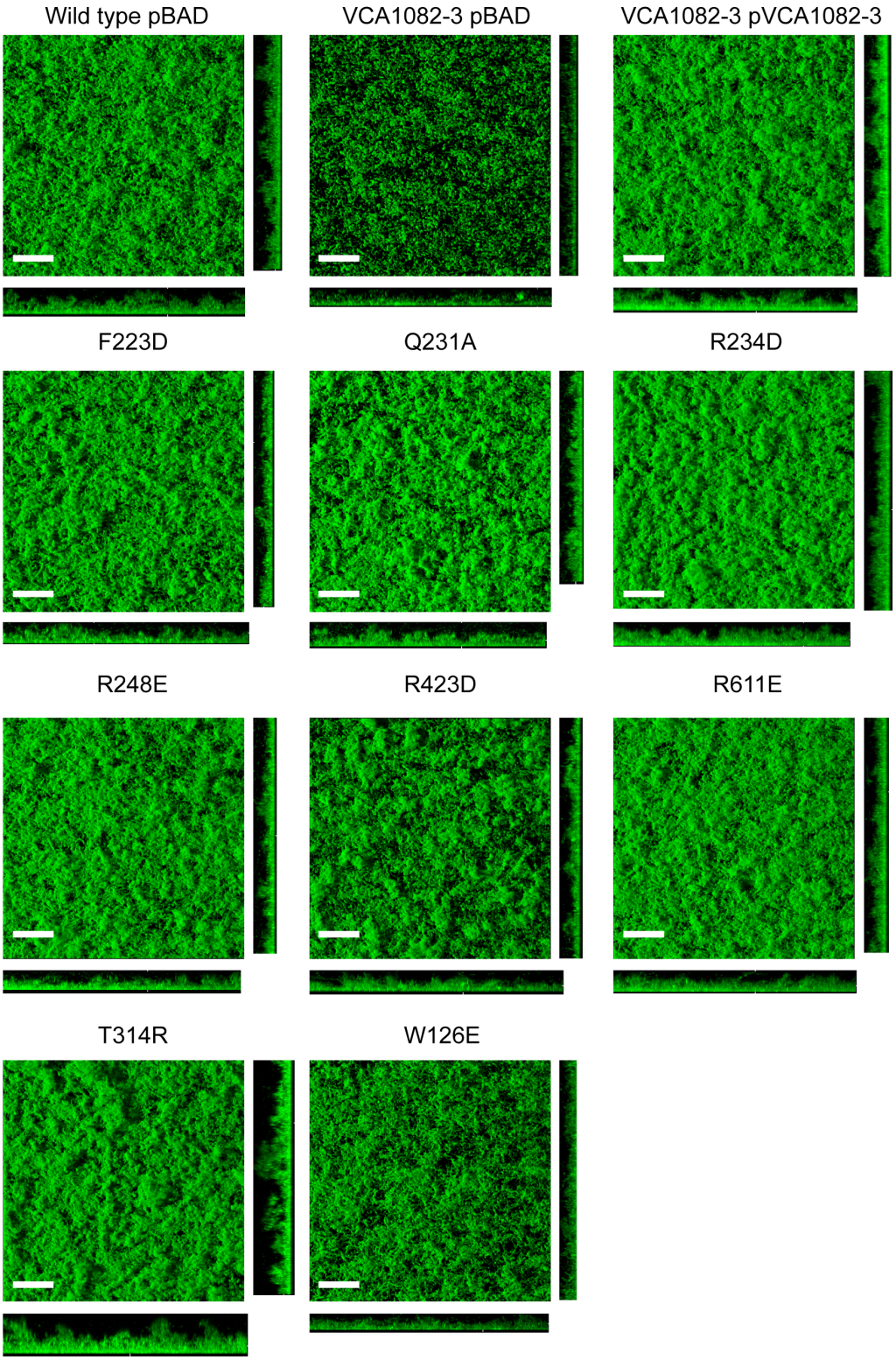
Wild type pBAD
VCA1082-3 pBAD
VCA1082-3 pVCA1082-3
F223D
Q231A
R234D
R248E
R423D
R611E
T314R
W126E

CONCLUSION

c-di-GMP signaling is important for integrating environmental signals to downstream receptors. Yet few studies in *V. cholerae* have observed a complete c-di-GMP signaling circuit that includes identification of the environmental signal, c-di-GMP receptor protein, and interacting partners responsible for the phenotypic output. Here we have just begun to characterize a putative c-di-GMP effector/ protease system in *V. cholerae* that is predicted to be functionally homologous to the LapD/G system in *P. fluorescens.* We determined that temperature is a key signal in regulating this system likely though increased levels of cellular c-di-GMP as well as via temperature modulation of VCA0849 and VC1620 mRNA message abundance. Based on our results we predict that at low temperatures high c-di-GMP levels cause VCA1082-3 to bind c-di-GMP and inhibit VCA1081 degradation of VCA0849, which increases biofilm compactness and thickness at low temperatures. Future studies will be needed to address the molecular details of this system.

EXPERIMENTAL PROCEDURES

Bacterial strains and growth conditions

Vibrio cholerae O1 El Tor A1552 was used as wild-type strain. *Escherichia coli* CC118 λpir and S17-1 λpir were used for cloning and conjugation respectively. Luria–Bertani medium (1% tryptone, 0.5% yeast extract, 0.2 M NaCl; pH 7.5) was used to grow all strains. Temperature-shift experiments were performed by inoculating overnight-grown cultures of *V. cholerae* in a 1:200 dilution in LB and incubating at 37°C until exponential phase (OD600 = 0.4); cultures were then shifted to 15°C or maintained at 37°C for 1 h. When needed, chloramphenicol was used at 5 μgml−1 , and ampicillin and rifampicin were used at 100 μgml−1 , except for biofilm complementation analysis where ampicillin was used at 25 μgml−1 . L-arabinose was added to growth medium at a final concentration of 0.1% (wt/vol) for complementation.

Expression analysis

Real-time PCR Total RNA was isolated from *V. cholerae* cells that were grown in LB that were exposed to cold-shift. For this, overnight-grown cultures of *V. cholerae* were diluted 1:200 in LB and incubated at 37°C until exponential phase (OD600 = 0.4); cultures were then shifted to 15°C or maintained at 37°C for 1 h. Two ml of each aliquot was collected by

centrifugation, immediately re-suspended in 1ml of Trizol reagent (Invitrogen), and RNA purification, cDNA synthesis, and Real Time PCR was performed as previously described (Townsley & Yildiz, 2015). Results are from three independent experiments performed in triplicate. All samples were normalized to the expression of the house- keeping gene 16S using the Pfaffl method (Pfaffl, 2001). Relative expression was calculated by normalizing expression at 15°C by that at 37°C. Statistical analysis was performed using two-tailed student's t test.

Luminescence assays

V. cholerae wild type and *vpsR, vpsT* mutants harboring the either the pVC1620p-lux or pVCA0849p-lux plasmids where grown overnight (15–17 h) aerobically in LB supplemented with chloramphenicol. Cells were diluted 1:200 in LB + chloramphenicol and grown at 30°C until OD600 = 0.4, at which time luminescence was measured using a Victor 3 Multi-label Counter (Perkin-Elmer) and is reported as counts min−1 ml−1 /OD600. Assays were repeated with three biological replicates for all strains tested. Four technical replicates were measured for all assays. Statistical analysis was performed using two-tailed student's *t* test.

Colony morphology and pellicle formation assays

Colonies were formed on LB agar plates at 37°C. After 24 h plates were transferred to 25°C for another 48 h, then colony morphology was imaged. *V. cholerae* were grown overnight at 37°C then a 1:200 dilution was performed into glass tubes containing 5 ml LB. Tubes were incubated at 15 °C, 25°C, and 37°C for 1 week then pellicles were imaged.

Hemagglutination assay

The hemagglutination assays were performed as previously described by Syed et al, 2011 with slight alternations. Briefly, *V. cholerae* strains were grown at 37°C to an OD_{600} of 0.4, then cells were pelleted, washed twice, and resuspended in KRT buffer at a concentration of 10^{10} CFU/ml. KRT-diluted cells were then serially diluted in a round-bottomed 96-well microtiter plate. Defibrinated equine erythrocytes (Hemostat Labs) were harvested by centrifugation, washed twice, and resuspended in KRT buffer at a 2% concentration. 0.1 ml of red blood cells were added to 0.1 ml KRT-suspended bacterial cells and the plate was incubated at 25°C for 30 min, then the hemagglutination titer was recorded. The titer reported represents the reciprocal of the greatest dilution at which hemagglutination was observed.

Biofilm imaging

Vibrio cholerae strains were tagged with GFP according to the procedure previously described (Fong et al., 2006). GFP-tagged *V. cholerae* from overnight-grown cultures were diluted into LB broth to an OD600 of about

0.02, then 3 ml were inoculated into glass chambers (Lab-Tek) and incubated statically at 15°C. After 24 h, planktonic bacteria were gently removed by inverting the glass chambers then gently washed twice with fresh LB. Biofilm formation was visualized using confocal laser-scanning microscopy with an LSM 5 Pascal laser-scanning microscope (Zeiss). Three- dimensional images were reconstructed using IMARIS 7.6 and analyzed using COMSTAT (Heydorn et al., 2000). Each experiment included three independent biological replicates, and three images were taken for each replicate.

Plasmid construction

Overexpression plasmids were constructed by cloning the open reading frame of VCA1082-3 into pBAD/Myc- His B (Invitrogen) using ligation-independent cloning. The insert was sequenced. Point mutations of pBADVCA1082-3 were generated using the QuikChange II Site-Directed Mutagenesis Kit (Agilent) and point mutants were confirmed by sequencing (UC Berkeley).

REFERENCES

Alam, M., Alam, M., Sultana, M., Sultana, M., Nair, G. B., Nair, G. B., Colwell, R. R. (2006). Vibrio cholerae. *Society*, *72*(4), 2849–2855.

Beyhan, S., Bilecen, K., Salama, S. R., Casper-Lindley, C., & Yildiz, F. H. (2007). Regulation of rugosity and biofilm formation in *Vibrio cholerae*: comparison of VpsT and VpsR regulons and epistasis analysis of *vpsT*, *vpsR*, and *hapR*. *Journal of Bacteriology*, *189*(2), 388–402.

Boyd, C. D., Chatterjee, D., Sondermann, H., & O'Toole, G. a. (2012). LapG, required for modulating biofilm formation by *Pseudomonas fluorescens* Pf0-1, is a calcium-dependent protease. *Journal of Bacteriology*, *194*(16), 4406–4414.

Boyd, C. D., Jarrod Smith, T., El-Kirat-Chatel, S., Newell, P. D., Dufrêne, Y. F., & O'Toolea, G. a. (2014). Structural features of the *Pseudomonas fluorescens* biofilm adhesin LapA required for LapG-dependent cleavage, biofilm formation, and cell surface localization. *Journal of Bacteriology*, *196*(15), 2775–2788.

Charles, R. C., & Ryan, E. T. (2011). Cholera in the 21st century. *Current Opinion in Infectious Diseases*, *24*(5), 472–7.

Chatterjee, D., Cooley, R. B., Boyd, C. D., Mehl, R. a, O'Toole, G. a, & Sondermann, H. (2014). Mechanistic insight into the conserved allosteric regulation of periplasmic proteolysis by the signaling molecule cyclic-di-GMP. *eLife*, *3*, 1–29.

Faruque, S. M., Albert, M. J., & Mekalanos, J. J. (1998). Epidemiology , Genetics , and Ecology of Toxigenic *Vibrio cholerae* Epidemiology , Genetics , and Ecology of Toxigenic Vibrio cholerae. *Microbiology and Molecular Biology Reviews*, *62*(4), 1301–1314.

Hinsa, S. M., & O'Toole, G. a. (2006). Biofilm formation by *Pseudomonas fluorescens* WCS365: A role for LapD. *Microbiology*, *152*(5), 1375–1383.

Karatan, E., Duncan, T. R., & Watnick, P. I. (2005). NspS , a Predicted Polyamine Sensor , Mediates Activation of *Vibrio cholerae* Biofilm Formation by Norspermidine NspS , a Predicted Polyamine Sensor , Mediates Activation of Vibrio cholerae Biofilm Formation by Norspermidine, *187*(21).

Koestler, B. J., & Waters, C. M. (2014). Bile Acids and Bicarbonate Inversely Regulate Intracellular Cyclic di-GMP in *Vibrio cholerae*. *Infection and Immunity*, *82*(7), 3002–3014.

Lipp, E. K., Huq, A., & Colwell, R. R. (2002). Effects of Global Climate on Infectious Disease : the Cholera Model. *Clinical Microbiology Reviews*, *15*(4), 757–770.

Matz, C., & Kjelleberg, S. (2005). Off the hook - How bacteria survive protozoan grazing. *Trends in Microbiology*, *13*(7), 302–307.

Navarro, M. V. a S., Newell, P. D., Krasteva, P. V., Chatterjee, D., Madden, D. R., O'Toole, G. a., & Sondermann, H. (2011). Structural basis for c-di-GMP-mediated inside-out signaling controlling periplasmic proteolysis. *PLoS Biology*, *9*(2).

Nelson, E. J., Harris, J. B., Morris, J. G., Calderwood, S. B., & Camilli, A. (2009). Cholera transmission: the host, pathogen and bacteriophage dynamic. *Nature Reviews. Microbiology*, *7*(10), 693–702.

Newell, P. D., Boyd, C. D., & Sondermann, H. (2011). A C-di-GMP Effector System Controls Cell Adhesion by Inside-out Signaling and Surface Protein Cleavage. *Plos Biology*, *9*(2), 1–17.

Newell, P. D., Monds, R. D., & Toole, G. A. O. (2009). protein that regulates surface attachment by *Pseudomonas fluorescens* Pf0 – 1. *PNAS*, *106*(9).

Römling, U., Galperin, M. Y., & Gomelsky, M. (2013). Cyclic di-GMP: the first 25 years of a universal bacterial second messenger. *Microbiology and Molecular Biology Reviews : MMBR*, *77*(1), 1–52.

Ryjenkov, D. A., Tarutina, M., Moskvin, O. V, & Gomelsky, M. (2005). Cyclic Diguanylate Is a Ubiquitous Signaling Molecule in Bacteria : Insights into Biochemistry of the GGDEF Protein Domain Cyclic Diguanylate Is a Ubiquitous Signaling Molecule in Bacteria : Insights into Biochemistry of the GGDEF Protein Domain. *Journal of bacteriology*, *187*(5), 1792-1798.

Schaller, R. a, Ali, S. K., Klose, K. E., & Kurtz, D. M. (2012). A bacterial hemerythrin domain regulates the activity of a *Vibrio cholerae* diguanylate cyclase. *Biochemistry*, *51*(43), 8563–70.

Schmidt, A. J., Ryjenkov, D. a., & Gomelsky, M. (2005). The ubiquitous protein domain EAL is a cyclic diguanylate-specific phosphodiesterase:

Enzymatically active and inactive EAL domains. *Journal of Bacteriology*, *187*(14), 4774–4781.

Syed, K. A., Beyhan, S., Correa, N., Queen, J., Liu, J., Peng, F., Klose, K. E. (2009). The *Vibrio cholerae* flagellar regulatory hierarchy controls expression of virulence factors. *Journal of Bacteriology*, *191*(21), 6555–6570.

Tamayo, R., Patimalla, B., & Camilli, A. (2010). Growth in a biofilm induces a hyperinfectious phenotype in *Vibrio cholerae*. *Infection and Immunity*, *78*(8), 3560–9.

Townsley, L., & Yildiz, F. H. (2015). Temperature affects c-di-GMP signaling and biofilm formation in *Vibrio cholerae*. *Environmental Microbiology* [Epub ahead of print].

Perspectives

V. cholerae is a facultative human pathogen that must endure drastic changes in temperature between its human hosts and aquatic reservoirs. To date, studies have focused on how temperature affects the prevalence and distribution of *V. cholerae* in the environment; however, little is known regarding temperature-mediated changes to physiology and cellular processes that facilitate survival of this pathogen in the environment.

Here we found that biofilm formation is enhanced at low temperatures in *V. cholerae* through temperature-modulation of cyclic diguanylate (c-di-GMP) levels. This low-temperature induction of c-di-GMP requires six diguanylate cycleases (DGCs), *cdgA, cdgH, cdgK cdgL, cdgM,* and *vpvC.* However, it remains unclear how these DGCs sense low-temperature signals. It is possible that these DGCs sense temperature themselves, either by sensing membrane alterations or through sensing domains. Or they may require an intermediate sensor required to relay temperature signals to the biofilm network. Further studies are required to elucidate the exact mechanism of low-temperature signal sensing by the c-di-GMP signaling network. In addition, we still do not know if the increase in c-di-GMP levels is due to an increase in abundance or activity of these DGCs, therefore studies in the future may focus on how temperature impacts translation, protein stability,

and enzymatic activity in order to gain a more clear understanding of low-temperatures affect the c-di-GMP signaling network.

In addition, we analyzed the genome-wide transcriptional profile of *V. cholerae* cells 1 h after a shift to 15°C or 25°C from 37 ° C. We determined differential expression in genes involved in virulence, biofilm formation, type VI secretion (T6SS), and cold shock. In particular we found the cold shock gene, *cspV* (encoding cold shock protein V) is the most highly induced gene upon low-temperate shift and demonstrated that it is important for biofilm formation and T6SS-mediated interspecies killing in *V. cholerae*. Yet the question remains exactly how *cspV* affects the expression of these genes. Cold shock proteins are predicted chaperones, however their actual physiological role has not been determined. In *E. coli* CspA has been shown to cooperatively bind RNA or single-stranded DNA that acts as a transcriptional anti-terminator by preventing secondary structures in nascent RNA. Future work may be directed in finding the exact mechanism of biofilm formation and T6SS gene regulation of *cspV.* In addition, it will be interesting to see if low-temperature growth and *cspV* play a role in infectivity. Preadaptation to low-temperatures has been shown to enable enhanced stress resistance in bacteria and therefore could facilitate survival in the host. In addition, *cspV* was shown to be up-regulated in the presence of bile and

therefore could impact survival in the host. Transmission and infectivity studies will bring *V. cholerae*'s lifecycle story full circle and provide important insight into how temperature adaptation influences the infectious cycle of this pathogen.

In Chapter 4 we provided evidence in support of the hypothesis that a putative c-di-GMP effector/ protease system in *V. cholerae* that is functionally homologous to the inside-out signal transduction system LapD/G found in *Pseudomonas fluorescens.* Future studies will be needed to show direct binding of c-di-GMP to VCA1082-3 and to characterize protein-protein interactions betwee VCA1081, VCA1082-3, VC1620, and VCA0849. It will also be interesting to see if low temperatures affect binding activity of VCA1082-3 as this has been shown in other c-di-GMP receptors and could add another level of temperature signal sensing into the system. Moreover, localization studies of VC11620 and VCA0849 could provide more insight into their specific functions in biofilm attachment. Future studies aimed at identifying other c-di-GMP effectors could also provide important insights into other c-di-GMP regulated processes that are important for low temperature survival.

Temperature is an important physical parameter that impacts the fundamental biochemical processes that support life. Here we have demonstrated that low-temperature shift causes global changes to transcriptome and affects intracellular signaling and cellular processes crucial to the survival of *V. cholerae.* A better understanding of how temperature affects the ecology of *V. cholerae* will provide insight into how seasonal changes and global warming effects may alter pathogenic microbial communities in the environment. Moreover, understanding temperature adaptation and how it affects bacterial behavior and survival will provide important insight into the prediction and control of microbial-associated diseases.